Supporting Information for

Collaborative Biosynthesis of Maleimide- and Succinimide-Containing Natural Products by Fungal Polyketide Megasynthases

Michio Sato,[1,3] Jacob E. Dander,[2] Chizuru Sato,[1] Yiu-Sun Hung,[1] Shu-Shan Gao,[1] Man-Cheng Tang,[2] Leibniz Hang,[2] Jaclyn M. Winter,[1,4] Neil K. Garg,[2*] Kenji Watanabe,[3*] and Yi Tang[1,2*]

[1] Departments of Chemical and Biomolecular Engineering, [2]Chemistry and Biochemistry, University of California, Los Angeles, California 90095, United States.

[3]Department of Pharmaceutical Sciences, University of Shizuoka, Shizuoka 422-8526, Japan;

[4]Medicinal Chemistry Department, University of Utah, Salt Lake City, Utah, 84112

Table of Contents

1. Supporting Methods

1.1. Strains and general techniques for DNA manipulation.

To confirm the modified genotype, the genomic DNA isolated from the transformants of *Penicillium oxalicum* was analyzed by PCR. Genomic DNA from above strains was prepared using the CTAB isolation buffer at pH 8.0 (20 g/L cetyl trimethylammonium bromide, 1.4 M sodium chloride and 20 mM EDTA). The gene-specific primers are listed in Table S1. PCR was performed using Phusion® High-Fidelity DNA polymerase (New England Biolab). The sequences of PCR products were confirmed by DNA sequencing. *Escherichia coli* XL1-Blue (Stratagene) was used for plasmid propagation. DNA restriction enzymes were used as recommended by the manufacturer (New England Biolab).

1.2. Spectroscopic analyses.

NMR spectra were obtained with a Bruker AV500 spectrometer with a 5 mm dual cryoprobe at the UCLA Molecular Instrumentation Center. (^{1}H 500 MHz, ^{13}C 125 MHz). ^{1}H NMR chemical shifts are reported in parts/million (ppm) using the proton resonance of residual solvent as reference: $CDCl_3$ δ 7.26, CD_3OD δ 3.31 and DMSO-d_6 δ 2.50.[1] ^{13}C NMR chemical shifts are reported relative to $CDCl_3$ δ 77.16, CD_3OD δ 49.00 and DMSO-d_6 δ 39.52. High resolution mass spectra were obtained from Thermo Fisher Scientific Exactive Plus with IonSense ID-CUBE DART source at the UCLA Molecular Instrumentation Center. All LC–MS analyses were performed on a Shimadzu 2020 EVLC–MS (Phenomenex kinetex, 1.7 μm, 2.0 x 100 mm, C18 column) using positive and negative mode electrospray ionization with a linear gradient of 5−95% MeCN−H_2O supplemented with 0.1% (v/v) formic acid in 15 min followed by 95% MeCN for 5 min with a flow rate of 0.3 mL/min.

1.3. Preparation of the overexpression strains.

The overexpression of a GAL4 gene in *P. oxalicum* was carried out by integration of an expression cassette containing *poxB* which was placed under control of the constitutive promoter *PgpdA*. The cassette comprised of *bar* gene, which encodes phosphinothricin acetyltransferase, as a selection marker and *poxB* was introduced into *P. oxalicum*. Overexpression of the target gene was confirmed by PCR.

1.4. Preparation of the deletion strains.

The deletion of the target gene in *P. oxalicum* was carried out by homologous recombination using the POX3 which is a strain expressing *poxB* constitutively. A disruption cassette comprised of selection markers *hph* (hygromycin B phosphotransferase[2]) flanked on both sides by a 2000-base pair fragment that is homologous to the site of recombination in the *P. oxalicum* genome was introduced to POX3 to replace the target gene with the selection marker. Disruption of the target gene was confirmed by amplifying the disrupted segment from the genomic DNA by PCR.

1.5. Transformation and cultivation for production of secondary metabolites.

A mutant *P. oxalicum* strain was initially cultured on PDA plates at 28 °C for 7 days. Then approximately 1×10^6 to 4×10^6 of sexual spores, or ascospores, collected from a single plate were inoculated into 200 mL of PD medium (Sigma-Aldrich), which was shaken for 16 h at 28 °C. The grown cells were collected by centrifugation and washed two times with osmotic buffer at pH5.8 (10 mM sodium phosphate buffer and 1.2 M magnesium sulfate). The cells were incubated with 10 mL of osmotic buffer containing 6 mg/mL lysing enzyme (Sigma-Aldrich) and 4 mg/mL yatalase (Takara) at 28 °C for 10 h. After the digestion, 10mL of trapping buffer at pH7.0 (0.1 M Tris-HCl and 0.6 M sorbitol) was overlaid to the resulting protoplasts solution and subsequently centrifuged at 6,800 × *g* for 15 min at 4 °C. The protoplast layer was collected and diluted with triple volume of STC buffer at pH7.5 (1.2 M sorbitol, 10 mM calcium chloride and 10 mM Tris-HCl) and centrifuged at 3,000 × *g* for 5 min at 4 °C. The protoplasts were suspended in STC buffer and combined with 1-5μg of cassette DNA fragment. The mixture was incubated on ice for 1 hour to allow the transformation to proceed. After incubation on ice, 600 μL of PEG solution at pH 7.5 (600 mg/mL polyethylene glycol 4,000, 50 mM calcium chloride and 50 mM Tris-HCl) was added to the reaction mixture, and the mixture was incubated at room temperature for additional 15 min. The DNA–protoplast mixture was plated on a PDA–sorbitol medium (PDA and 1.2 M sorbitol) supplemented with 300 μL/mL hygromycin B for *hph* cassette or 30 μL/mL glufosinate (extracted from herbicide (BAYER)) for *bar* cassette. These plates were incubated for several days at 28 °C. The resultant cells were transferred onto PDA plates with hygromycin B or glufosinate, and incubated for 3 days at 28 °C. The spores from the plate were inoculated into 0.5–5 L of PD liquid medium at 28 °C for 4 days shaken at 250 rpm or

PDA plates at 28 °C for 5days. The broth and cells were extracted with organic solvents for isolation of compounds.

1.6. Compound purification and structural characterization.

To purify **1-10** for structural analysis, POX3 was cultured in PD medium, which was shaken at 28 °C for 4 days. After 4 days of incubation, the culture was centrifuged to separate the supernatant and the cells. The EtOAc extract from the supernatant and acetone extract from the cells were combined and concentrated *in vacuo* to give an oily residue, which was then fractionated by silica gel flash column chromatography with $CHCl_3$/MeOH (1:0→0:1). The fraction containing the compound was further purified by a reversed-phase HPLC (Nacalai Tesque Inc., COSMOSIL 5C18 MS-II, 20 × 250 mm). To purify **12** for structural analysis, POX3/*ΔpoxO* was cultured in PDA plates at 28 °C for 5 days. After 5 days of incubation, the culture was extracted with acetone. After concentration of the extract, the residue was resuspended with water, which was adjusted to pH12 with 10 M NaOH to dissolve fatty acids. Subsequently, the solution was extracted with EtOAc and the extract was concentrated *in vacuo* to give an oily residue, which was then fractionated by ODS gel (Nacalai Tesque Inc., COSMOSIL 140 C_{18}-OPN) flash column chromatography with MeOH/H_2O (30/70→100/0). The sample was further purified by a reversed-phase HPLC as describe above. Chemical structures of the isolated compounds **1-10** were identified from HRESIMS and NMR. For the [1,2-^{13}C]acetate feeding study, the labeled acetate was added to 500 mL of PD medium to the final concentration of 1.0 mM at the same time of inoculation.

1.7. Construction of overexpression and disruption cassette.

To prepare GAL4 expressing strain, an overexpression cassette was constructed (pMIS3). It contains GAL4 gene (*poxB*) which replaces the promoter to constitutive one, *PgpdA* from *A. nidulans*, and selection marker (*bar*). PCR was carried out using Phusion HF DNA polymerase (New England Biolab) as recommended by the manufacturer. The fragment for *PgpdA* and *bar* gene were amplified from pAN7-1[3] and pBARGPE1 (Fungal Genetics Stock Center), respectively. The following primer sets were used to prepare the cassette:

Target gene	Primer set for *PgpdA*	Primer set for *poxB*	Primer set for *bar*
poxB	pMIS3_Fw1 pMIS3_Rv1	pMIS3_Fw2 pMIS3_Rv2	bar_Fw1 pMIS3_Rv3

To prepare a deletion strain of *P. oxalicum* missing a functional copy of a target *pox* gene, initially a disruption cassette of each of the target gene was constructed (pMIS33, 35 and 36). A disruption cassette included a selection marker (*hph*) flanked on both sides by a 2,000-base pair fragment that is homologous to the site of recombination at or near the ends of the target gene in the *P. oxalicum* genome. The disruption cassette was introduced into POX3 which is overexpressing *poxB*, to allow homologous recombination to take place through which the target gene would be replaced by the selection marker. For the 2,000-base pair homologous region that is to be appended to each terminal of the selection marker (designated KO1 for 5' side-flanking fragment and KO2 for 3' side-flanking fragment as shown in Figure S1) to knock out the target gene via homologous recombination, both regions were amplified from the *P. oxalicum* genomic DNA, and *hph* gene was amplified from pAN7-1 by PCR. PCR was carried out as described above. The following primer sets were used to prepare the required flanking homologous regions and selectable marker for each of the target genes:

Target gene	Primer set for KO1	Primer set for *hph*	Primer set for KO2
poxE	pMIS35_Fw1 pMIS35_Rv1	PgpdA_Fw1 TtrpC_Rv1	pMIS35_Fw2 pMIS35_Rv2
poxF	pMIS36_Fw1 pMIS36_Rv1	PgpdA_Fw1 TtrpC_Rv1	pMIS36_Fw2 pMIS36_Rv2
poxO	pMIS33_Fw1 pMIS33_Rv1	PgpdA_Fw1 TtrpC_Rv1	pMIS33_Fw2 pMIS33_Rv2

Amplified DNA fragments were visualized by agarose gel electrophoresis with ethidium bromide using UV (365 nm) transilluminator and purified with Gel DNA Recovery Kit

(Zymo Research). Three purified fragments (KO1, KO2 and the selectable marker) were mixed with the vector backbone from XW55 amplified by PCR using XW55-inverse_Fw1/ Rv1 as a primer set at the concentration of ca 100 ng in a total volume of 10 μL. The mixture was transformed into *Saccharomyces cerevisiae* BJ5464-NpgA[4] for *in vivo* homologous recombination. These four DNA fragments were joined *in situ* by the endogenous homologous recombination activity of *S. cerevisiae* through the 25-bp homologous sequences present at the ends of those DNA fragments. The desired transformants were selected by the presence of the selection marker *URA3* on a uracil-deficient plate. The resulting plasmids (Figure S1) were recovered from the yeast transformant and then amplified in *E. coli* for subsequent characterization by restriction enzyme digestion and DNA sequencing to confirm its identity.

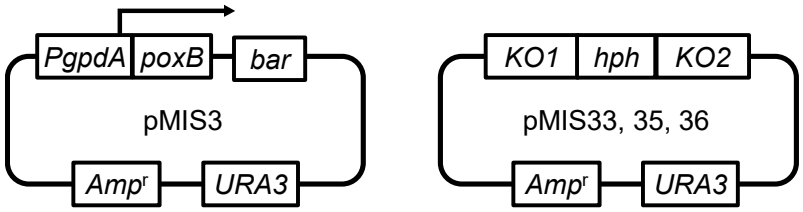

Figure S1. Map of plasmids for making the overexpression and deletion mutants. pMIS3 for *poxB*; pMIS33 for *poxO*; pMIS35 for *poxE*; pMIS36 for *poxF.* KO1: 2,000-bp 5'-side-flanking fragment homologous to one side of the recombination site in the POX3 genome; KO2: 2,000-bp 3'-side-flanking fragment homologous to the other side of the recombination site in the POX3 genome.

1.8. Confirmation of targeted deletion for *poxE*, *F* and *O* genes by PCR.

To verify that the cassette was inserted into the target gene, the genomic DNA isolated from the transformants was analyzed by PCR. Two sets of PCR primers were designed for this verification (Figure S2). For the first set, one primer that anneals at the 5' side of the KO1 region and another primer that anneals to the selection marker were designed. For the second primer set, one primer that anneals to the selection marker and another primer that anneals at the 3' side of the KO2 region were designed. With these primer sets, POX3 genomic DNA will not produce any PCR product with this primer set. However, a PCR product will be formed from the genomic DNA of a strain containing desired gene deletion. Combination of the results from those two separate PCR reactions (Figure S5) ensured us that we had the targeted gene replaced by our desired selection marker.

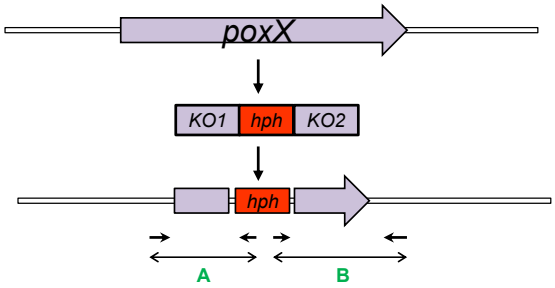

Figure S2. Detection strategy for the deletion strains by using PCR. Deficiency of the target genes by *hph*. A: left border of the marker region; B: right border of the marker region. *poxX*: *pox*E, *F*, or *O*.

Following are primer sets used for each of the deletion strains, where sequences of those primers are given in Table S1:

Deletion strain	PCR fragment	Forward primer	Reverse primer
ΔpoxE	A	PDE_04017KO_Fw2	PgpdA_Rv2
	B	TtrpC_Fw1	PDE_04017KO_Rv2
ΔpoxF	A	PDE_04018KO_Fw2	PgpdA_Rv2
	B	TtrpC_Fw1	PDE_04018KO_Rv2
ΔpoxO	A	PDE_04027KO_Fw1	PgpdA_Rv2
	B	TtrpC_Fw1	PDE_04027KO_Rv1

1.9. Engineered biosynthesis of **14** by expression of *poxF*, *poxL and poxM* in *Aspergillus nidulans* A1145.

For molecular cloning of *poxF* from *P. oxalicum*, this strain was cultured in a PDA for 5 days. The genomic DNA extraction was performed as described above. The *poxF* was amplified by PCR with two sets of primers pMIS113_Fw1/Rv1, pMIS113_Fw2/ Rv2 (Table S1) and combined with PacI and BamHI-digested (10 units) pYTR[5] expression vector to generate pMIS113 (Figure S3) using yeast-based homologous recombination. The identity of the resulting vector MIS113 was confirmed by DNA sequencing. This plasmid was used for expression of *poxF* for *in vivo* reactions.

The *poxL* and *poxM* were amplified by PCR with three primer sets pMIS116_Fw1/Rv1, pMIS116_Fw2/Rv2 and pMIS116_Fw3/Rv3 (Table S1), and combined with PacI and HindIIII-digested (10 units) pYTP[5] to generate pMIS116 (Figure S3) using yeast-based homologous recombination. The expression vector which encodes only *poxM*, pMIS129, was constructed as describe above. The identity of the resulting vector pMIS116 and pMIS129 were confirmed by DNA sequencing. These plasmids were used for expression of *poxL* and *poxM*.

Engineered biosynthesis of **14, 15** and **16** was performed by using engineered *A. nidulans* A1145 that was transformed with pMIS113/pMIS116 or pMIS113/pMIS129 and grown with essentially the same procedure described in our report elsewhere[6]. Briefly, selected cells were grown overnight in CD-ST medium at 28 °C for 3 days with shaking at 250 rpm. The analysis and purification of **14**, **15** and **16** were performed using essentially the same experimental procedure as described above, and the chemical structure of **15** was confirmed by HRESIMS and NMR. The results of the HPLC traces of metabolic extracts from engineered *A. nidulans* A1145 are given in **Figure 2e** in the main text.

1.10. Reverse transcriptional PCR analysis of expression of *pox* genes.

Total RNA was isolated from *P. oxalicum* and *P. aethiopicum* using Ambion RNAqueous kit (Thermo Fisher Scientific Inc.). First strand cDNA synthesis was performed using a SuperScript III First-Strand Synthesis SuperMix kit (Thermo Fisher Scientific Inc.). Primer sets used for amplifying the target genes are listed below. Amplified products were visualized by agarose gel electrophoresis with ethidium bromide using UV (254 nm) transilluminator (Figure S6).

gene	primer sets	gene	primer sets
beta-actin	Poxactin_Fw1/Rv1	*poxI*	PDE_04021_Fw1/Rv1
PKS-NRPS(P.aethiopicum)	PaePKSNRPS_Fw1/Rv1	*poxJ*	PDE_04022_Fw1/Rv1
poxA	PDE_04008_Fw1/Rv1	*poxK*	PDE_04023_Fw1/Rv1
poxB	PDE_04009_Fw1/Rv1	*poxL*	PDE_04024_Fw1/Rv1
poxC	PDE_04015_Fw1/Rv1	*poxM*	PDE_04025_Fw1/Rv1
poxD	PDE_04016_Fw1/Rv1	*poxN*	PDE_04026_Fw1/Rv1
poxE	PDE_04017_Fw1/Rv1	*poxO*	PDE_04027_Fw1/Rv1
poxF	PDE_04018_Fw1/Rv1	*poxP*	PDE_04028_Fw1/Rv1
poxG	PDE_04019_Fw1/Rv1	*poxQ*	PDE_04029_Fw1/Rv1
poxH	PDE_04020_Fw1/Rv1		

1.11. Organic synthesis of (*S,E*)-2-amino-4-decenoic acid (**14**).

Prior to use, CH_2Cl_2 was passed through an activated alumina column. *N*-Fmoc-(L)-allylglycine was purchased from Combi-Blocks and used as received. 1-Heptene was obtained from TCI and used as received. Hoveyda–Grubbs second-generation metathesis catalyst was obtained from Materia, stored in an inert atmosphere glove box, and used as recieved. Reaction temperatures were controlled using an IKAmag temperature modulator. Thin-layer chromatography (TLC) was conducted with EMD gel 60 F254 pre-coated plates (0.25 mm for analytical chromatography and 0.50 mm for preparative chromatography) and visualized using UV. Silicycle Siliaflash P60 (particle size 0.040–0.063 mm) was used for flash column chromatography.

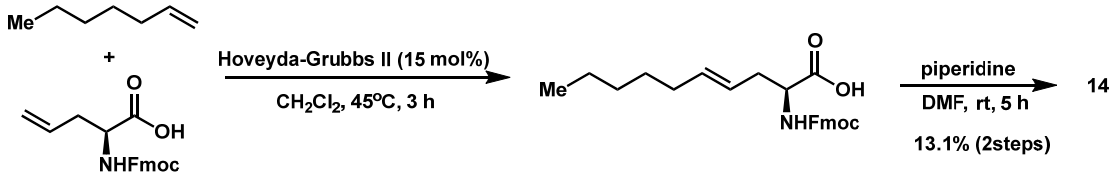

A 25 mL round-bottom flask was equipped with a magnetic stir bar, flame-dried, and cooled under N_2. *N*-Fmoc-(L)-allylglycine (100 mg, 0.30 mmol) was added, and the system was flushed with N_2 for 5 min. CH_2Cl_2 (5 mL) and 1-heptene (63 μL, 0.45 mmol) were then added sequentially via syringe. The mixture was stirred at room temperature for 5 min. Hoveyda–Grubbs second generation catalyst (28.2 mg, 0.45 mmol) was then added to the

mixture and an air condenser was attached. The reaction was then heated to 45 °C (reflux) via oil bath and stirred for 3 h. The reaction was removed from heat and allowed to cool to room temperature. Once cooled, 100 μL of ethylvinylether was added to quench the catalyst, and the mixture was stirred for 30 min at room temperature. The mixture was then concentrated *in vacuo* to provide a crude, golden-brown oil that was then purified by flash chromatography (9:1 → 3:1 Hexanes: EtOAc) to afford the protected amino acid product as a golden oil (49.9 mg). The Fmoc protected amino acid (5 mg, 12.3 μmol) was dissolved with 1 mL of 30% piperidine/*N,N*-dimethylformamide and stirred at room temperature for 5 h. The reaction mixture was purified by a reversed-phase HPLC (Nacalai Tesque Inc., COSMOSIL 5C18 AR-II, 20 × 250 mm) to give (*S,E*)-2-aminodec-4-enoic acid (**14**) (0.91 mg, 13.1%).

1.12. Preparation of (*R*)- and (*S*)-PGME amides of oxaleimide A (**1**) to determine absolute stereochemistry.

To determine the absolute stereochemistry at C7 position of **1**, PGME (phenylglycine methyl ester) derivatization was performed. **1** (2.0 mg, 4.3 μmol) was dissolved with 5 mL of dichloromethane followed by addition of *N*-(3-dimethylaminopropyl)-*N′*-ethylcarbodiimide hydrochloride (3.3 mg, 17 μmol), *N,N*-dimethyl-4-aminopyridine (2.4 mg, 20 μmol), trimethylamine (4.0 mg, 40 μmol) and (*R*)-(–) or (*S*)-(+)-2-phenylglycine methyl ester hydrochloride (4.1 mg, 17 μmol). The reaction mixture was incubated at 0 °C for 1 h and room temperature for overnight. The residue obtained after evaporation of the solvent was partitioned between EtOAc (5 mL × 2) and saturated $NaHCO_3$ solution (5 mL). The EtOAc layer was further partitioned with 0.1 N HCl (5 mL × 3). The extract was dried *in vacuo* and the residue was purified by C_{18} HPLC. The derivatized samples, (*R*)-PGME amide (**11a**) and (*S*)-PGME amide (**11b**), were characterized by NMR (Figure S7 and Table S3). X-ray single crystal analysis was performed with (*R*)-PGME derivative (**11a**) in Figure 2C in the main text.

1.13. Feeding experiments of **14** and **15** in POX3/*ΔpoxF*.

The synthetic amino acid **14** were added to 10 mL of PD medium to a final concentration of 0.1 mM at the time of inoculation of POX3/*ΔpoxF*. The medium was incubated at 28 °C for 3 days. The resultant culture was filtrated to separate the liquid medium and the cells. 2.0 mL of the liquid medium was extracted with ethyl acetate (2 × 2.0 mL). The extract was combined and concentrated *in vacuo*. The dried residue was dissolved in *N*,*N*-dimethylformamide (150 μL), and the resulting solution was subjected to LC–MS analysis (Figure 2F in the main text).

1.14. Construction of pMIS49 for expression of *poxL* in *E. coli*.

For expression of *poxL* in *E. coli*, poxL gene was amplified from cDNA that was synthesized from mRNA isolated from POX3 with a primer set pMIS49_Fw1/Rv1 (Table S1). A plasmid backbone was also amplified from pET21c vector with a primer set pET21c-inverse_Fw1/Rv1 (Table S1). These DNA fragments were then simultaneously joined together by using GeneArt Seamless Cloning and Assembly kit (Thermo Fisher Scientific Inc.). The resulting plasmid was sequenced to confirm its identity. This plasmid was named pMIS49. This vector allowed production of PoxL having a C-terminal His_6-tag.

1.15. Protein production and purification of PoxL.

Overexpression and subsequent protein purification of PoxL was performed as follows: *E. coli* BL21 (DE3) harboring the plasmid pMIS49 was grown in 20 mL of LB with 100 μg/mL carbenicillin at 37 °C overnight. 1 liter of fresh LB with 100 μg/mL carbenicillin was inoculated with 10 mL of the overnight culture and incubated at 37 °C until the optical density at 600 nm reached 0.5. Then expression of each gene was induced with 100 μM isopropylthio-β-D-galactoside at 18 °C. Incubation was continued for another 15 h and then the cells were harvested by centrifugation at 4,000 × *g*. All subsequent procedures were performed at 4 °C or on ice. Harvested cells were resuspended in buffer A (50 mM sodium phosphate buffer (pH 7.5), 500 mM NaCl). Cells were disrupted by sonication, and the lysate was centrifuged at 16,000 × *g* for 1 h. The supernatant and the pellet were recovered as soluble and insoluble fractions, respectively. The soluble fraction containing the protein of interest was applied to 2 mL of Ni-NTA Sepharose resin (GE Healthcare Life Sciences) previously equilibrated in buffer A supplemented with 20 mM imidazole. The column was washed, then the protein was eluted with 10 mL of buffer A supplemented with 250 mM of

imidazole. Fractions containing proteins having the target molecular weight were pooled and dialyzed against 50 mM sodium phosphate buffer (pH 7.5), 50 mM NaCl. Protein concentration was estimated using the Bio-Rad protein assay kit (Bio-Rad Laboratories) with bovine immunoglobulin G as a standard. Purified protein samples were analyzed by SDS–PAGE using Tris-HCl gel stained with Coomassie Brilliant Blue R-250 staining solution (Figure S4). The purified protein was concentrated using a centrifugal filtration, and was flash frozen in liquid nitrogen and stored at –80 °C until use for *in vitro* assays.

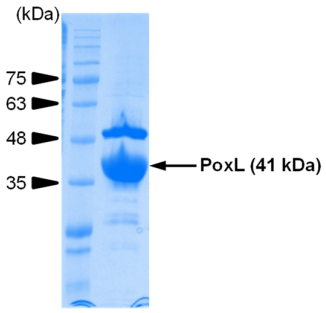

Figure S4. SDS–PAGE analysis of the purified PoxL.

1.16. *In vitro* assay of PoxL for elucidating the biosynthesis of **14**.

The purified protein PoxL (1.0 μM) was added to the assay mixture (50 μL) containing 1.0 mM of L-aspartic acid or L-glutamic acid, 10 μM of pyridoxal-5'-phosphate and 50 μM of (*E*)-2-oxodec-4-enoic acid (**16**) in 50 mM sodium phosphate buffer (pH7.5). After the mixture was incubated at 30 °C for 10 min, equal volume of EtOAc was added to quench the reaction and extract the compounds. The EtOAc layer was concentrated *in vacuo*, and the residue was dissolved with *N*,*N*-dimethylformamide (30 μL) for LC–MS analysis. The analysis was performed described as above.

Table S1. Oligonucleotide primer sequences. DNA primers were designed on the basis of sequence data obtained from the *C. globosum* and *Streptomyces hygroscopicus* (for *hph*) genome sequence database.

Primer name	Sequence
XW55-inverse_Fw1	5'- ACAGTTGCGCAGCCTGAATGGCGAAT -3'
XW55-inverse_Rv1	5'- CGGGGAGAGGCGGTTTGCGTATTGG -3'
pMIS3_Fw1	5'- CCAATACGCAAACCGCCTCTCCCCGGGTGGAGAGCTTATACCGAGCTCC-3'
pMIS3_Rv1	5'- CGGCCTCACTCATGGTGATGTCTGCTCAAGCGGGG -3'
pMIS3_Fw2	5'- AGCAGACATCACCATGAGTGAGGCCGAACCATCTG -3'
pMIS3_Rv2	5'- CTCCTTCAATATCATCTTCTGTCGACATTCCGATGTCCTGGACGTCGT -3'
bar_Fw1	5'- TCGACAGAAGATGATATTGAAGGAG -3'
pMIS3_Rv3	5'- TTCGCCATTCAGGCTGCGCAACTGTTCAGATCTCGGTGACGGGCAG -3'
pMIS33_Fw1	5'- CCAATACGCAAACCGCCTCTCCCCGCCAGAGCAGCAAGGCTGCGGCC -3'
pMIS33_Rv1	5'- GGGAGCTCGGTATAAGCTCTCCACCACCGATGCATCATGAGTGTATT -3'
pMIS33_Fw2	5'- TTTAGAGGTAATCCTTCTTTCTAGAAGCATCTTAATGTTACGCGGTA -3'
pMIS33_Rv2	5'- ATTCGCCATTCAGGCTGCGCAACTGTCGAGGAGAGGTAGTCGACGGTG -3'
pMIS35_Fw1	5'- CCAATACGCAAACCGCCTCTCCCCGGGTGATTGAATCCTGCATTCATC -3'
pMIS35_Rv1	5'- GGGAGCTCGGTATAAGCTCTCCACCCCATTTCGGGGAATAGTTGAGCAT -3'
pMIS35_Fw2	5'- TTTAGAGGTAATCCTTCTTTCTAGAGAAGGGCCTTATGTGGGACTGCTC -3'
pMIS35_Rv2	5'- ATTCGCCATTCAGGCTGCGCAACTGTCACCAAAACACCGCCTGGACTAAT -3
pMIS36_Fw1	5'- CCAATACGCAAACCGCCTCTCCCCGGTTTCCGTGCCCGAGAAGACCTC -3'
pMIS36_Rv1	5'- GGGAGCTCGGTATAAGCTCTCCACCATTAGGTAGAGATGTTGTGGTCAA -3'
pMIS36_Fw2	5'- TTTAGAGGTAATCCTTCTTTCTAGACGACGAGGCGAACGAGCCACCAAC -3'
pMIS36_Rv2	5'- ATTCGCCATTCAGGCTGCGCAACTGTGGTGAAGGGGATGCGCACCTTGG -3'
PgpdA_Fw1	5'- GGTGGAGAGCTTATACCGAGCTCCC -3'
TtrpC_Rv1	5'- TCTAGAAAGAAGGATTACCTCTAAA -3'
PDE_04017KO_Fw2	5'- CACGGATGGACCTGAGAATGTTCTCCGG -3'
PDE_04017KO_Rv2	5'- CGACCCAGTTTGGACGCTCGGGTGC -3'
PDE_04018KO_Fw2	5'- GCCACTCCTGCAGCTGTGGACGCCG -3'
PDE_04018KO_Rv2	5'- AGGTCAACCAGTGCATGGTACGCCG -3'
PDE_04027KO_Fw1	5'- AGCAAGCTCCTCGCCGACCG -3'
PDE_04027KO_Rv1	5'- GGGACCAGATGCCGACCACT -3'
PgpdA_Rv2	5'- GAGGCGGCGGATTTTAGGCTCAAGTC -3'
TtrpC_Fw1	5'- GAGTCGTTTACCCAGAATGCACAGGTAC -3'
pMIS113_Fw1	5'- CCCGCCACATAGACACATCTAAACAATGATCGCCCCAGTAAATGCAGGCGAC -3'
pMIS113_Rv1	5'- GCGCGTCAACGCCTTCGCAAACATC -3'
pMIS113_Fw2	5'- GTTGTGTCGATTTGGGGAGCGTCTCC -3'
pMIS113_Rv2	5'- CATCGAAAGGGAGTCATCCAATTTTGTCTGATGATTTCTGGGGCGCAACC -3'
pMIS116_Fw1	5'- ACAATAAACCCCACAGAAGGCATTTATGAATGCCCTGATCGGACAGTTGTTG -3'
pMIS116_Rv1	5'- CAATTCACCGGAGTCCGCATGTCGCGATGGAGTTGTTGGCAG -3'
pMIS116_Fw2	5'- CATCGCGACATGCGGACTCCGGTGAATTGATTTGGG -3'
pMIS116_Rv2	5'- GTCTTTGGGTGCCATTGTTTAGATGTGTCTATGTGGC -3'
pMIS116_Fw3	5'- GACACATCTAAACAATGGCACCCAAAGACTTCTTTCCAC -3'
pMIS116_Rv3	5'- CCCCTCGAGGTCGACGGTATCGATACCGCTGTGTTAATATGACTGATGATTTG -3'
Poxactin_Fw1	5'- GCTGCTCTCGTCATTGACAAT -3'
Poxactin_Rv1	5'- CGTACAGATCCTTACGGACATC -3'
PaeHR-PKS_Fw1	5'- CAGTCTGGCACGGCGGTCATC -3'
PaeHR-PKS_Rv1	5'- GAGAGACACGAGGCATAGGTG -3'
PDE_04008_Fw1	5'- GCAGTGCCGTGATGTTACTAC -3'
PDE_04008_Rv1	5'- CCCAAATAATGCCGCTGCCG -3'
PDE_04009_Fw1	5'- CCATTGACCACCTGCCAGAT -3'
PDE_04009_Rv1	5'- TGGTTGAGTATGTGCGTGCT -3'
PDE_04015_Fw1	5'- ATTTAGTGCCCGGGCTTTGA -3'

PDE_04015_Rv1	5'- TTGGCCAGGGTAATTCGCAT -3'
PDE_04016_Fw1	5'- TCACCATCATGGTCCGTGATG -3'
PDE_04016_Rv1	5'- AAGTGCATCAAACCACAGGG -3'
PDE_04017_Fw1	5'- AGAGTCGCTTTACAGTCCCGA -3'
PDE_04017_Rv1	5'- GGCCGCAGCACGATTCATGAC -3'
PDE_04018_Fw1	5'- GGACCCGACGATTGAAGAGA -3'
PDE_04018_Rv1	5'- GCCAGGGAGTTGAGGACTAC -3'
PDE_04019_Fw1	5'- GGTCAACTATTGGCGTTGTTG -3'
PDE_04019_Rv1	5'- CCGTCATCTCACACTTGTCAC -3'
PDE_04020_Fw1	5'- CAGCACCACCTATATCCCTC -3'
PDE_04020_Rv1	5'- CCTTTGCTCTCTTACTCTCC -3'
PDE_04021_Fw1	5'- TTACGTTCACGGGTATCACC -3'
PDE_04021_Rv1	5'- CCTTGGCCACCACCTCATCT -3'
PDE_04022_Fw1	5'- GCGAGTCTATGCGATGGATC -3'
PDE_04022_Rv1	5'- TCGTCAACTGGGTGGCATAC -3'
PDE_04023_Fw1	5'- GACTCGCTCCAAGTCCTGCA -3'
PDE_04023_Rv1	5'- CCTGAGTGATGCCACTAAGG -3'
PDE_04024_Fw1	5'- CAAGTTGTCAAGGGCATTGA -3'
PDE_04024_Rv1	5'- CCCATCATCATCTCTAACACC -3'
PDE_04025_Fw1	5'- GGAAAGGCGACATTCACGAG -3'
PDE_04025_Rv1	5'- GATCACCGACCGGTATTTCTC -3'
PDE_04026_Fw1	5'- ATGGCGCTCGATCTCCTGGT -3'
PDE_04026_Rv1	5'- CCCTCCAGGGTGGCCCAAAC -3'
PDE_04027_Fw1	5'- CTAGACACCGGCGAAGCAAG -3'
PDE_04027_Rv1	5'- CATATGTCGCAGCGTCTGCG -3'
PDE_04028_Fw1	5'- CTCTGTGGATTGCCCTGTAC -3'
PDE_04028_Rv1	5'- GCCCTCGTCTACTAGTCGTTG -3'
PDE_04029_Fw1	5'- GCTGGCTGGATCTCATGACG -3'
PDE_04029_Rv1	5'- GCAGGCCACCCAGATATCCG -3'
pET21c-inverse_Fw1	5'- GAGCACCACCACCACCACCACTGAGATCCGGCTGCTAACAAAGCCC -3'
pET21c-inverse_Rv1	5'- GTATATCTCCTTCTTAAAGTTAAACAAAATTATTTCTAGAGGGGAA -3'
pMIS49_Fw1	5'- AAGAAGGAGATATACATGGCACCCAAAGACTTCTTTC -3'
pMIS49_Rv1	5'- GTGGTGGTGGTGCTCGGCGGAAACAGGCTGGAAATATG -3'

Table S2. Deduced functions of the ORFs in the *pox* or *pae* biosynthetic gene cluster from *P. oxalicum* and *P. aethiopicum.*

Gene name	Amino acids (no.)	Deduced function (homolog, NCBI accession number, species)	Identity/ Similarity (%) *pox*, *pae*
poxA/paeF	567/560	MFS transporter (*A. aculeatus*, OJK01149.1)	95/97, 90/95
poxB/paeE	574/570	GAL4-like transcription factor (*A. aculeatus,* OJK01148.1)	73/77, 66/72
poxC/paeM	477/516	cytochrome P450 (*A. aculeatus,* OJK01157.1)	85/89, 93/97
poxD/paeN	484/485	cytochrome P450 (*A. aculeatus,* OJK01158.1)	94/95, 94/95
poxE/paeO	4080/4075	PKS-NRPS (*A. aculeatus,* OJK01159.1)	88/92, 88/92
poxF/paeP	2503/2421	HR-PKS (*A. aculeatus,* OJK01160.1)	82/87, 81/86
poxG	303	thioesterase (*P. brasilianum*, CEJ57900.1)	74/77
poxH/paeA	385/379	enoyl reductase (*A. aculeatus,* OJK01145.1)	84/90, 83/89
poxI/paeB	314/302	NADP-binding protein (*A. aculeatus,* OJK01146.1)	90/94, 89/94
poxJ/paeD	345	WD40 (*A. aculeatus*, OJK01147.1)	88/93, 88/94
poxK	325	hypothetical protein (*A. aculeatus*, OJK01150.1)	89/93
poxL/paeG	365/372	transaminase (*P. roquefoti*, CDM28613.1)	68/80, 68/79
poxM/paeH	512/512	cytochrome P450 (*A. aculeatus*, OJK01152.1)	84/89, 84/89
poxN/paeI	176/176	hypothetical protein (*A. aculeatus*, OJK01153.1)	92/97, 90/97
poxO/paeJ	421/421	alpha/beta hydrolase (*A. aculeatus*, OJK01154.1)	92/96, 91/95
poxP/paeK	378/378	enoyl reductase (*A. aculeatus*, OJK01155.1)	91/95, 92/96
poxQ/paeL	443/446	putative Diels-Alderase (*A. aculeatus*, OJK01156.1)	61/65, 61/65

Deduced function of the ORFs was determined based on the sequence similarity/identity to known proteins as determined by Protein BLAST (BLASTP) search[7] against the NCBI non-redundant database.

2. Supporting Results

2.1. PCR analysis for confirming the deletion.

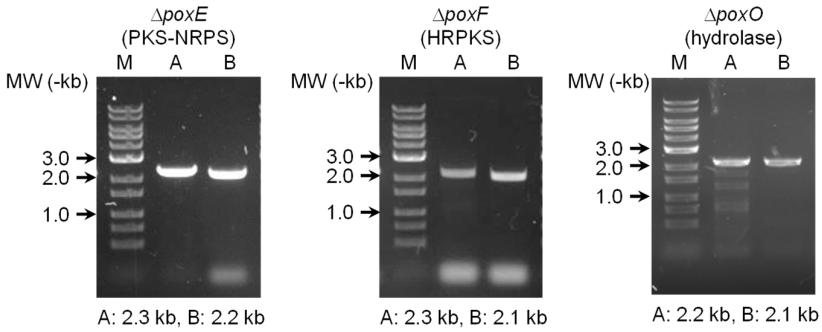

Figure S5. PCR analysis for confirming the deletion of *poxE, F* and *O* using the genomic DNA of each deletion strain as a template. M, molecular marker; Lane A, PCR fragment A; Lane B, PCR fragment B. Expected DNA size were shown below the pictures.

2.2. RT-PCR analysis in fungi.

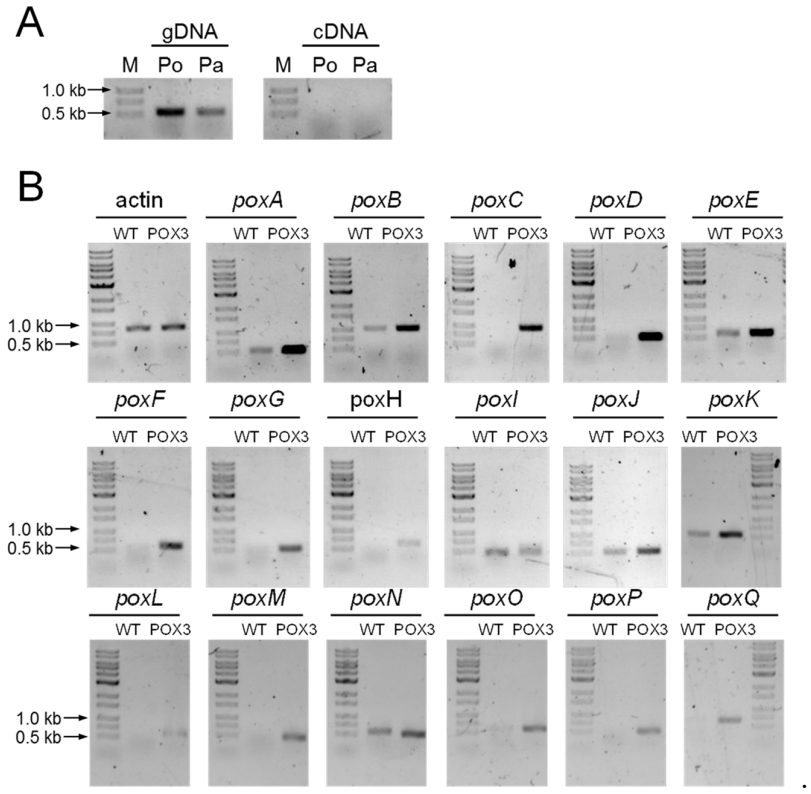

Figure S6. RT-PCR analysis in fungi. (A) PCR analysis of the expression of HR-PKS gene in *P. oxalicum* and *P. aethiopicum*. gDNA and cDNA were used as templates. M, marker; Po, *P. oxalicum*; Pa, *P. aethiopicum*. (B) RT-PCR analysis of the expression of *poxA-Q* in *P. oxalicum*. *β-actin* was used as a control

2.3. Determination of the stereochemistry of oxaleimide (**1**)

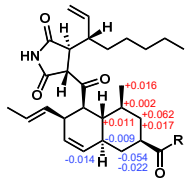

11a: R = (*R*)-PGME
11b: R = (*S*)-PGME

Δδ values [Δδ(in ppm) = δ_S-δ_R]

Figure S7. Structure of PGME-amide of **1** and Δδ values of PGME-amide.

Table S3. NMR data of compound **11a** and **11b** in $CDCl_3$.

	11a		**11b**	
Position	δ_H [ppm]	δ_C [ppm]	δ_H [ppm]	δ_C [ppm]
1	3.627	52.7	3.630	52.6
2	2.955	41.7	2.960	41.7
3	5.481	127.8	5.466	127.8
4	5.480	130.8	5.465	130.8
5	1.912	41.1	1.902	41.1
6	1.436	36.0	1.426	36.0
	2.018		1.964	
7	2.428	45.2	2.435	45.2
8	1.442	39.6	1.457	39.6
	1.768		1.830	
9	1.390	38.4	1.393	38.4
10	1.565	42.1	1.566	42.1
11	5.149	131.5	5.140	131.5
12	5.281	126.2	5.280	126.2
13	1.628	17.9	1.630	17.9
14		200.9		200.9
15	3.656	59.4	3.650	59.4
16		171.8		171.8
17		176.6		176.6
18	3.600	45.4	3.610	45.4
19	2.130	46.0	2.130	46.0
20	5.499	137.4	5.490	137.4
21	5.076	118.8	5.080	118.8
	5.152		5.150	
22	1.610	31.9	1.630	31.9
23	1.240	27.3	1.250	27.3
	1.310		1.320	
24	1.249	31.6	1.250	31.6
25	1.290	22.7	1.290	22.7
26	0.870	14.2	0.870	14.2
7-COOR		174.4		174.4
9-Me	0.569	23.6	0.585	23.6
NH	7.686		7.760	

^1H and ^{13}C NMR spectra were recorded at 500 MHz and 125 MHz, respectively.

2.4. Growth inhibitory effects of oxaleimides on Hela cell.

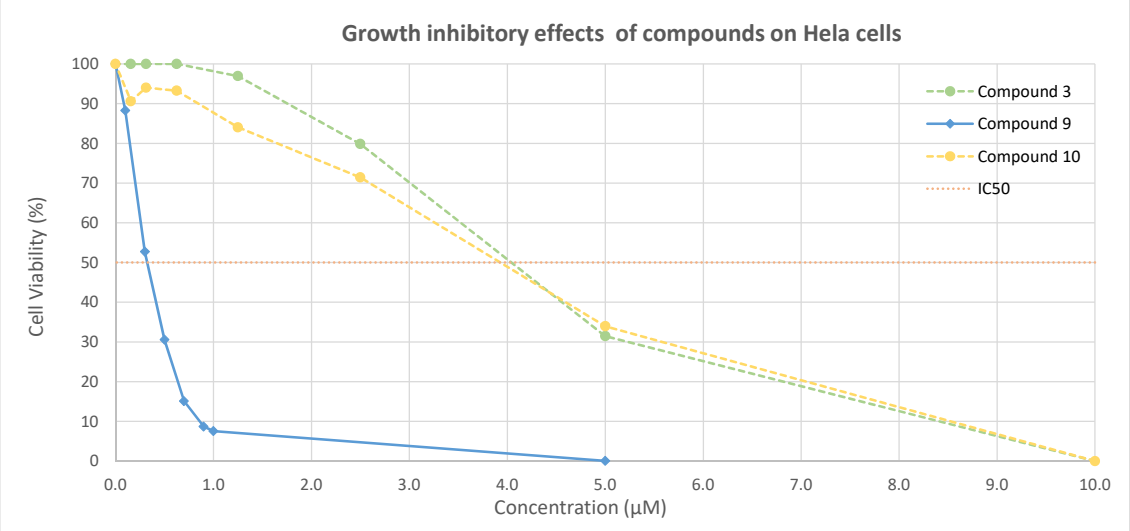

Figure S8. Growth inhibitory effects of **3**, **9** and **10** on Hela cell.

2.5. Bmt biosynthetic pathway[8].

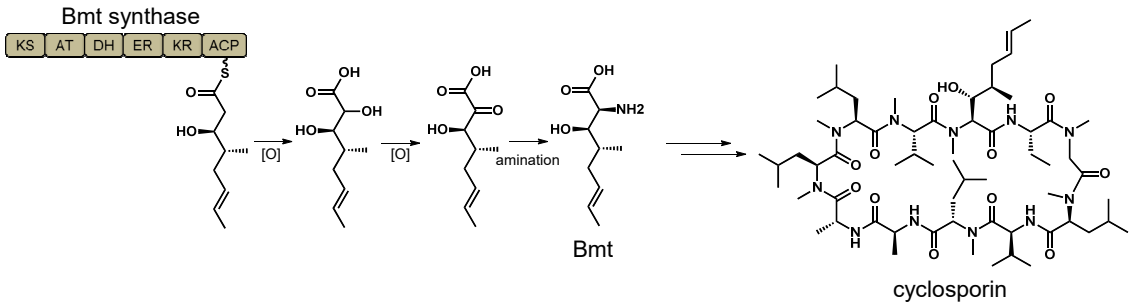

Figure S9. Proposed biosynthetic pathway of Bmt

2.6. Characterization of PoxL

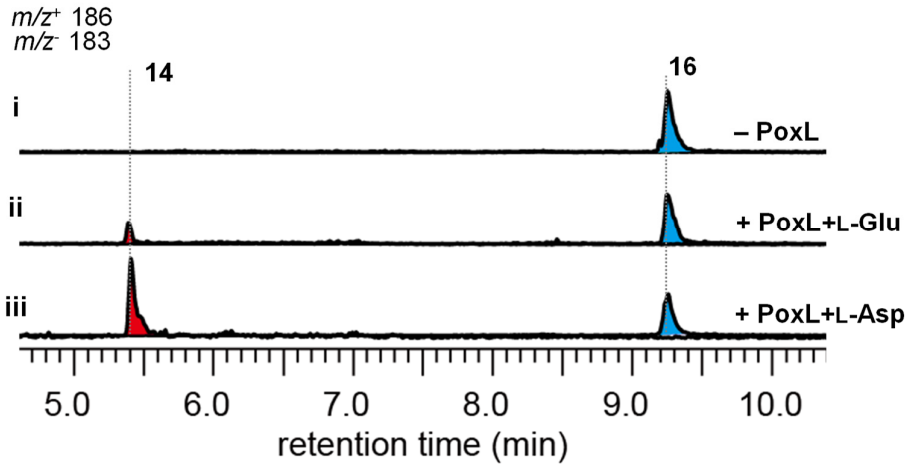

Figure S10. In vitro characterization of PoxL. HPLC analysis of PoxL using **16** as a substrate. Extracted LC traces corresponding to the m/z^+ for **14** (m/z^+ = 186) and m/z^- for **16** (m/z^- = 183). (i) Negative control with **16** lacking PoxL. (ii) Reaction containing PoxL and **16**. L-glutamic acid was used as an amino donor. (iii) Reaction containing PoxL and **16**. L-aspartic acid was used as an amino donor.

2.7. Chemical characterization of **1**.

Table S4. NMR data of oxaleimide A (**1**) in $CDCl_3$. The molecular formula of **1** was established by mass data [ESI–MS: *m/z* 468 $(M–H)^–$; HRESIMS: *m/z* 468.2754 $(M–H)^–$, calcd. for $C_{28}H_{37}NO_5^–$, 468.2756, Δ = 0.16 mmu]; $[\alpha]_D^{31}$: –103.1 (*c* 0.5, MeOH).

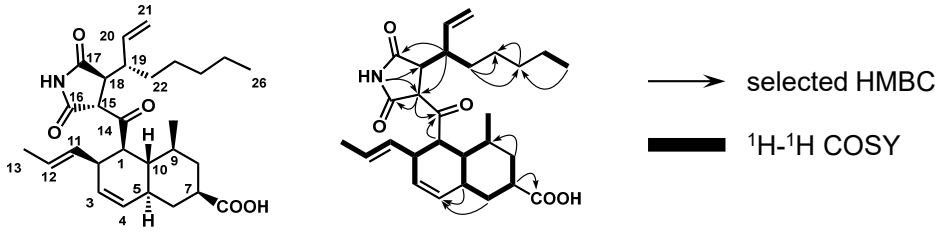

Position	δ_H [ppm]		mult. (*J* in Hz)	HMBC	δ_C [ppm]	*J*cc (Hz) [1,2-^{13}C]acetate
1	3.64	1H	dd (11.2, 6.0)	2, 9, 11, 14	52.7	42.1
2	2.96	1H	m	1, 3, 10, 11, 12	41.7	42.9
3	5.49	1H	m	1, 2	127.9	68.2
4	5.49	1H	m		130.7	68.2
5	1.91	1H	m	3, 4, 6, 9, 10	41.0	33.7
6	2.09	1H	m	4, 5, 8	35.4	33.7
	1.40	1H	m	4, 5, 7, 7-CO		
7	2.57	1H	m	6, 8, 7-CO	43.0	32.0
8	1.91	1H	m	9, 9-Me	38.9	32.0
	1.40	1H	m			
9	1.40	1H	m		38.2	34.5
10	1.56	1H	m	1, 5, 6, 9, 14	42.2	34.5
11	5.17	1H	m	2, 12, 13	131.5	42.9
12	5.29	1H	dq (14.9, 6.4)	2, 11, 13	126.2	42.9
13	1.63	3H	dd (6.4, 1.4)	11, 12	17.9	42.9
14					201.0	42.1
15	3.66	1H	d (4.6)	16, 17, 18, 19	59.4	42.9
16					172.0	42.9
17					177.2	45.4
18	3.61	1H	dd (3.7,3.7)	14,15,16,17,19,20,22	45.4	45.4
19	2.14	1H	m	15,17,18,20,21,22,23	46.0	33.7
20	5.49	1H	m		137.3	69.0
21	5.16	1H	m		118.8	69.0
	5.08	1H	dd (16.9, 0.92)	19, 20		
22	1.62	1H	m		31.9	33.7
23	1.29	1H	m		27.3	34.5
	1.24	1H	m			
24	1.25	2H	m	25,26	31.6	34.5
25	1.28	2H	m	24	22.7	35.3
26	0.87	3H	t (7.1)	24,25	14.2	35.3
7-COOH					180.3	
9-Me	0.59	3H	d (5.5)	9,10	23.6	
NH	8.17	1H	brs	15, 18		

Figure S11. ^{1}H NMR spectrum of **1** in $CDCl_3$ (500 MHz)

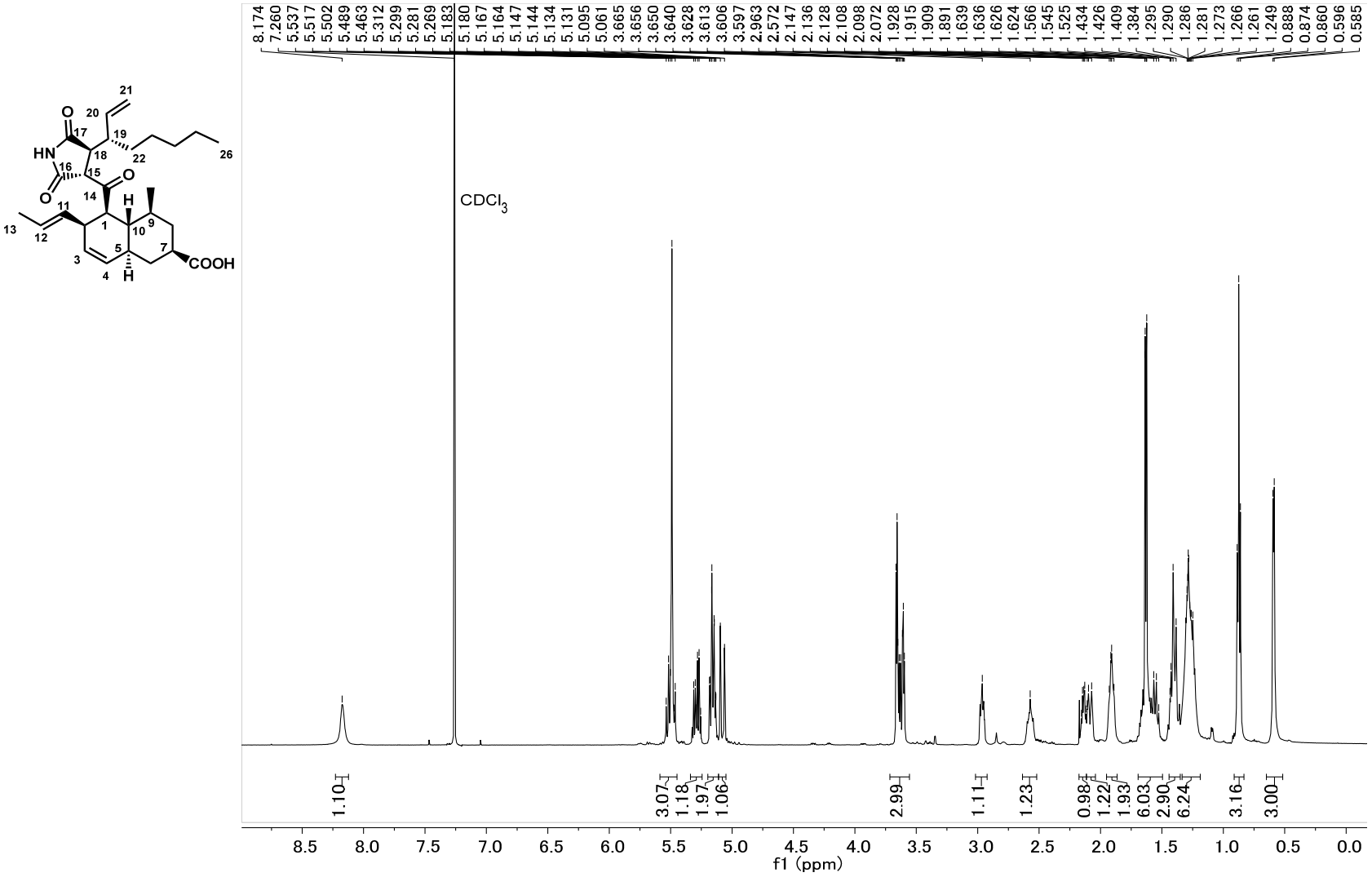

Figure S12. ^{13}CNMR spectrum of **1** in $CDCl_3$ (125 MHz)

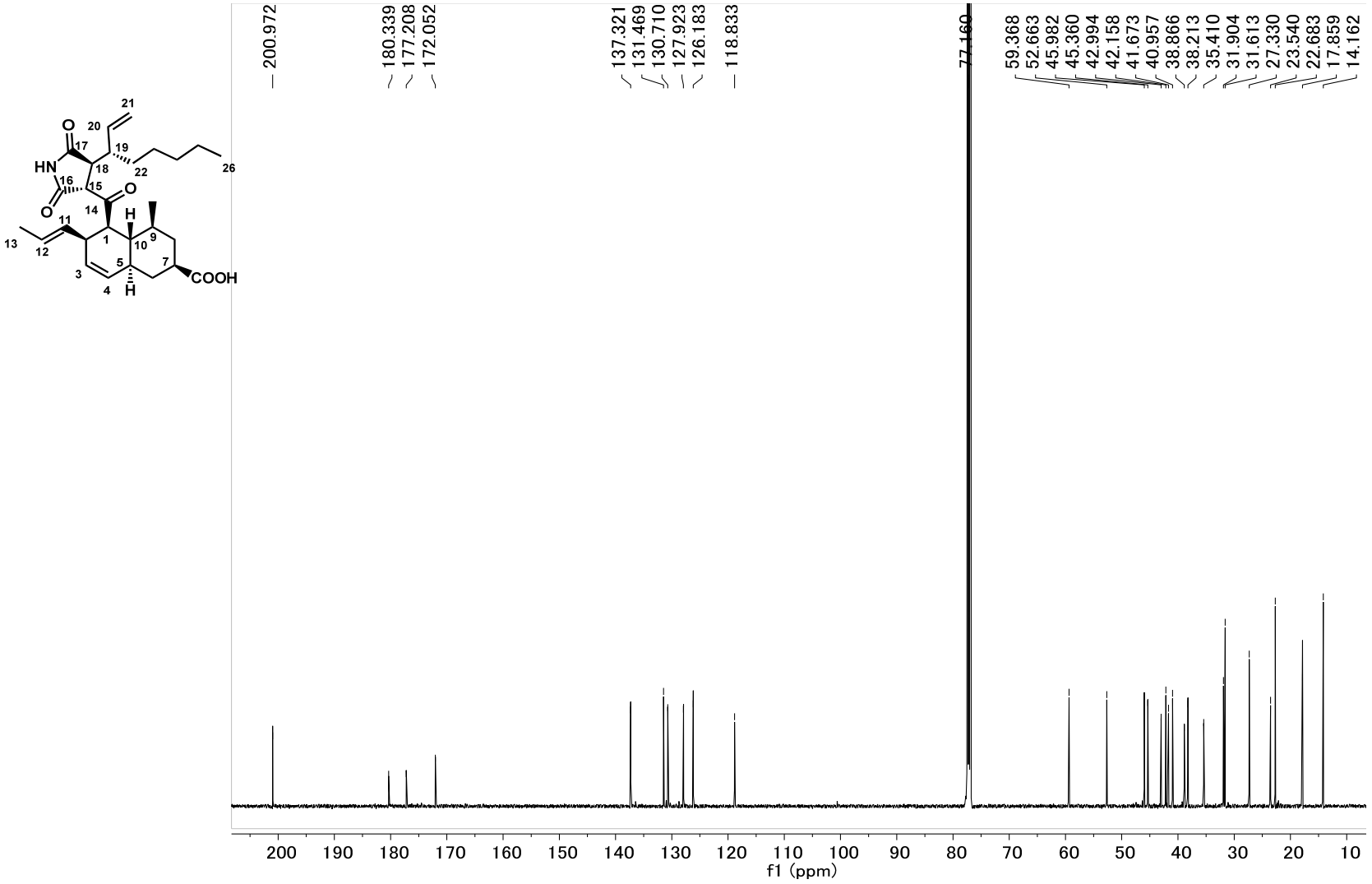

Figure S13. ^{1}H-^{1}H COSY spectrum of **1** in $CDCl_3$ (500 MHz).

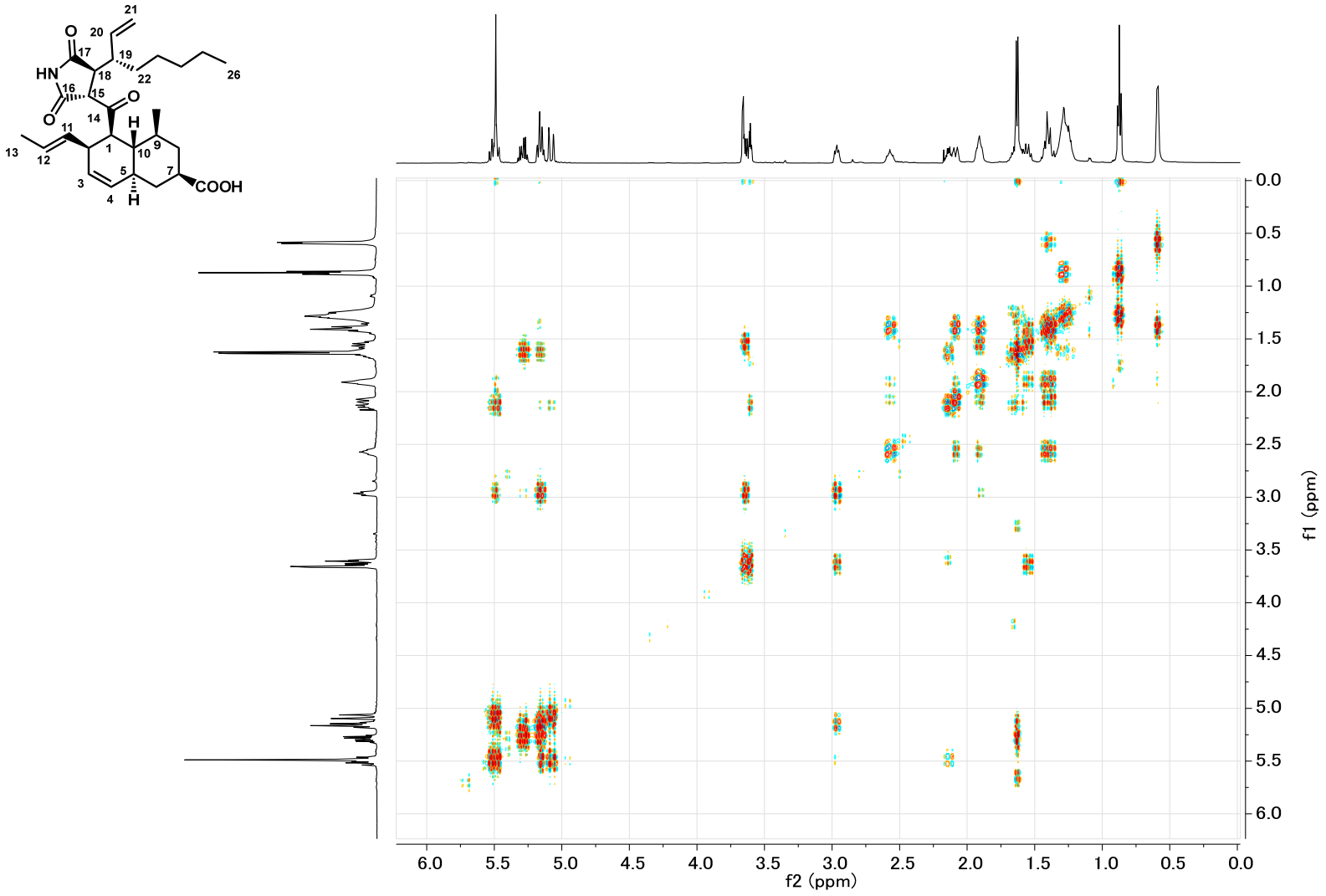

Figure S14. HSQC spectrum of **1** in $CDCl_3$ (500 MHz).

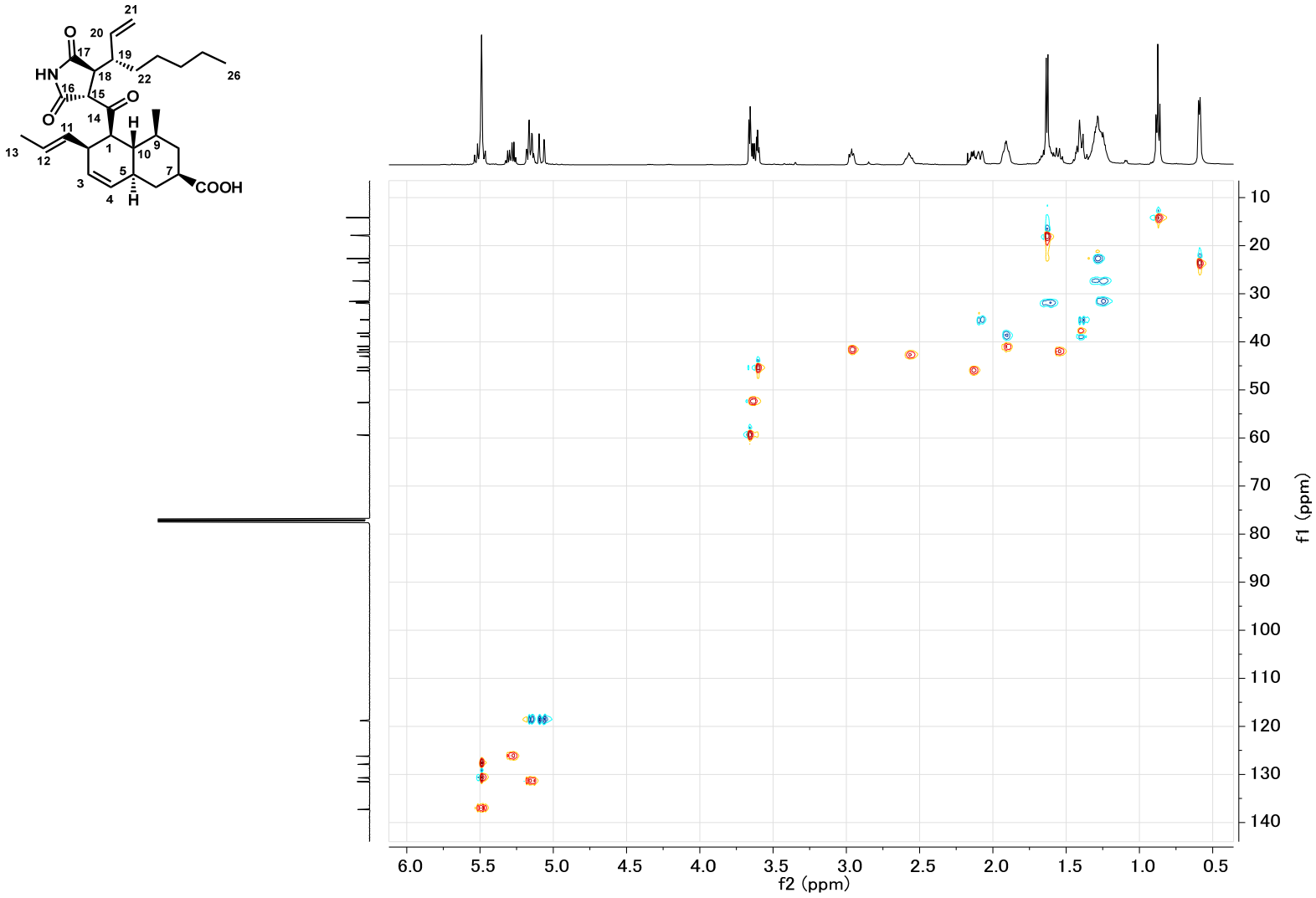

Figure S15. HMBC spectrum of **1** in $CDCl_3$ (500 MHz).

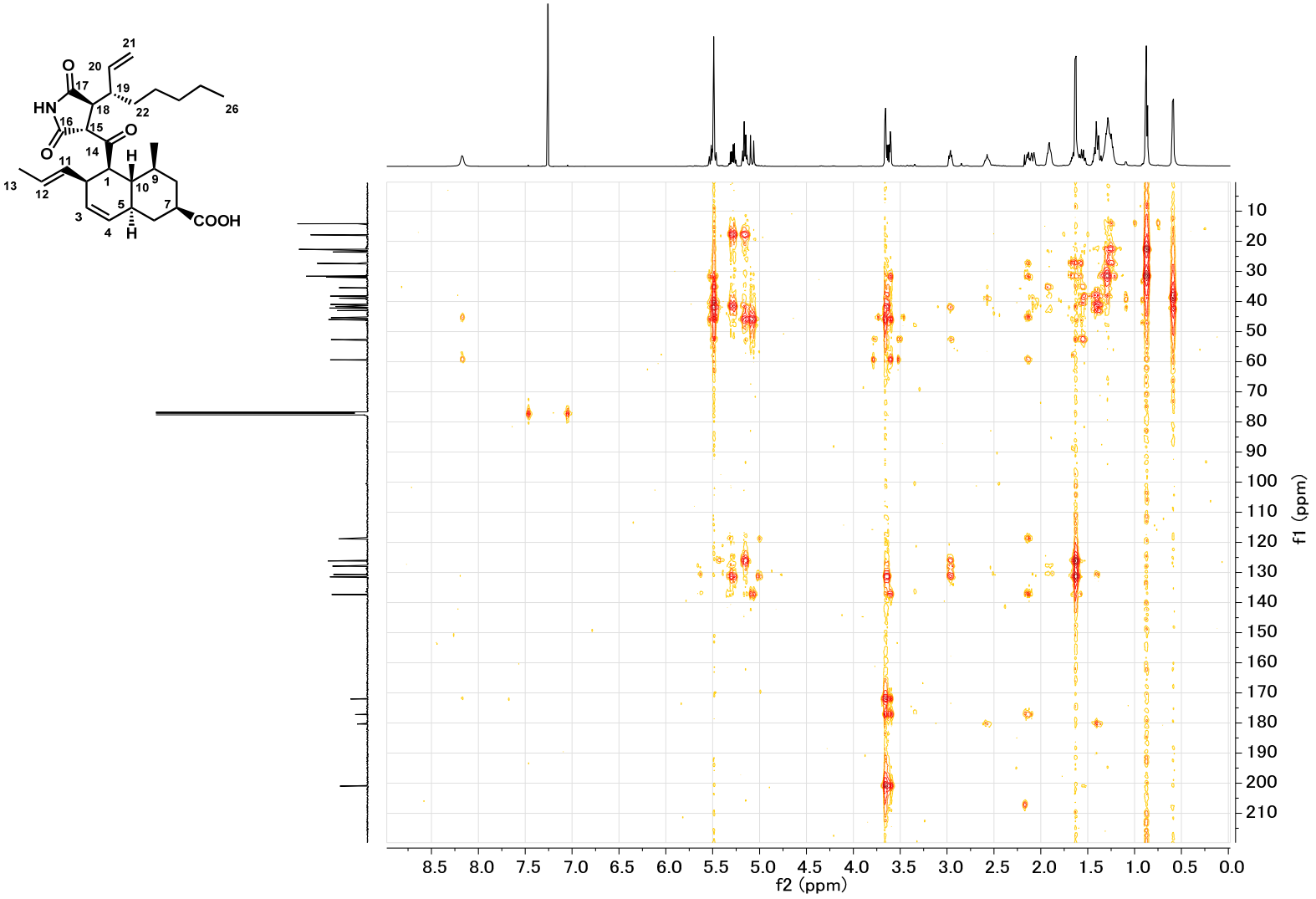

Figure S16. NOESY spectrum of **1** in $CDCl_3$ (500 MHz).

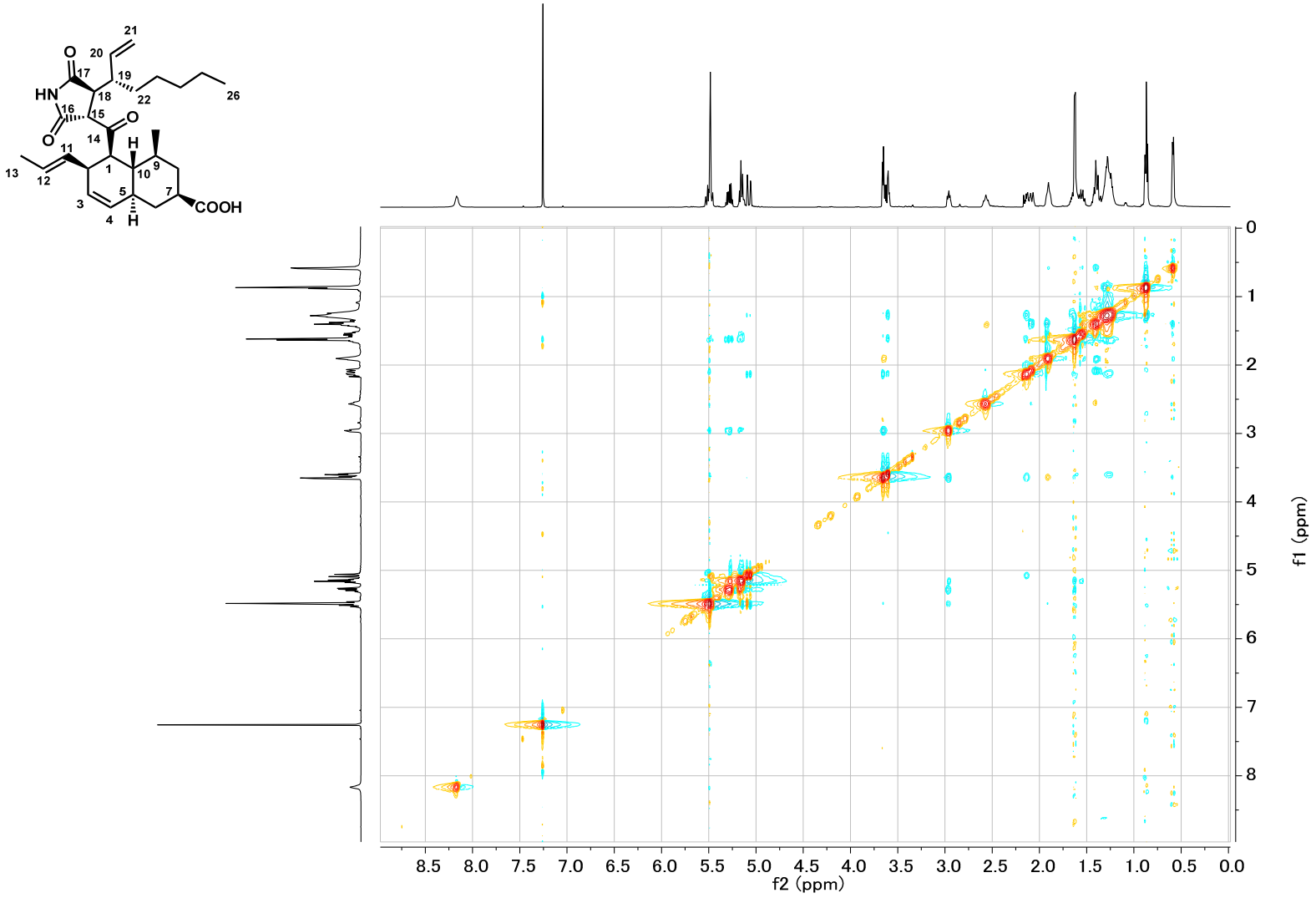

Figure S17. ^{13}C NMR spectrum (125 MHz) of **1** enriched with [1,2-^{13}C]acetate in CDCl3. (a) Full spectrum, (b) each ^{13}C-^{13}C couplings and structure of **1**. Bold lines in structure of **1** show enrichment from [1,2-^{13}C]acetate..

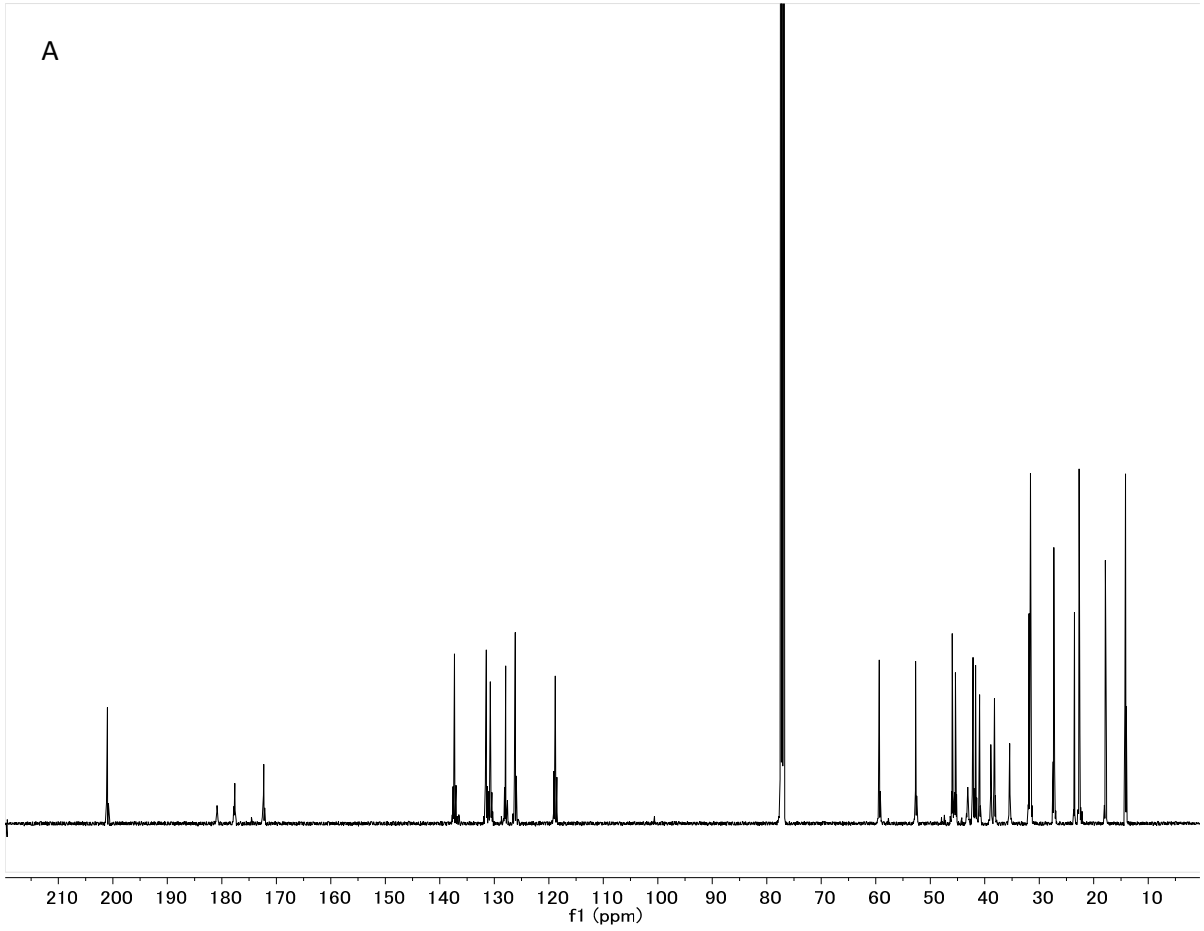

B

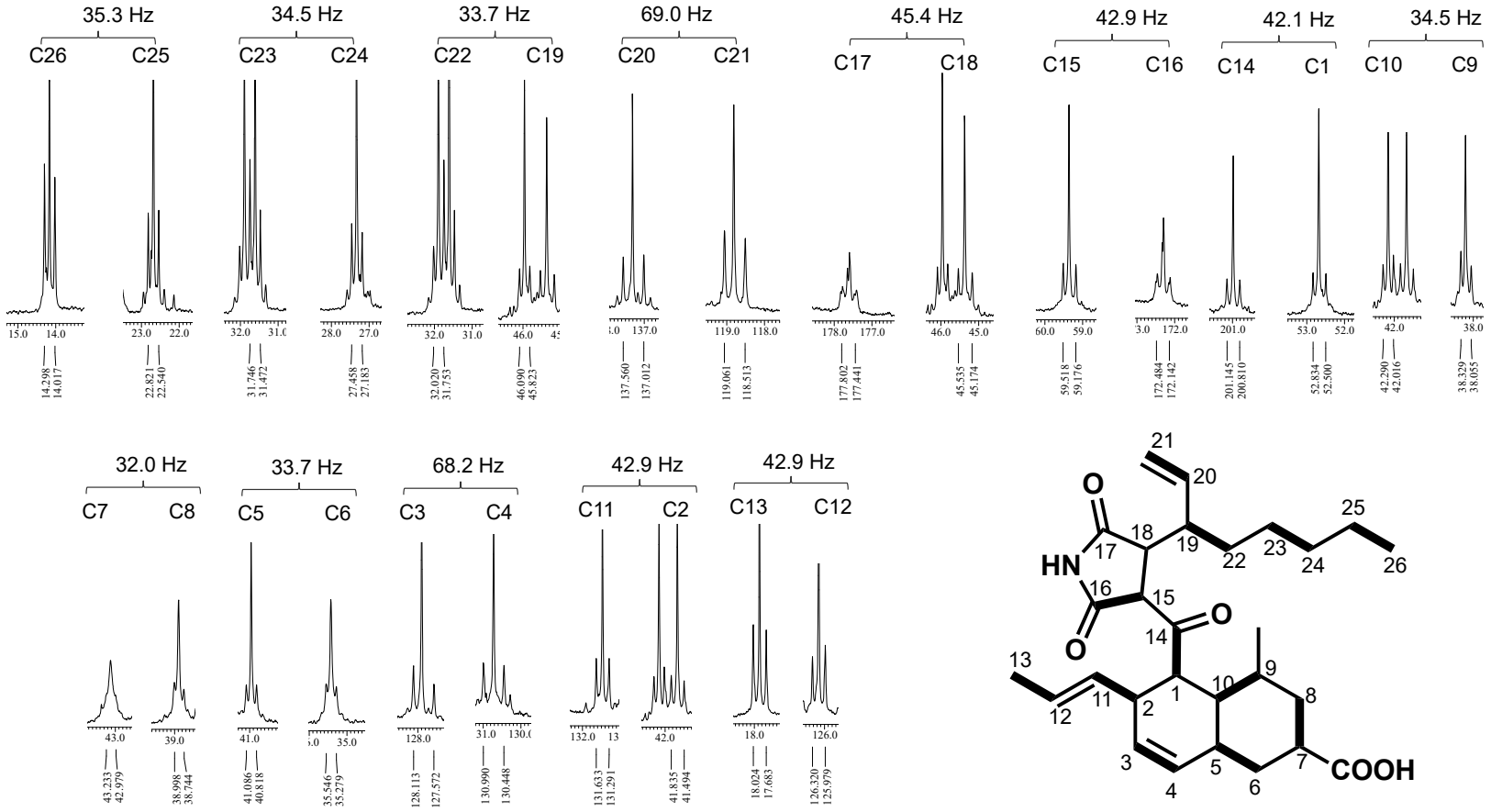
35.3 Hz
C26
C25
34.5 Hz
C23
C24
33.7 Hz
C22
C19
69.0 Hz
C20
C21
45.4 Hz
C17
C18
42.9 Hz
C15
C16
42.1 Hz
C14
C1
34.5 Hz
C10
C9
32.0 Hz
C7
C8
33.7 Hz
C5
C6
68.2 Hz
C3
C4
42.9 Hz
C11
C2
42.9 Hz
C13
C12
HN
O
COOH

2.8. Chemical characterization of **2**.

Table S5. NMR data of oxaleimide B (**2**) in $CDCl_3$. The molecular formula of **2** was established by mass data [ESI–MS: *m/z* 500 $(M-H)^-$; HRESIMS: *m/z* 500. 2659$(M–H)^-$, calcd. for $C_{28}H_{37}NO_7^-$, 500.2654, Δ = 0.51 mmu]; $[\alpha]_D^{31}$: –3.5 (*c* 1.2, MeOH).

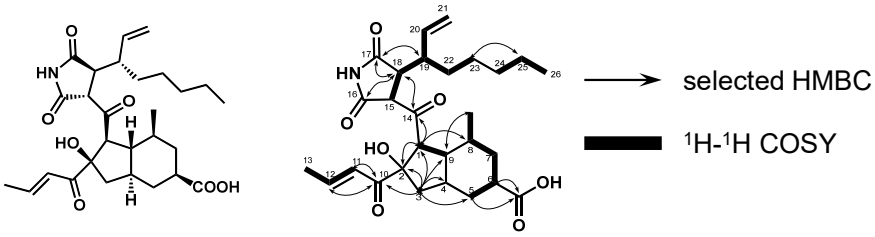

Position	δ_H [ppm]		mult. (*J* in Hz)	HMBC	δ_C [ppm]
1	3.72	1H	d (11.3)	2,8,9,14	69.5
2					87.3
3α	1.85	1H	m		46.0
β	1.76	1H	m	1,4,5,9,10	
4	1.97	1H	m	1,2,4,5,9	43.1
5	1.36	1H	m	6,7,9,6-CO	33.1
	2.23	1H	brd (12.5)	6,7,9	
6	2.55	1H	brt (11.9)	4,5,7,6-CO	43.0
7	1.31	1H	m		37.5
	2.00	1H	m	5,6,8,9	
8	1.50	1H	m		37.6
9	1.72	1H	m	1,8,14,8-Me	52.1
10					199.4
11	6.08	1H	d (15.1)	10,12,13	125.9
12	7.12	1H	dd (15.1, 7.1)	10,11,13	147.7
13	1.95	3H	d (6.9)	10,11,12	18.8
14					200.6
15	3.52	1H	d (4.0)	16,17,18	59.9
16					171.8
17					177.4
18	3.29	1H	dd (3.5, 3.5)	14,15,16,17,19,22	45.7
19	1.87	1H	m	15,18,22,23	45.9
20	5.38	1H	ddd (16.9, 10.0, 9.9)	19,21,22	136.4
21	5.19	1H	d (16.8)	19,20	119.8
	5.14	1H	d (10.0)	19,20	
22	1.65	1H	m	19,22,23	32.5
	1.52		m	19,20,22,23	
23	1.20	2H	m	25	27.4
24	1.22	2H	m	23	31.6
25	1.28	2H	m	24	22.7
26	0.89	3H	t (6.8)	24,25	14.2
6-COOH					180.6
8-Me	0.67	3H	d (6.5)	7,9	20.8
NH	8.39	1H	brs		

Figure S18. ^{1}H NMR spectrum of **2** in $CDCl_3$ (500 MHz).

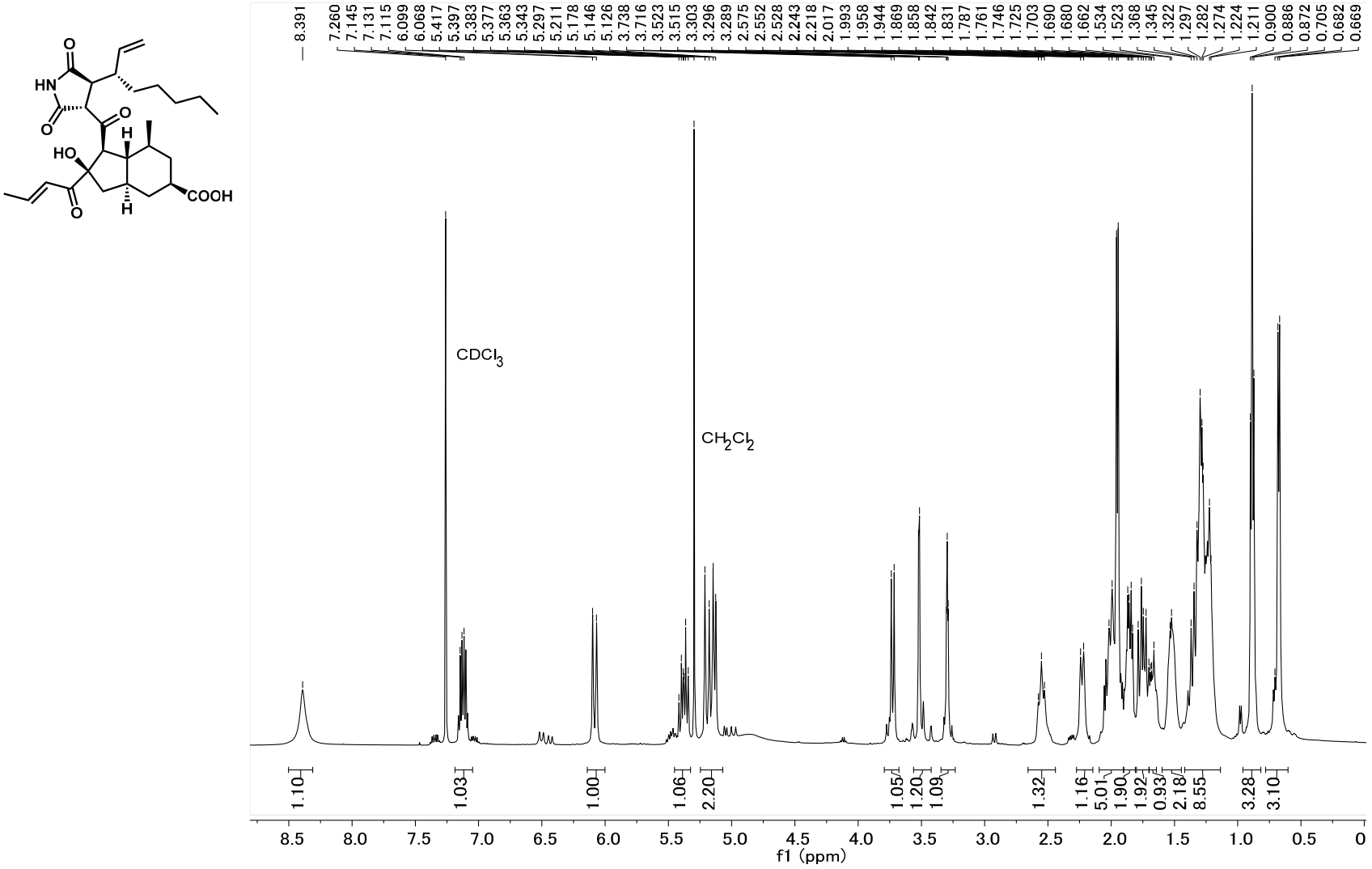

Figure S19. ^{13}CNMR spectrum of **2** in $CDCl_3$ (125 MHz).

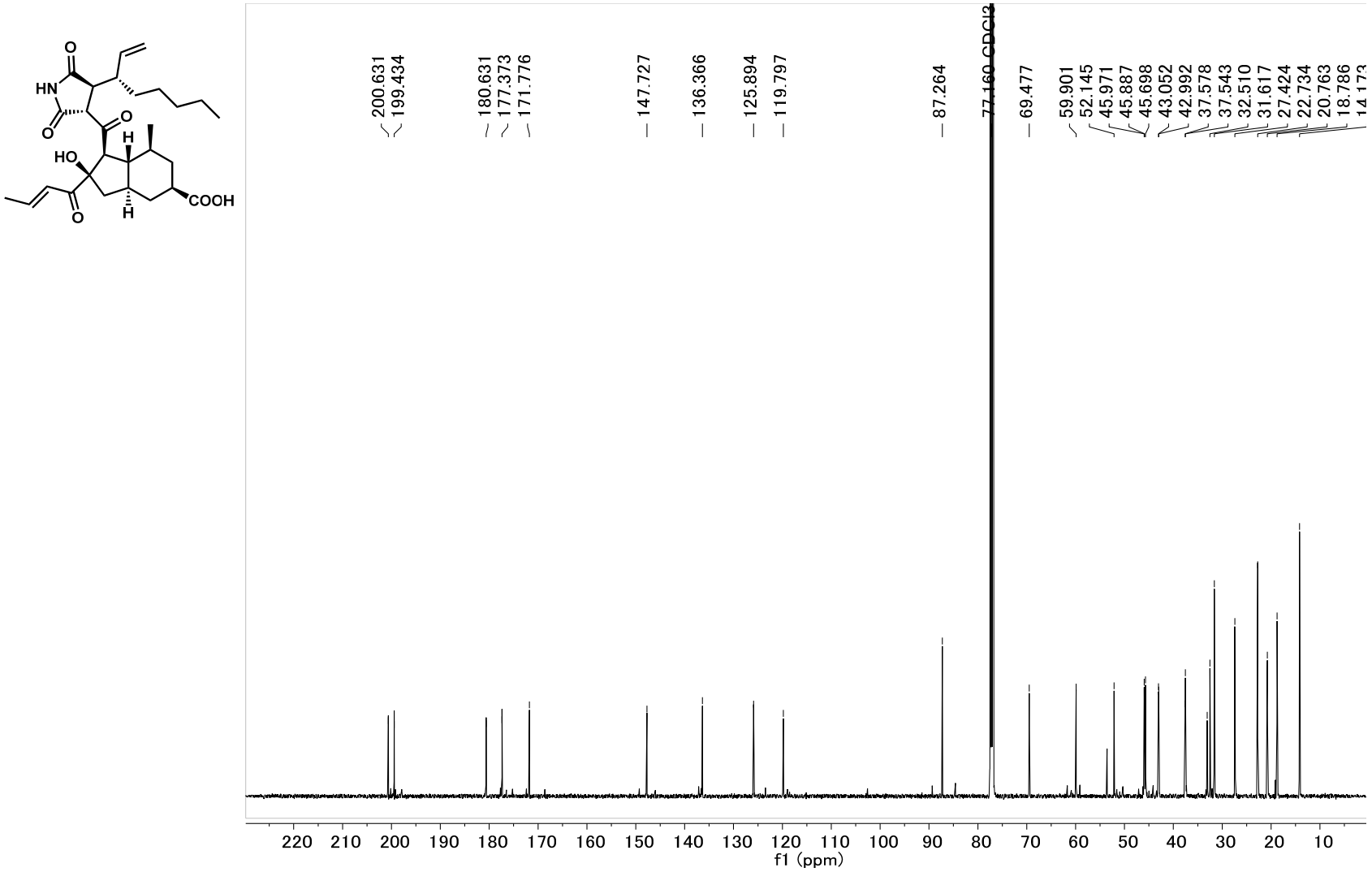

Figure S20. ^{1}H-^{1}H COSY spectrum of **2** in $CDCl_3$ (500 MHz).

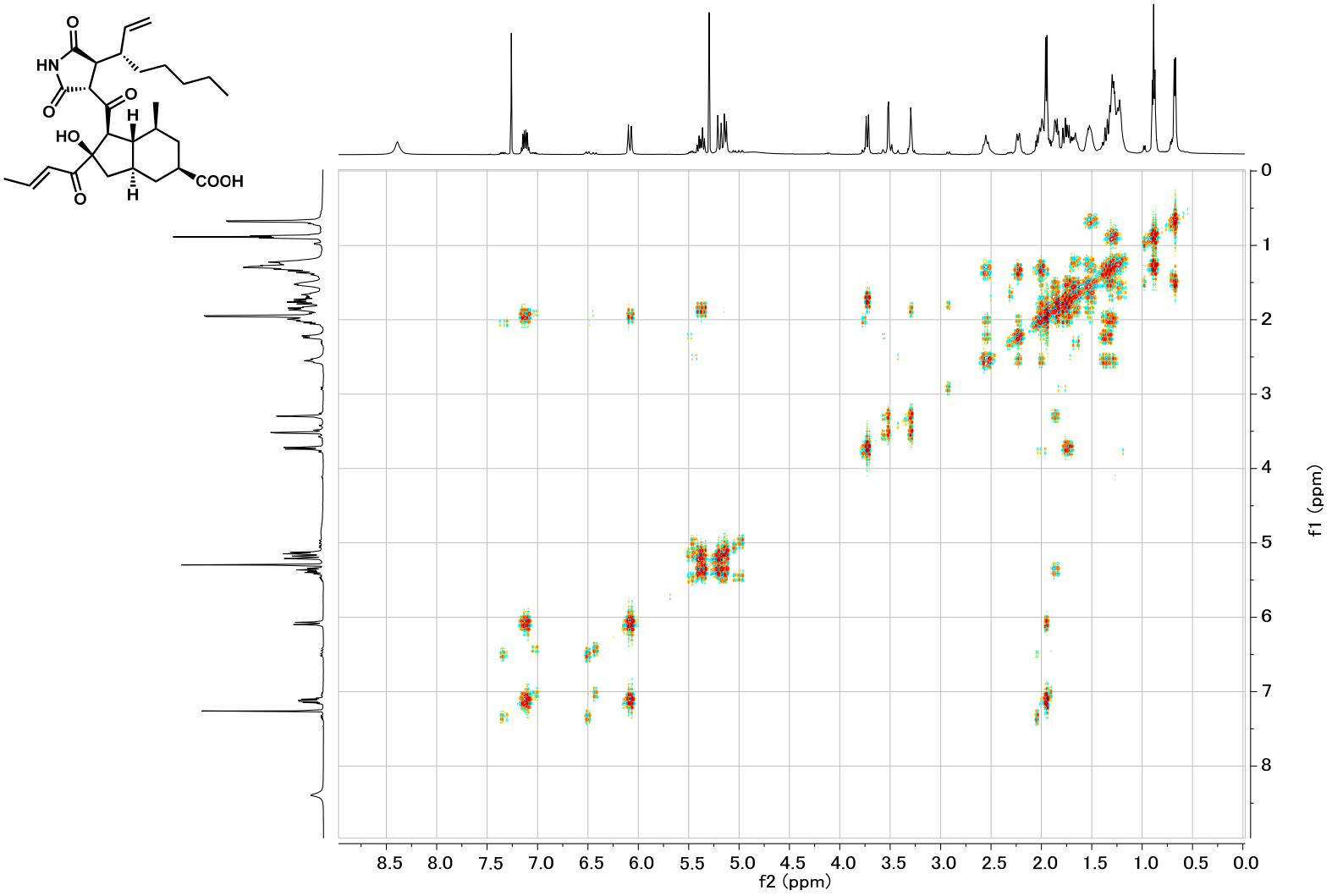

Figure S21. HSQC spectrum of **2** in $CDCl_3$ (500 MHz).

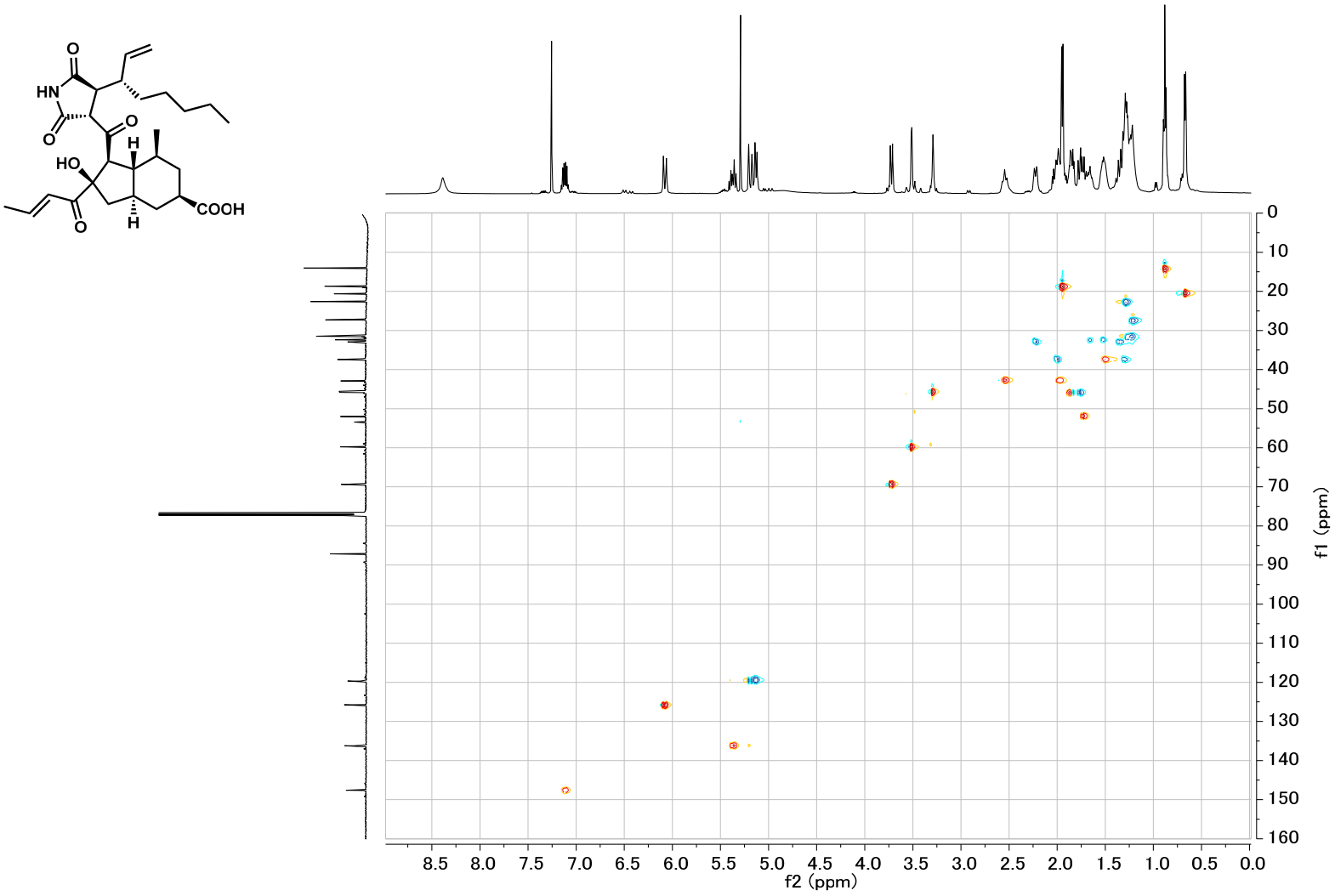

Figure S22. HMBC spectrum of **2** in $CDCl_3$ (500 MHz).

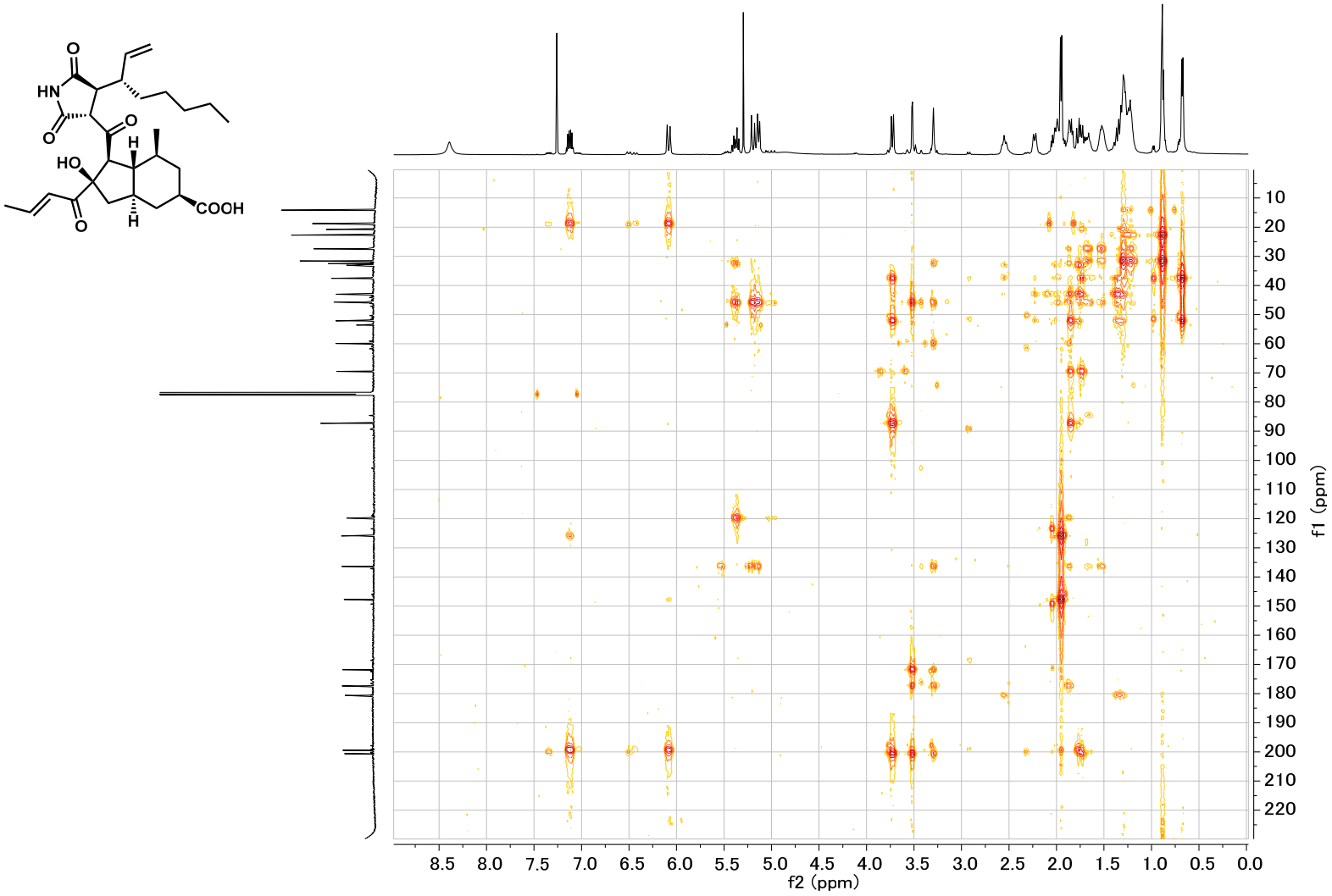

Figure S23. NOESY spectrum of **2** in $CDCl_3$ (500 MHz).

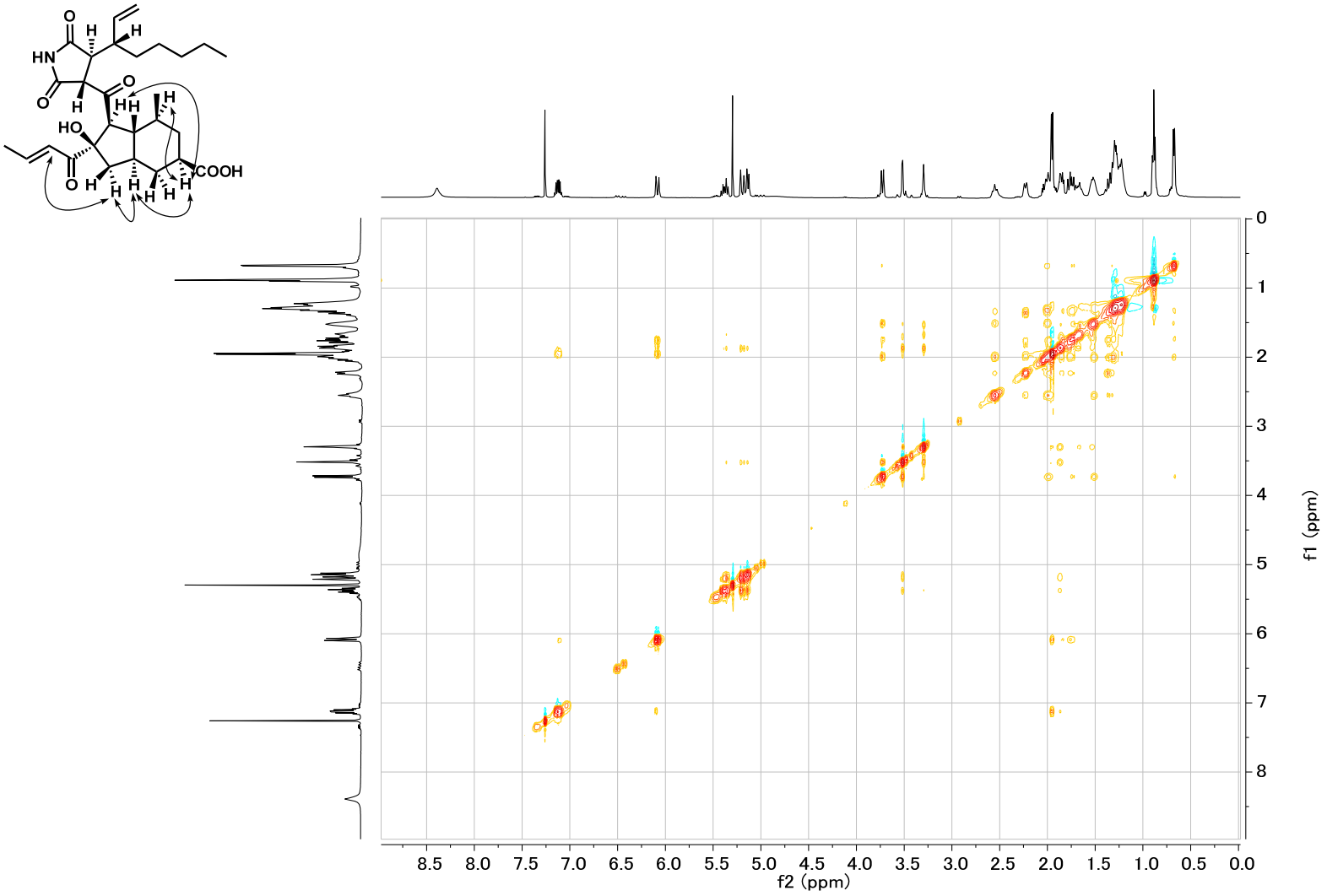

2.9. Chemical characterization of **3** and **3′** .

Table S6. NMR data of oxaleimide C and C′ (**3** and **3′**) in $CDCl_3$. The molecular formula of **3** was established by mass data [ESI–MS: *m/z* 498 $(M–H)^–$; HRESIMS: *m/z* 498.2499$(M–H)^–$, calcd. for $C_{28}H_{37}NO_7^–$,498.2497, Δ = 0.19 mmu]; $[\alpha]_D^{30}$: 57.6 (*c* 1.4, MeOH).

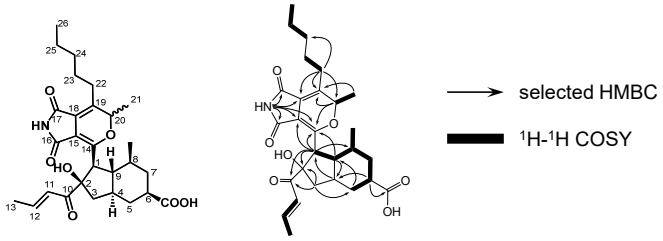

	3			**3′**			
Position	δ_H [ppm]	mult. (Hz)	δ_C [ppm]	δ_H [ppm]	mult. (Hz)	δ_C [ppm]	HMBC
1	3.28	d (11.2)	60.0	3.62	d (11.0)	59.9	2,4,8,9,10,14,15
2			89.9			90.9	
3	1.91	m	45.2	1.89	m	44.4	2,4,5,9,10
4	1.89	m	43.1	1.89	m	43.1	1,9
5	1.35	m	33.1	1.35	m	33.0	
	2.22	m		2.22	m		6,7,9
6	2.53	m	43.0	2.53	m	43.0	5,7,6-CO
7	1.25	m	37.6	1.25	m	37.6	
	1.99			1.99	m		6
8	1.40	m	37.7	1.49	m	37.6	
9	1.72	m	51.2	1.66	m	201.2	1,4,5,8,14
10			202.0				
11	6.82	m	126.3	6.69	dd (15.2, 2.2)	126.2	10,12,13
12	6.84	m	144.5	6.85	m	144.1	10,11,13
13	1.86	m	18.7	1.86	m	18.6	10,11,12
14			162.5			162.5	
15			101.5			101.8	
16			168.0			167.9	
17			165.3			165.0	
18			118.5			118.3	
19			139.7			139.5	
20	5.06	m	78.0	5.06	m	77.9	14,18,19,21,22
21	1.39	d (6.7)	20.0	1.48	d (6.7)	19.7	19,20
22	2.12	m	27.6	2.12	m	27.6	18,19,20,23,24
	3.03	m		3.03	m		
23	1.39	m	27.9	1.39	m	27.8	
	1.49	m		1.49	m		
24	1.28	m	31.6	1.28	m	31.5	
25	1.30	m	22.5	1.30	m	22.5	
26	0.89		14.1	0.86		14.1	24,25
6-COOH			180.5			180.5	
8-Me	0.80	d (6.5)	20.5	0.89	m	20.7	8,9
NH	8.26	brs		8.23	brs		14-19

Figure S24. ^{1}H NMR spectrum of **3** and **3′** in $CDCl_3$ (500 MHz).

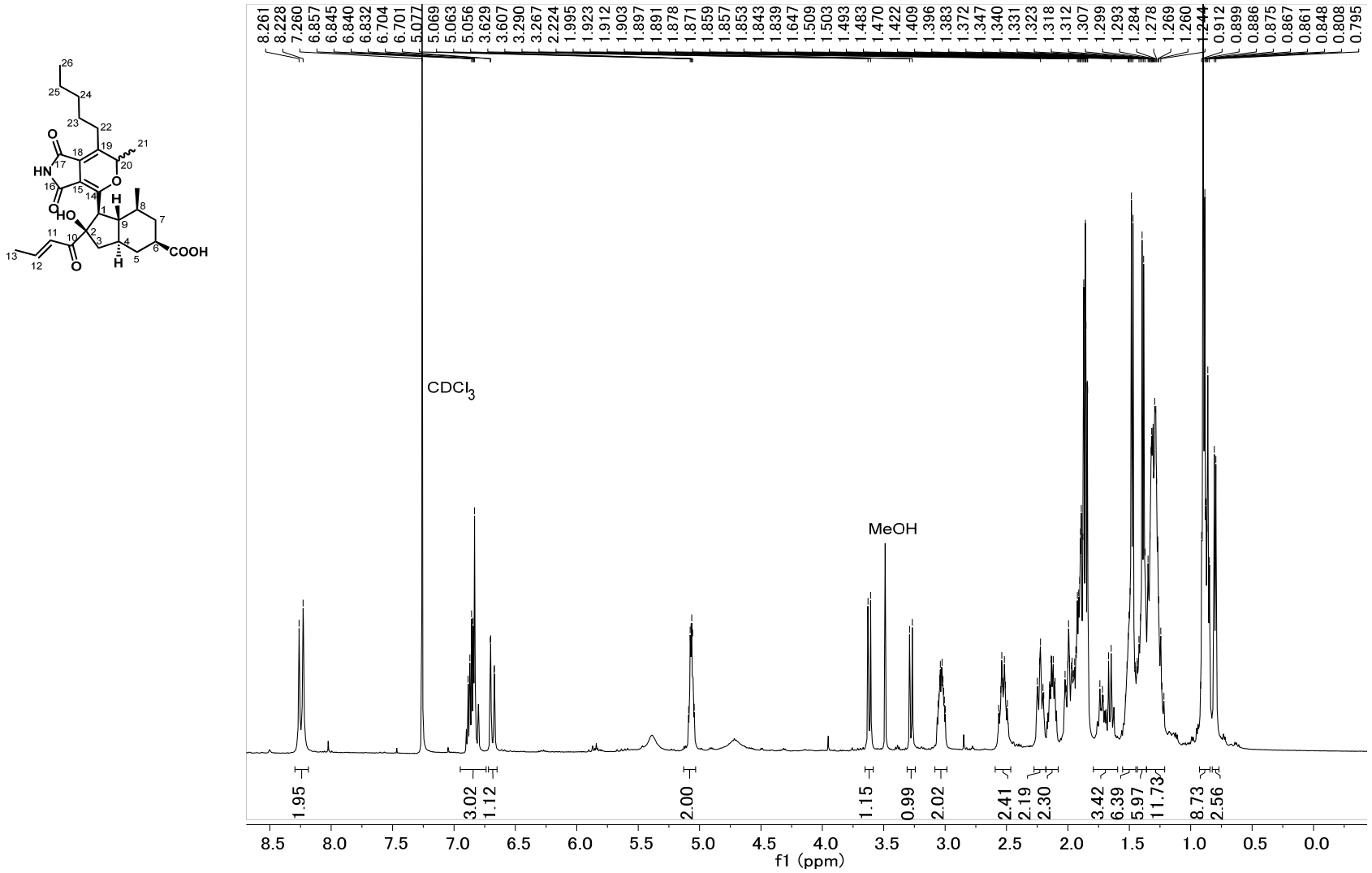

Figure S25. ^{13}CNMR spectrum of **3** and **3′** in $CDCl_3$ (125 MHz)

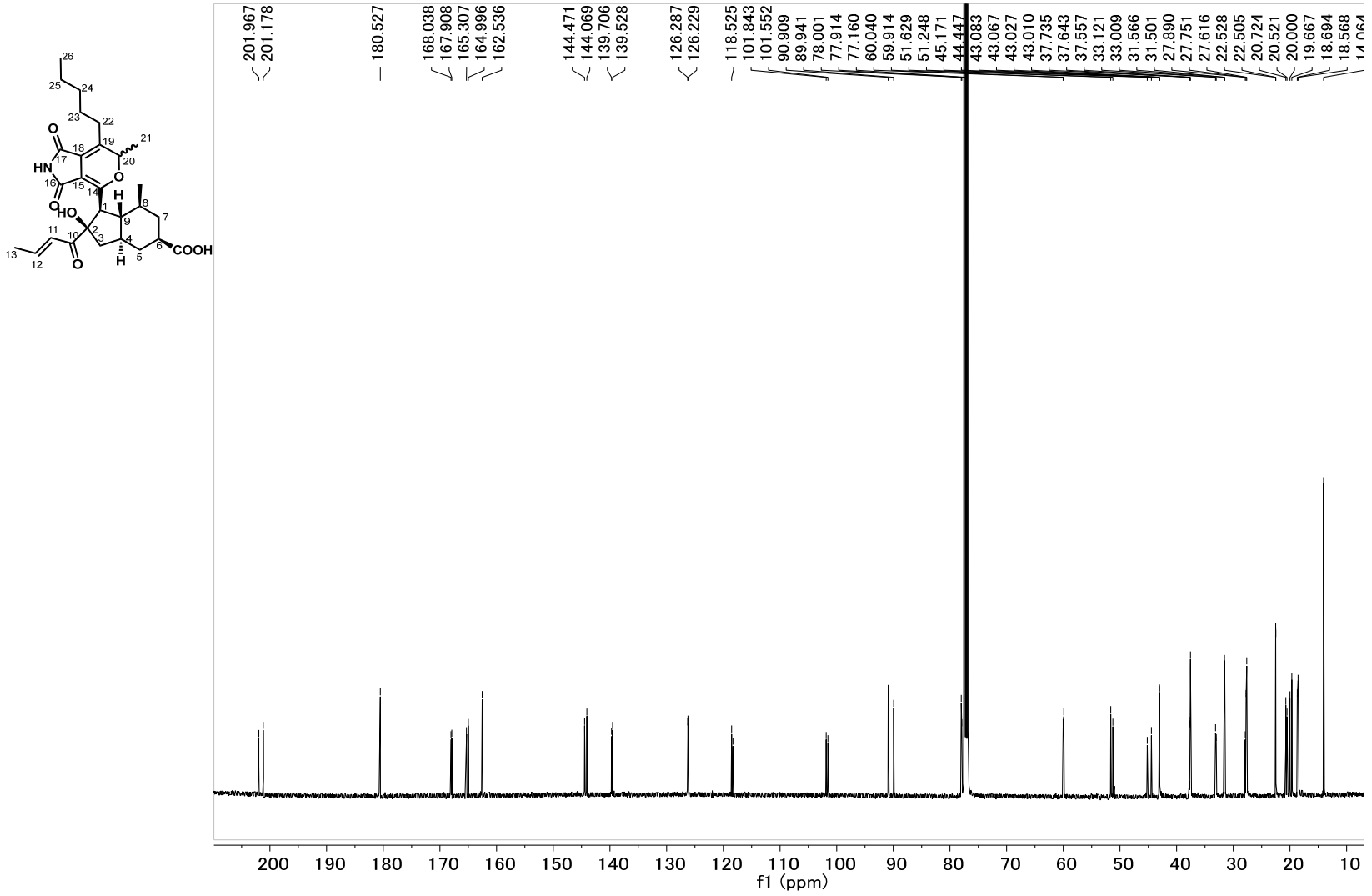

Figure S26. ^{1}H-^{1}H COSY spectrum of **3** and **3′** in $CDCl_3$ (500 MHz).

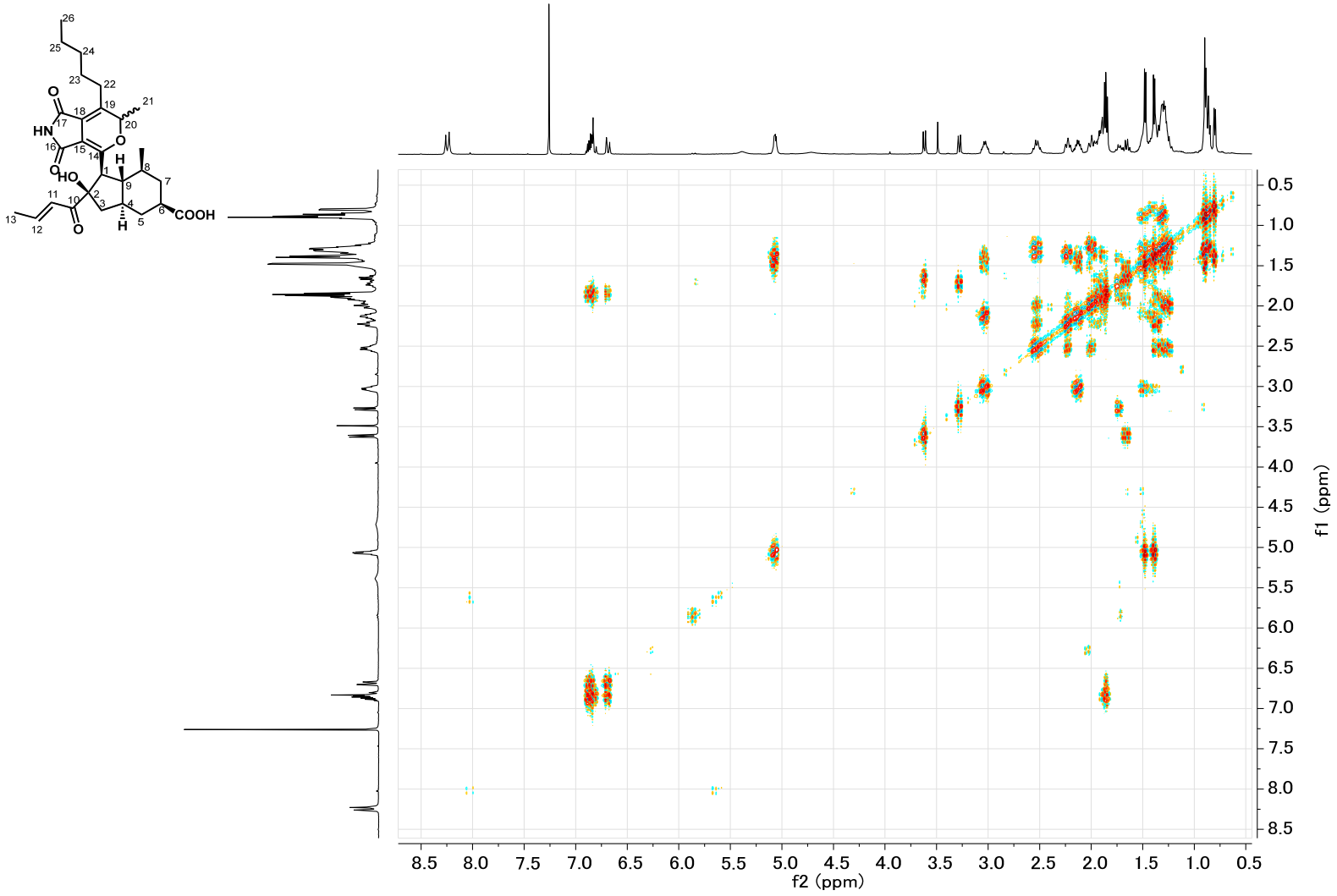

Figure S27. HSQC spectrum of **3** and **3′** in $CDCl_3$ (500 MHz).

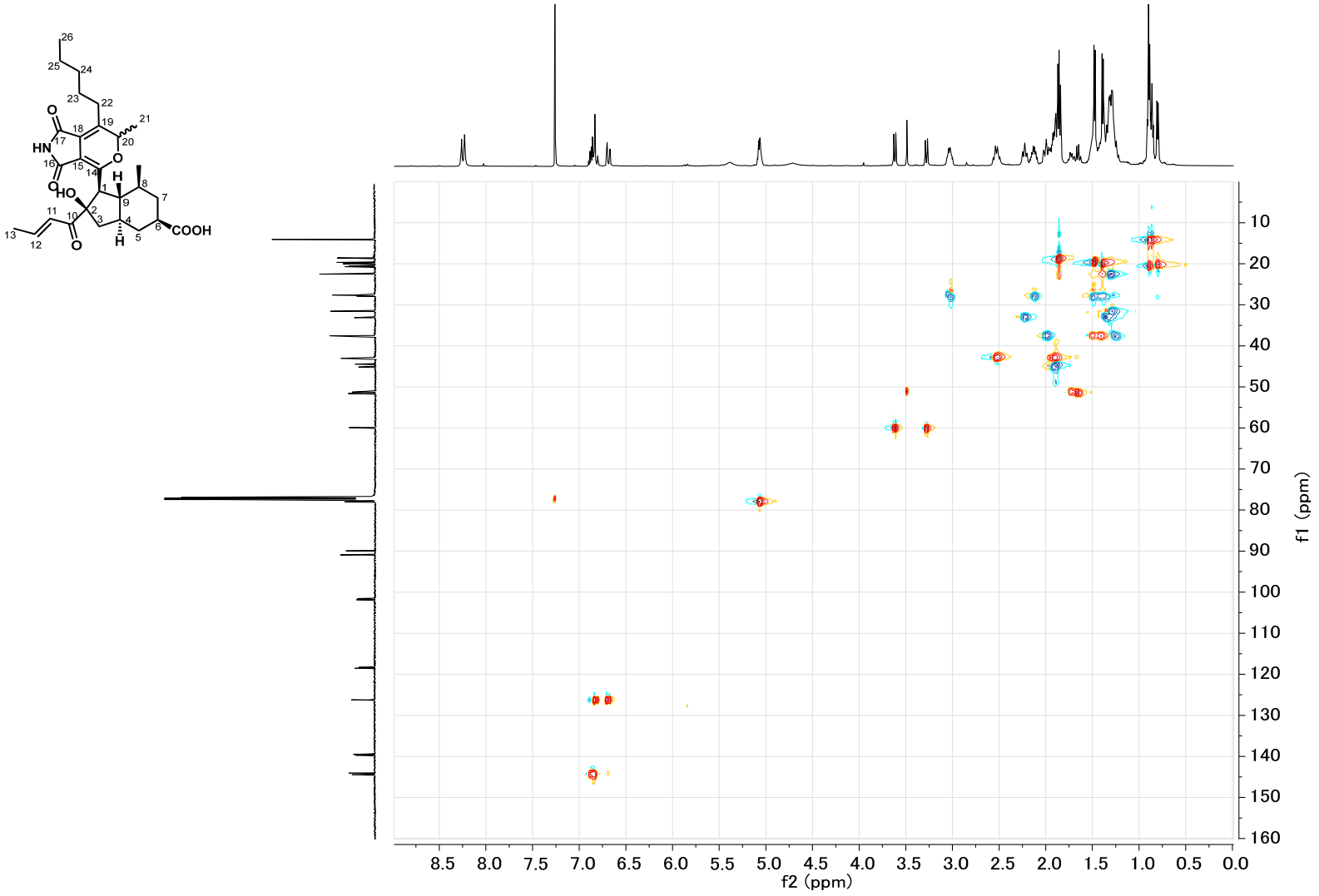

Figure S28. HMBC spectrum of **3** and **3′** in $CDCl_3$ (500 MHz).

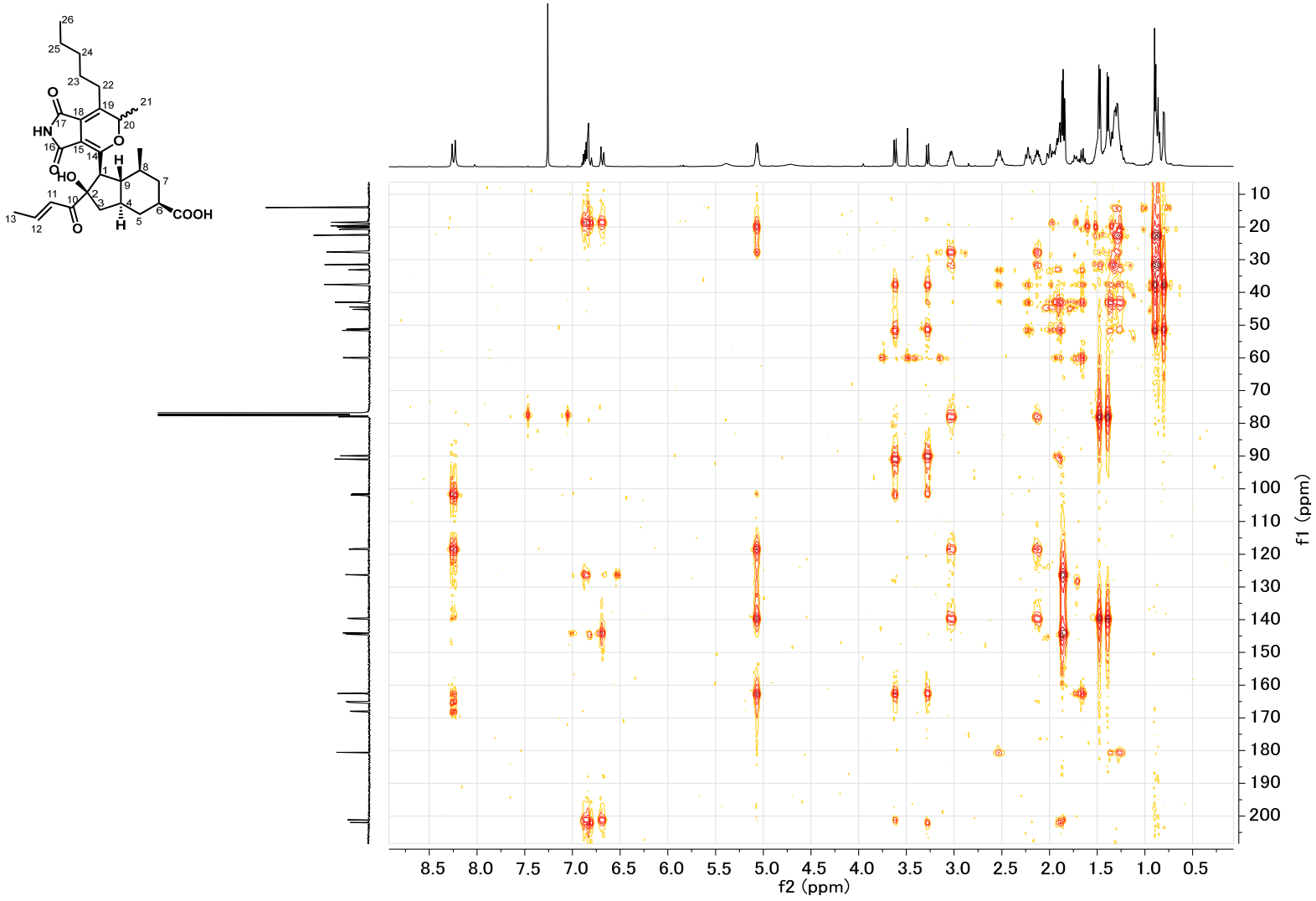

2.10. Chemical characterization of **4**

Table S7. NMR data of oxaleimide D (**4**) in DMSO-*d*$_6$. The molecular formula of **4** was established by mass data [ESI–MS: *m/z* 484 $(M–H)^-$; HRESIMS: *m/z* 484.2704 $(M–H)^-$, calcd. for $C_{28}H_{38}NO_6^-$, 484.2705, Δ = 0.06 mmu]; $[\alpha]_D^{31}$: –132.1 (*c* 0.28, MeOH).

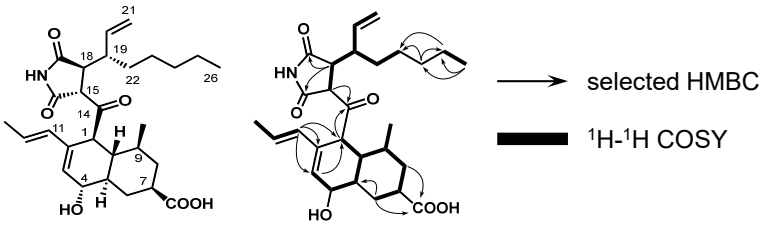

Position	δ_H [ppm]		mult. (*J* in Hz)	HMBC	δ_C [ppm]
1	3.63	1H	brd (5.9)	2,3,9,10,11,15	55.8
2					
3	5.95	1H	s	1,5,11,14	129.8
4	3.74	1H	m	3	137.8
5	1.00	1H			69.4
6	1.02	1H	m		31.9
	2.43	1H	m		
7	2.24	1H	m		41.3
8	1.09	1H	m	9,10,9-Me,7-CO	38.5
	1.86	1H	brd (12.6)		
9	1.42	1H	m		37.6
10	1.30	1H	m	1,4,5,14	41.5
11	6.02	1H	d (16.2)	1,2,3,13	132.1
12	5.71	1H	dq (15.9, 6.7)	11,13	124.7
13	1.67	3H	d (6.6)	11,12	18.1
14					204.4
15	3.75	1H	d (3.4)	14,16,17,18,19	55.3
16					173.0
17					178.0
18	2.84	1H	dd (3.5, 3.5)	15-17,19,20,22	49.4
19	2.29	1H	m	15,17,18,20,22,23	45.2
20	5.44	1H	ddd (16.9, 9.8, 9.8)	18,19,22	137.2
21	5.11	1H	m	19,20	118.6
	5.13	1H	m		
22	1.45	2H	m	23,24	30.6
23	1.20	2H	m	25	26.4
24	1.21	2H	m	23,25	30.9
25	1.24	2H	m	23,24	22.0
26	0.84	3H	m	24,25	13.8
7-COOH				8,9,10	176.3
9-Me	0.79	3H			20.2

Figure S29. ^{1}H NMR spectrum of **4** in DMSO-*d*$_6$ (500 MHz).

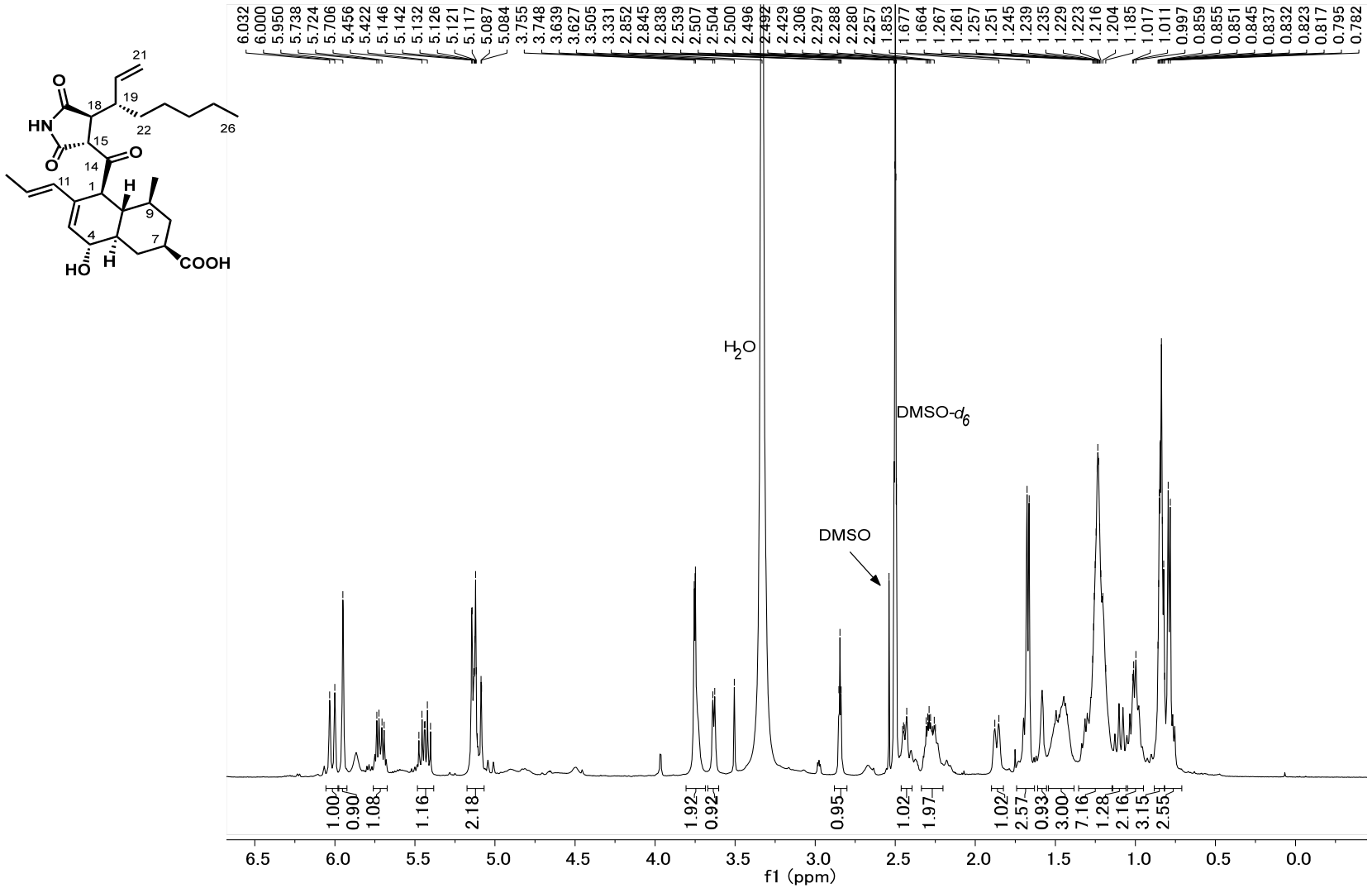

Figure S30. ^{13}CNMR spectrum of **4** in DMSO-*d*$_6$ (125 MHz)

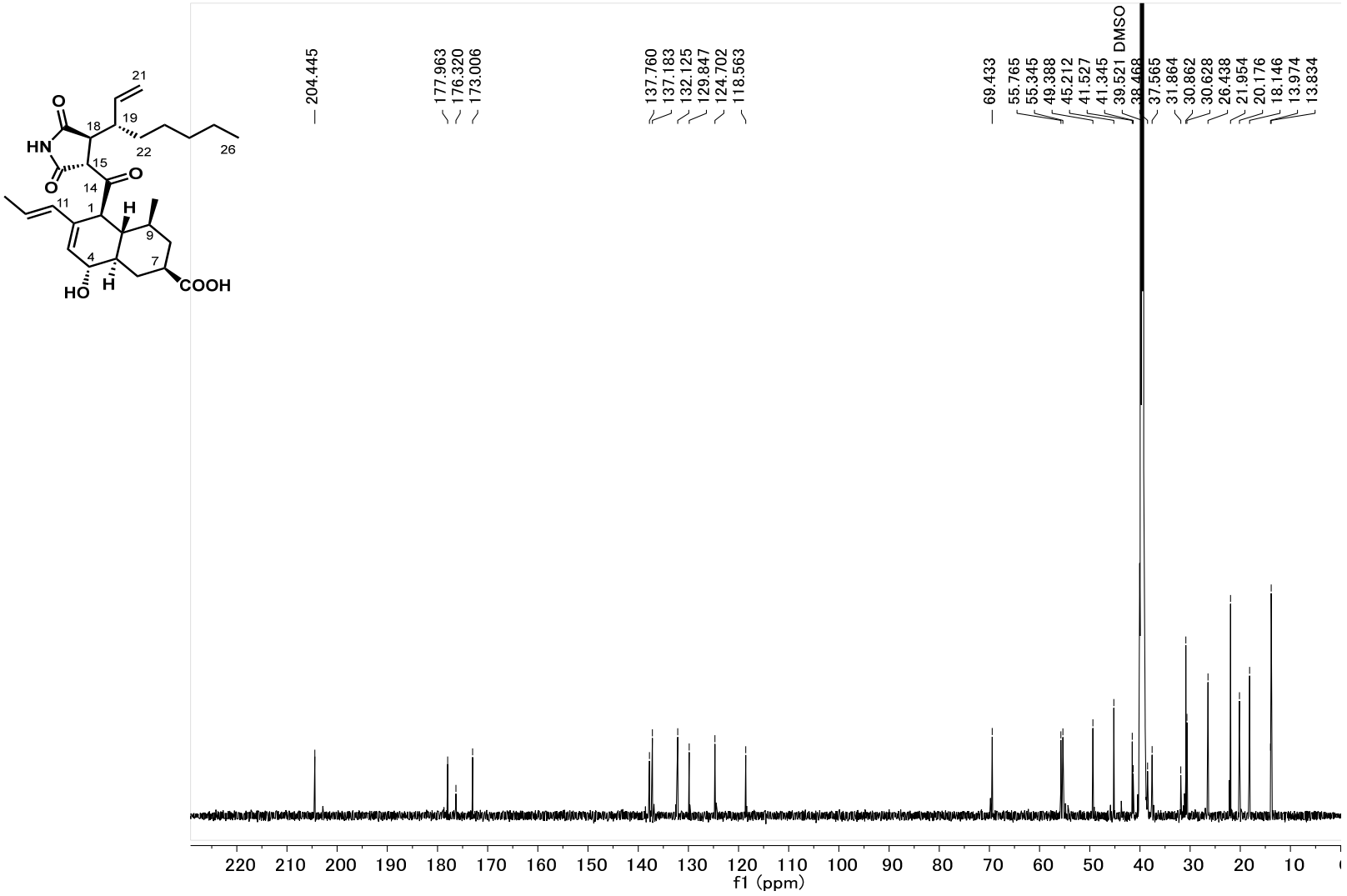

Figure S31. ^{1}H-^{1}H COSY spectrum of **4** in DMSO-*d*$_6$ (500 MHz).

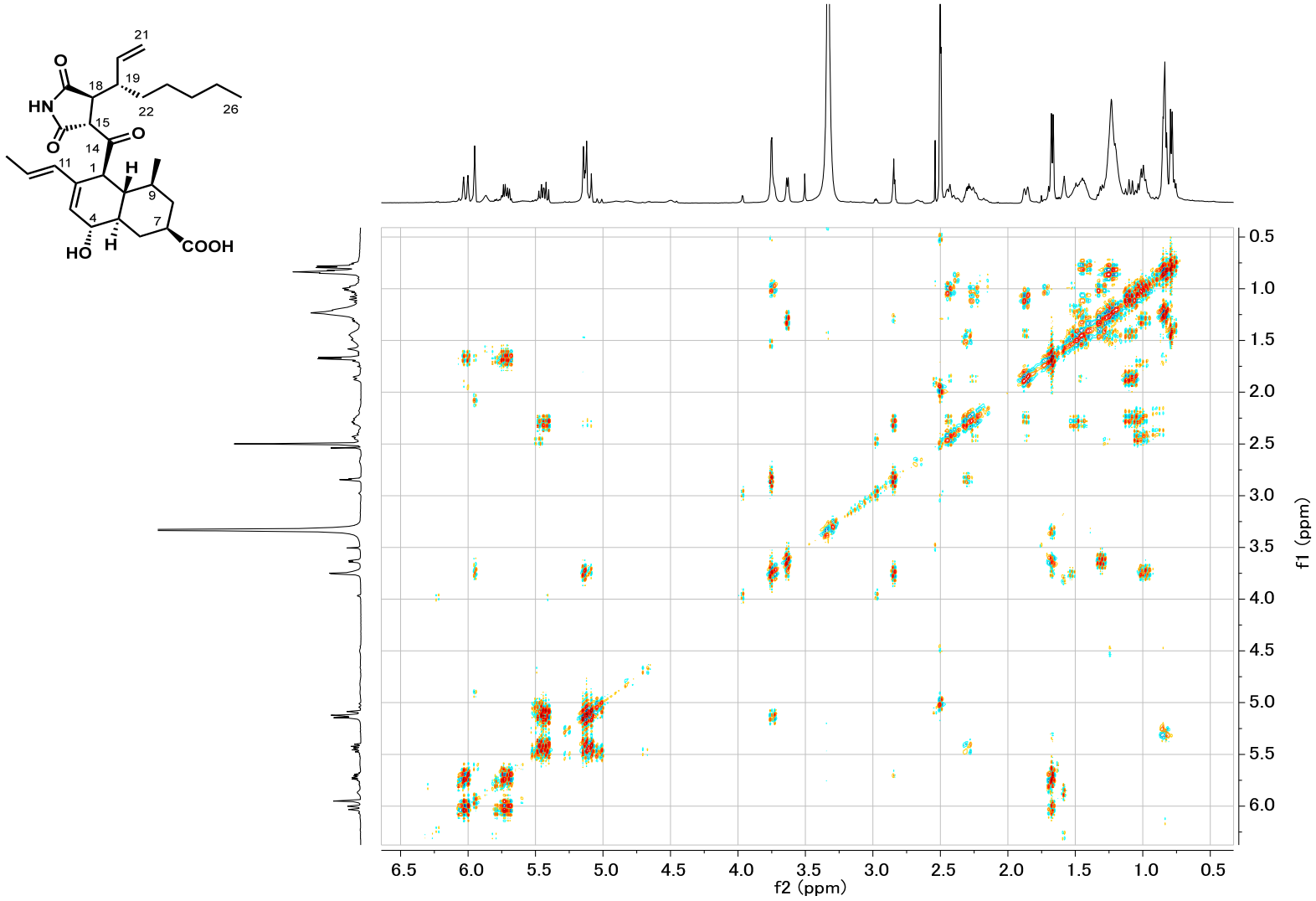

Figure S32. HSQC spectrum of **4** in DMSO-*d*$_6$ (500 MHz).

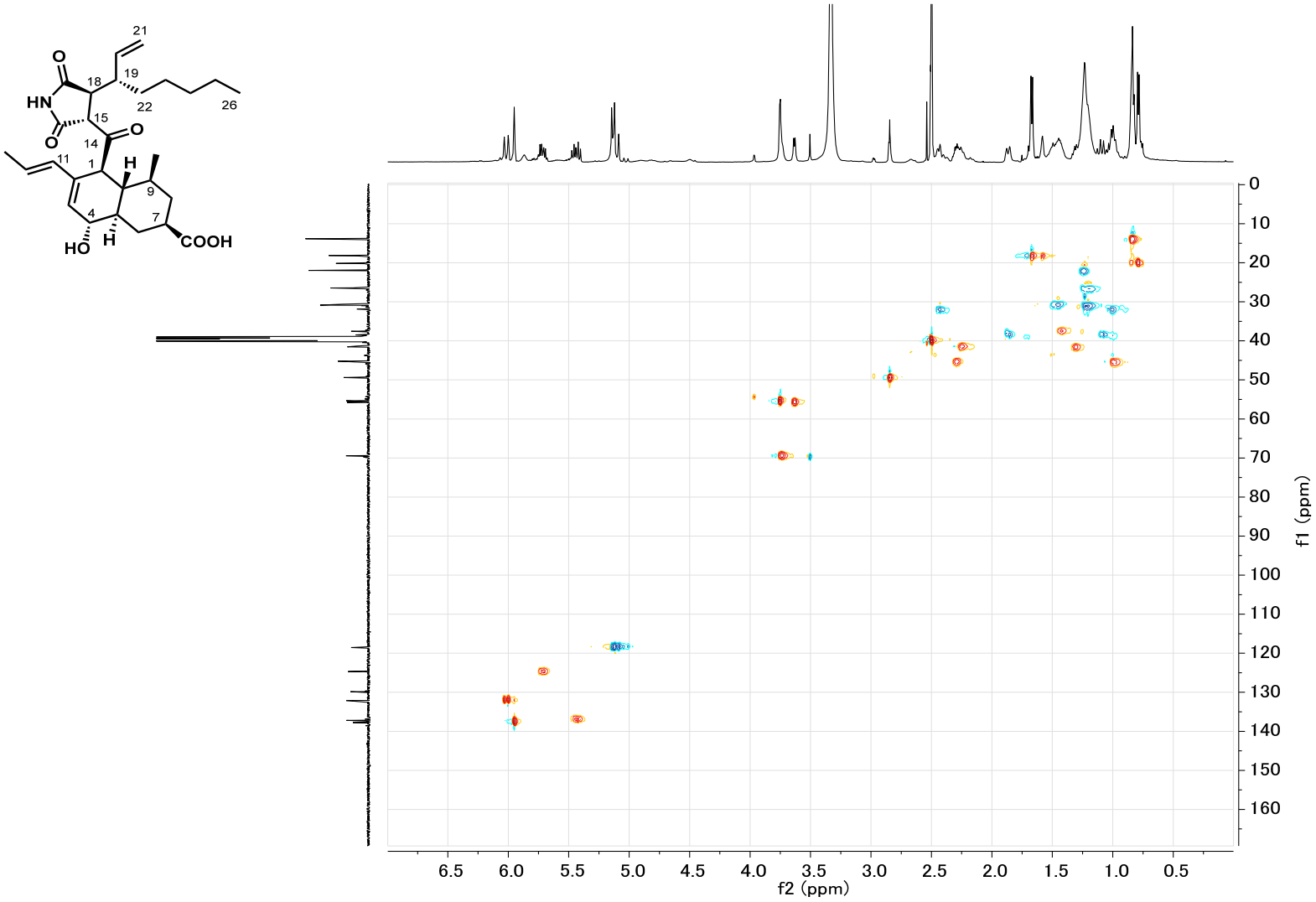

Figure S33. HMBC spectrum of **4** in DMSO-*d*$_6$ (500 MHz).

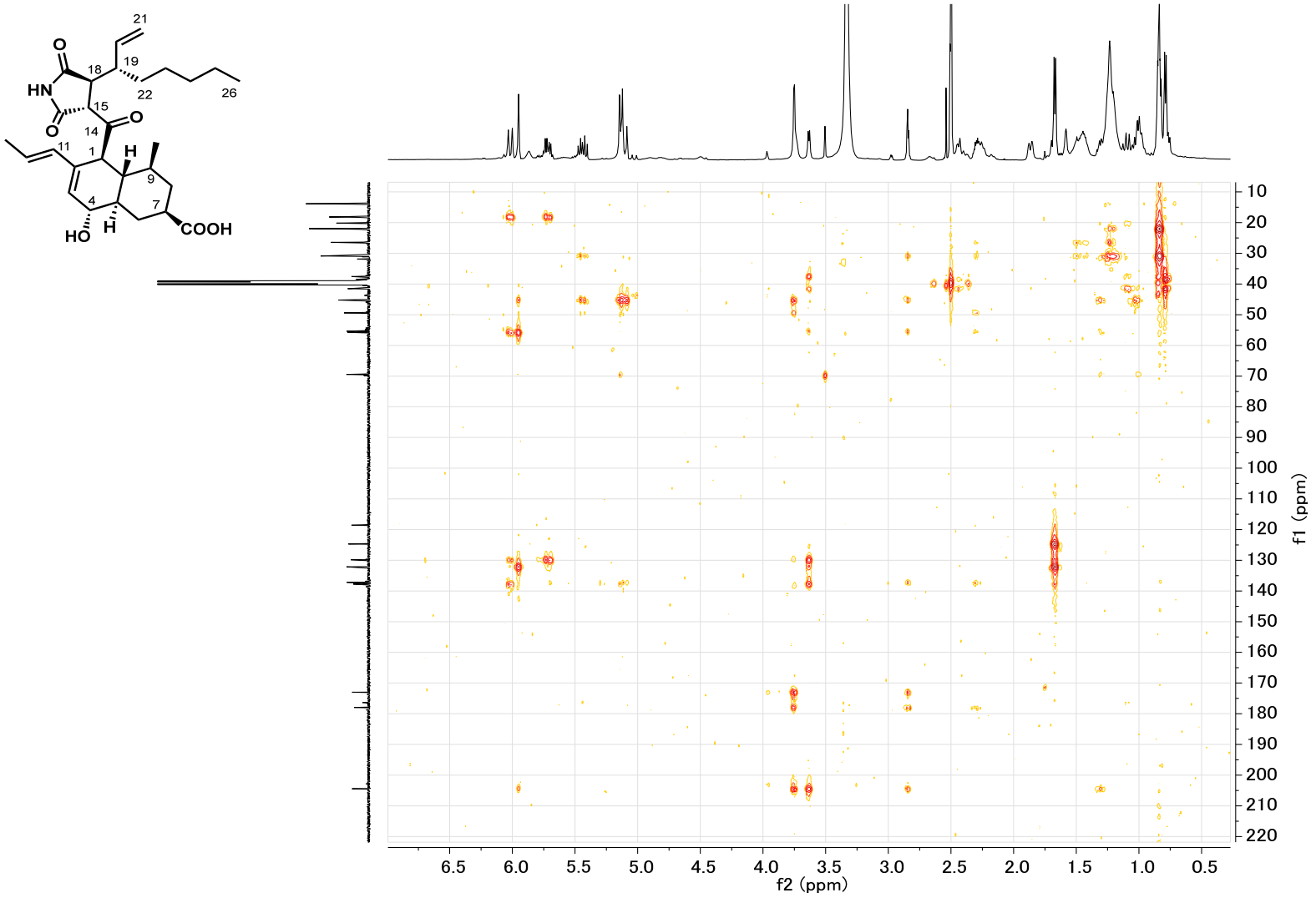

Figure S34. NOESY spectrum of **4** in DMSO-*d*$_6$ (500 MHz).

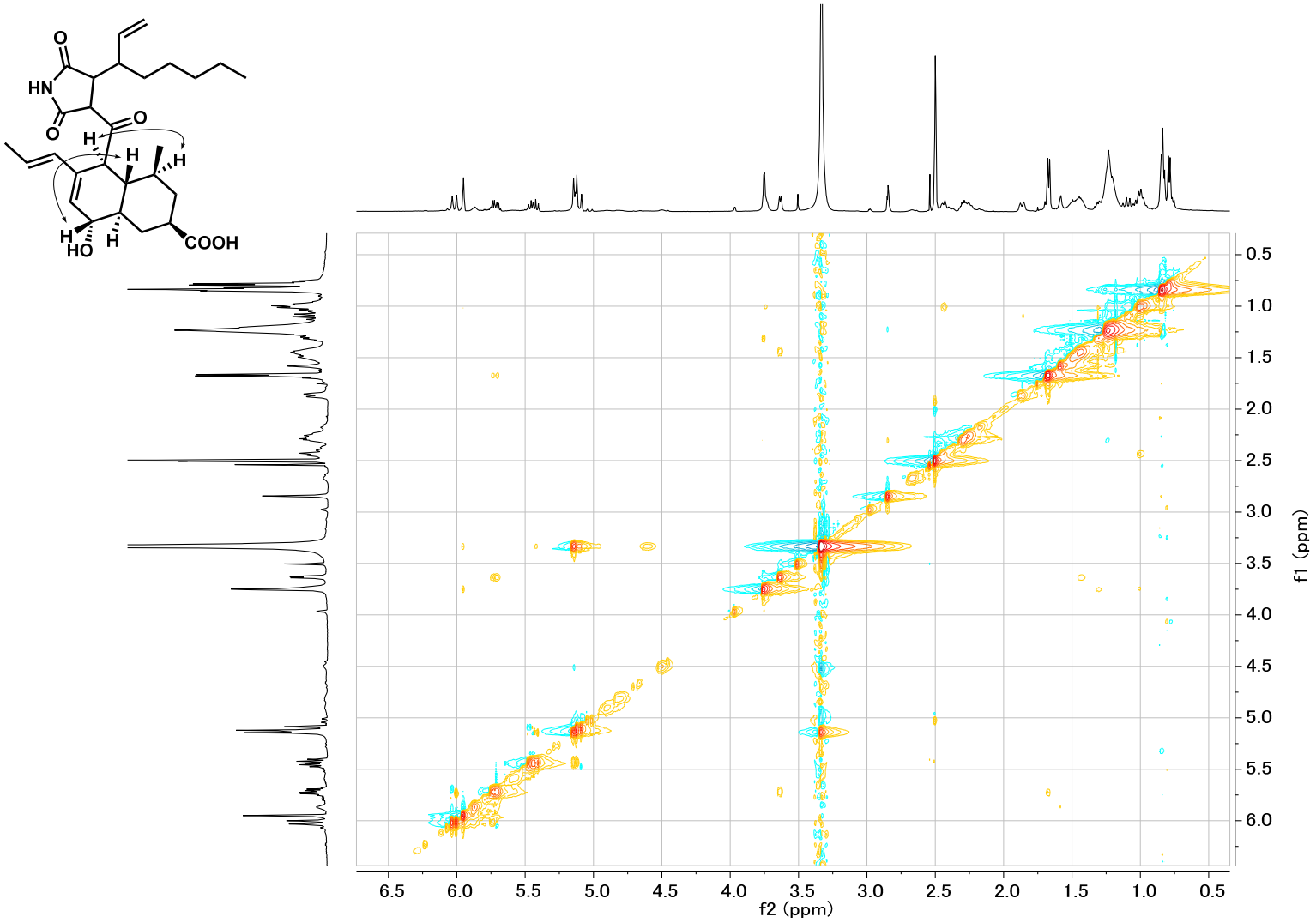

2.11. Chemical characterization of **5**

Table S8. NMR data of oxaleimide E (**5**) in $CDCl_3$. The molecular formula of **4** was established by mass data [ESI–MS: *m/z* 484 $(M–H)^–$; HRESIMS: *m/z* 484.2724 $(M–H)^–$, calcd. for $C_{28}H_{38}NO_6^–$, 484.2705, Δ = 0.19 mmu]; $[\alpha]_D^{31}$: –32.1 (*c* 0.15, MeOH).

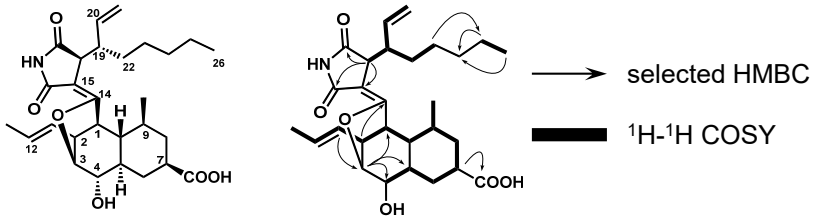

Position	δ_H [ppm]		mult. (*J* in Hz)	HMBC	δ_C [ppm]
1	3.78	1H	brs	2,3,5,9,10,11	42.4
2	3.07	1H	brd (6.3)	1,10,11,14	40.5
3	4.37	1H	s	1,4,5,11,14	88.9
4	3.37	1H	m		73.9
5	1.33	1H			43.3
6	1.13	1H			32.1
	2.27	1H	m		
7	2.46	1H	m	7-CO	42.7
8	1.18	1H	m		38.5
	2.06	1H	m		
9	1.47	1H	m	9-Me	36.7
10	0.85	1H	m		49.2
11	5.30	1H	ddd (15.4,6.6,1.5)	1,2,3,13	128.3
12	5.61	1H	dq (15.3, 6.6)	2,13	128.1
13	1.64	3H	d (6.4)	2,12,13	18.2
14					171.9
15					99.1
16					170.9
17					177.4
18	3.40	1H	m	15-17,19,20,22	49.0
19	2.68	1H	m	15,17,18,20-23	44.7
20	5.48	1H	ddd (16.9, 9.8, 9.8)	18,20,22	137.3
21	4.93	1H	dd (16.8, 1.7)	19,20	118.1
	5.03	1H	dd (10.1, 1.7)	19,20	
22	1.64	1H	m		32.3
	1.77	1H	m		
23	1.22	1H	m		27.7
	1.29	1H	m		
24	1.29	2H	m		32.1
25	1.29	2H	m		22.8
26	0.88	3H	t (6.7)	24,25	14.3
7-COOH					179.9
9-Me	1.13	3H	d (6.4)	8,9,10	20.5
NH		1H			

Figure S35. ^{1}H NMR spectrum of **5** in $CDCl_3$ (500 MHz).

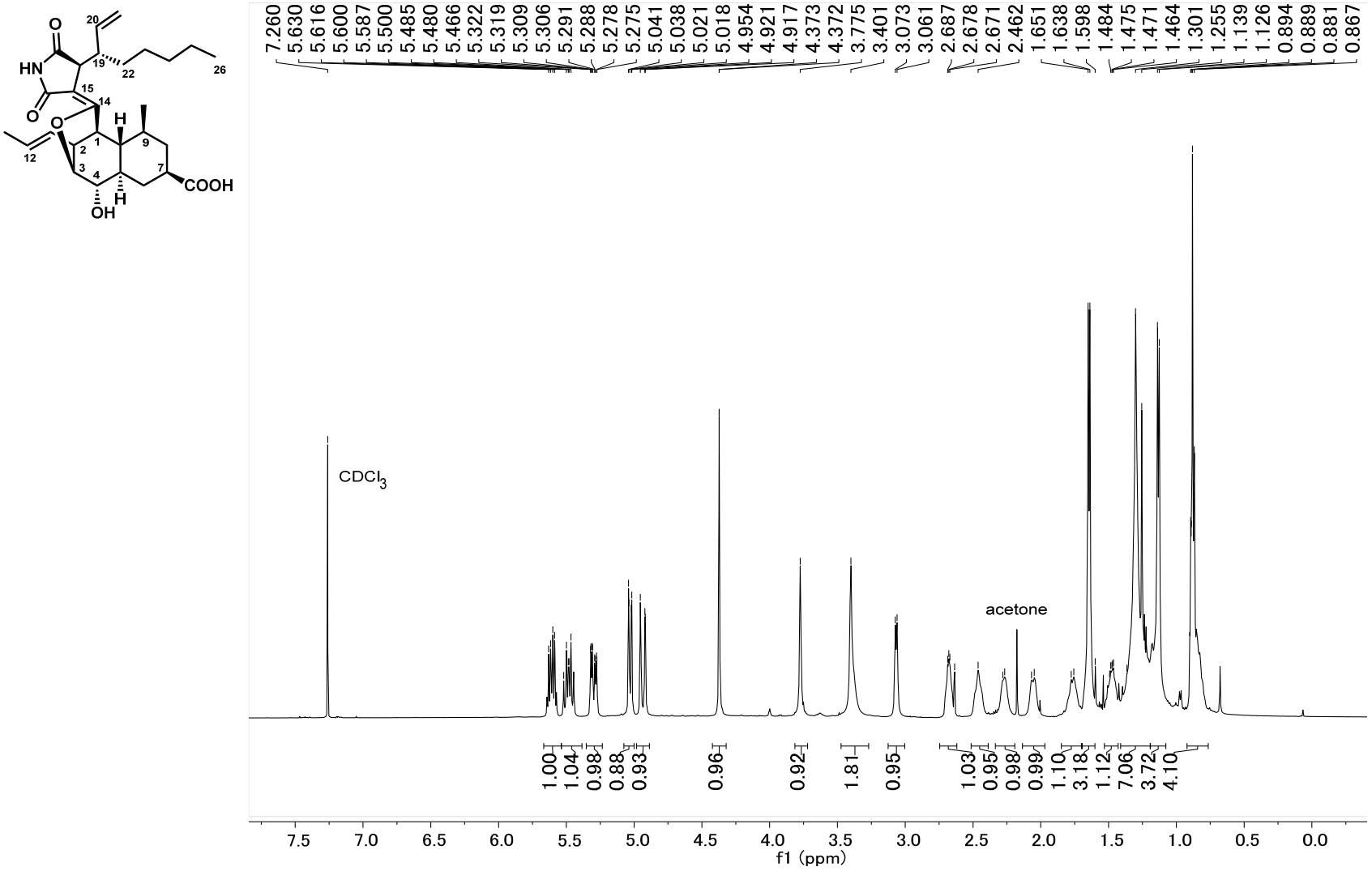

Figure S36. ^{13}CNMR spectrum of **5** in $CDCl_3$ (125 MHz)

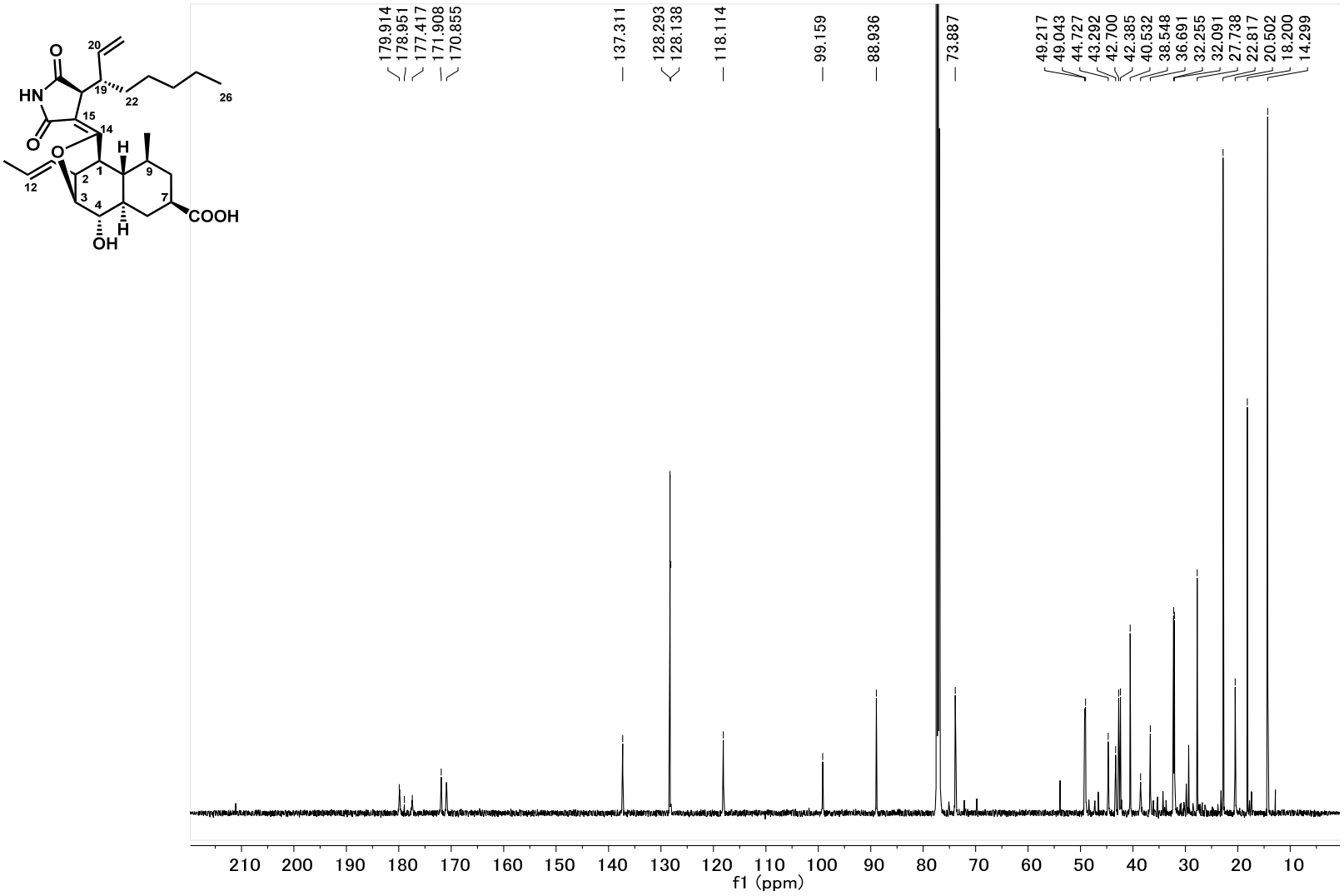

Figure S37. ^{1}H-^{1}H COSY spectrum of **5** in $CDCl_3$ (500 MHz).

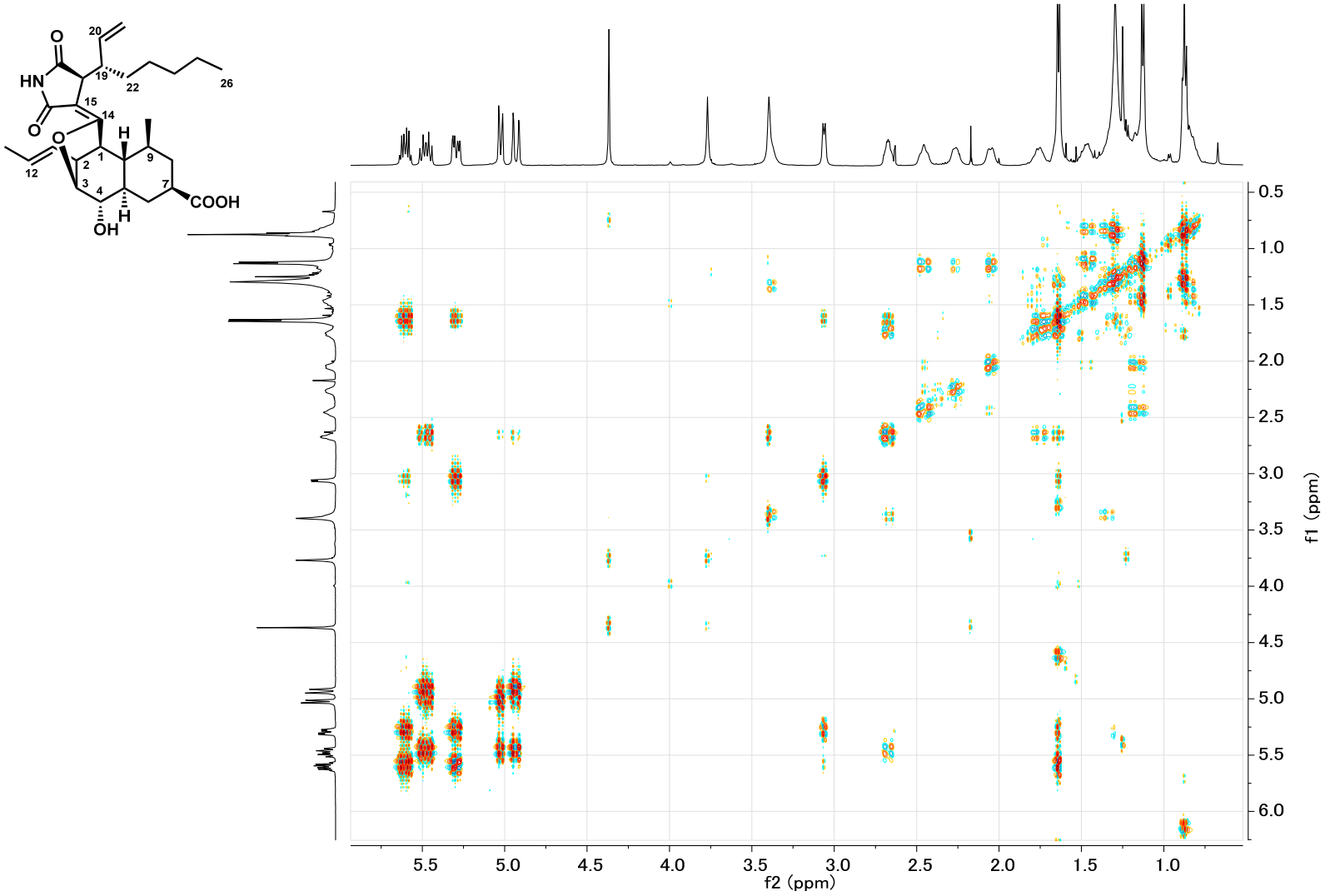

Figure S38. HSQC spectrum of **5** in $CDCl_3$ (500 MHz).

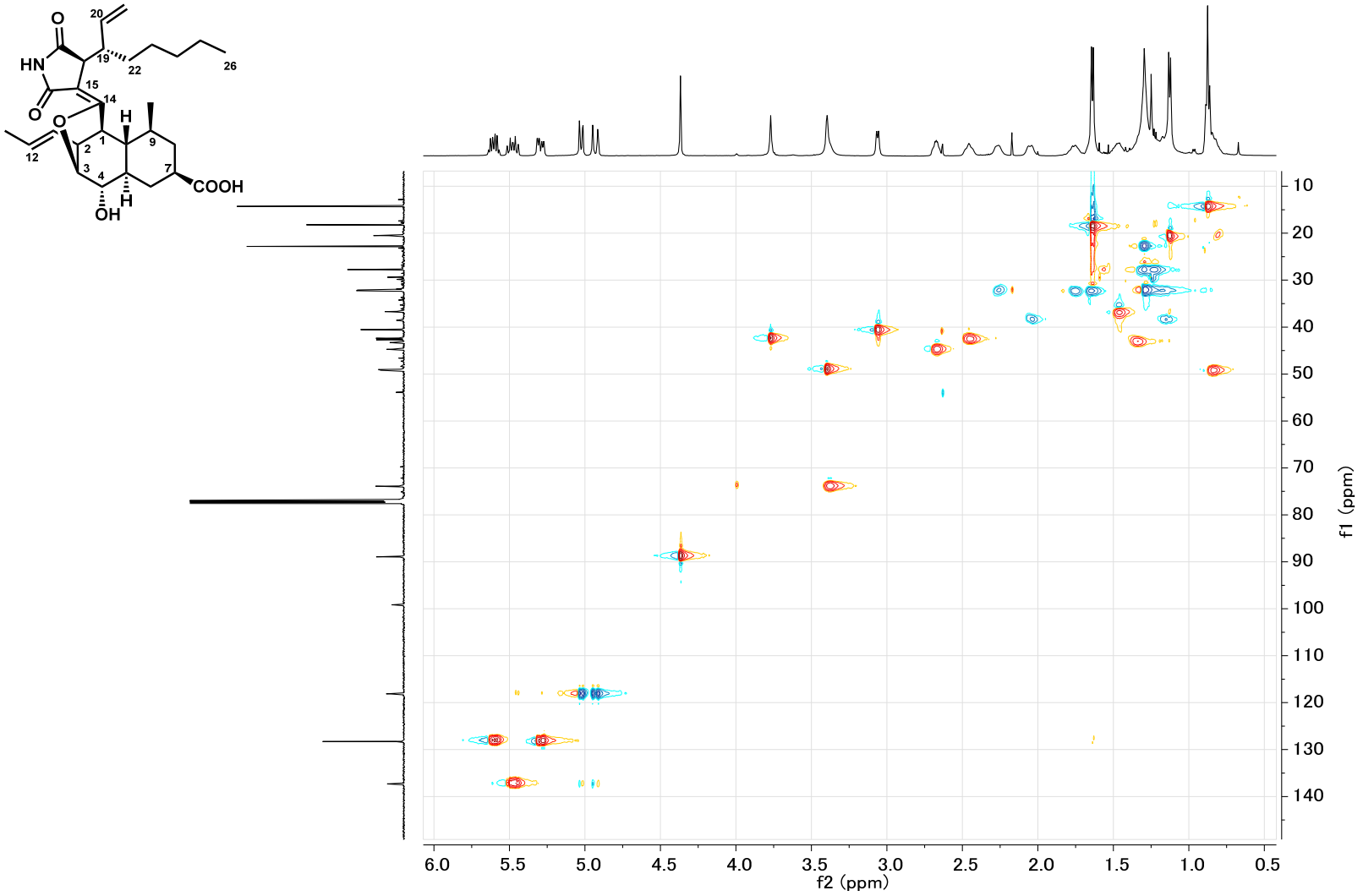

Figure. S39. HMBC spectrum of **5** in $CDCl_3$ (500 MHz).

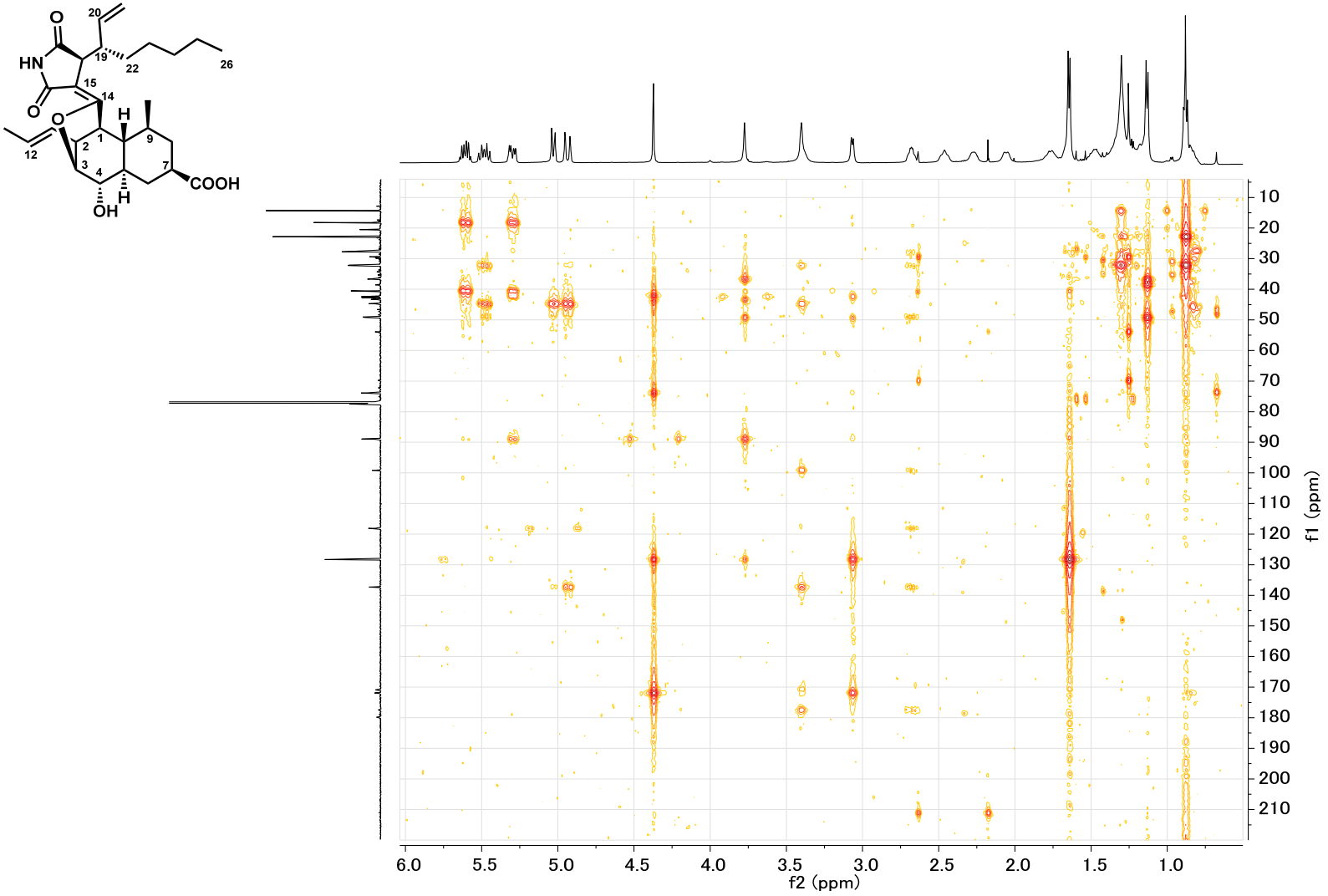

Figure. S40. NOESY spectrum of **5** in $CDCl_3$ (500 MHz).

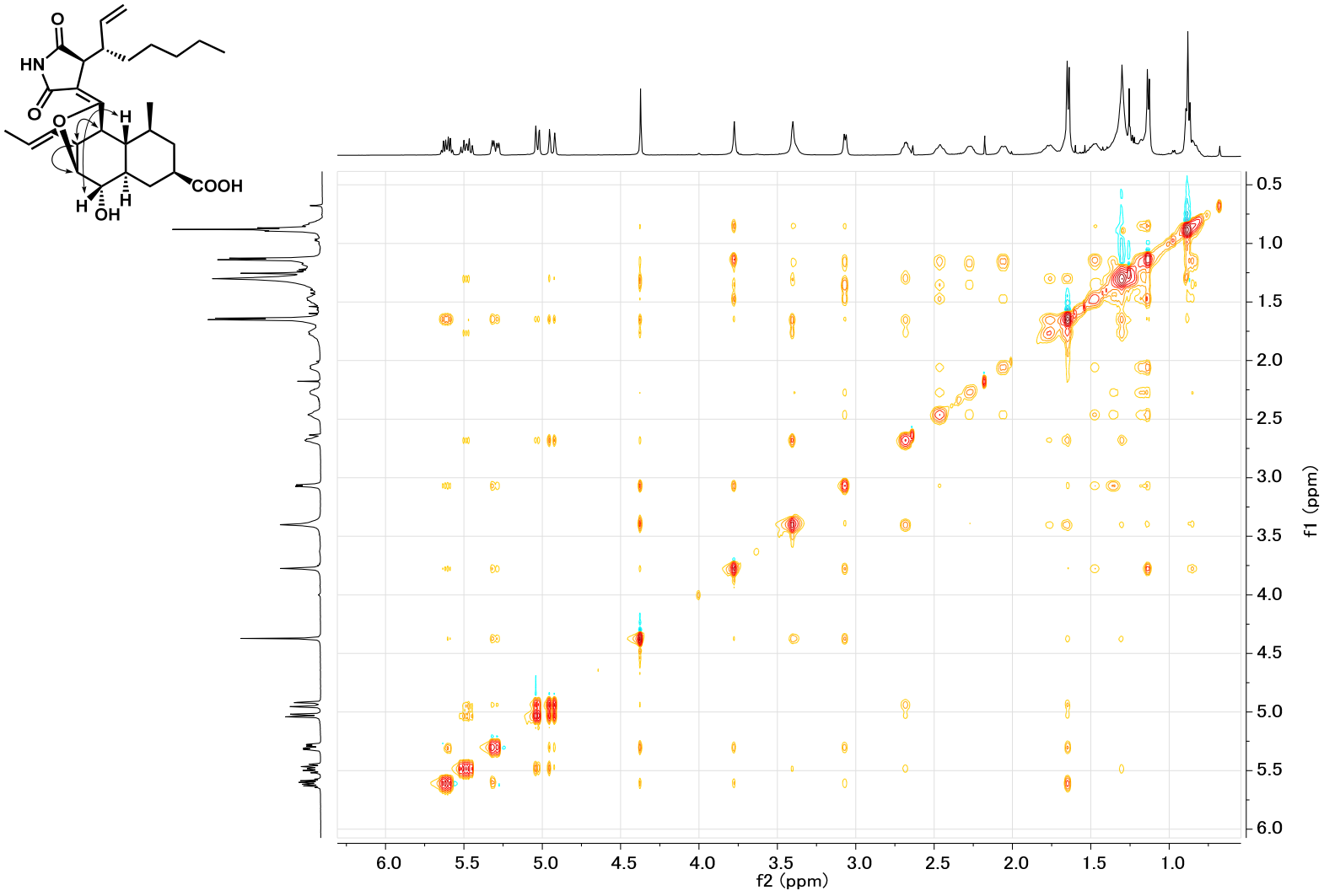

2.12. Chemical characterization of **6**

Table S9. NMR data of oxaleimide F (**6**) in DMSO-*d*$_6$. The molecular formula of **6** was established by mass data [ESI–MS: *m/z* 500 $(M–H)^–$; HRESIMS: *m/z* 500.2656 $(M–H)^–$, calcd. for $C_{28}H_{38}NO_7^–$,500.2654, Δ = 0.2mmu]; $[\alpha]_D^{30}$: 48.6 (*c* 0.14, MeOH).

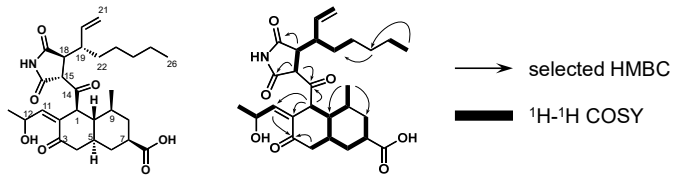

Position	δ_H [ppm]		mult. (*J* in Hz)	HMBC	δ_C [ppm]
1	4.58	1H	brd (3.7)	2,9,10,11,14	52.2
2					137.8
3					201.9
4	2.01	1H	dd (17.7, 13.7)	3,5,10	44.7
	2.23	1H	m		
5	1.51	1H	m		35.0
6	1.18	1H	m	10	34.2
	1.90	1H			
7	2.23	1H	m		41.9
8	1.08	1H	m	10	37.6
	1.89	1H	m		
9	1.36	1H	m		35.7
10	1.90	1H	m	1,14	44.6
11	6.18	1H	d (9.7)	1,3,13	139.8
12	5.01	1H	m	13	74.9
13	1.20	3H	d (6.3)	11,12	17.2
14					201.6
15	3.78	1H	d (5.2)	14,16,18,19	53.9
16					172.9
17					177.7
18	3.21	1H	dd (4.4, 4.4)	14,15,17,19,20,22	46.8
19	2.16	1H	m		43.6
20	5.36	1H	ddd (16.9, 9.9, 9.9)	19,22	137.6
21	4.99	1H	m	19,20	118.0
	5.03	1H	m		
22	1.31	1H	m	23	30.3
	1.34	1H	m		
23	1.10	1H	m		26.4
	1.20	1H	m		
24	1.14	1H	m	22	30.9
	1.19	1H	m		
25	1.23	2H	m	24	21.9
26	0.83	3H	m	24,25	13.9
7-COOH					176.0
9-Me	0.84	3H	m	8,9,10	19.1

Figure S41. [1]H NMR spectrum of **6** in DMSO-*d*$_6$ (500 MHz) (* are unidentified impurities)

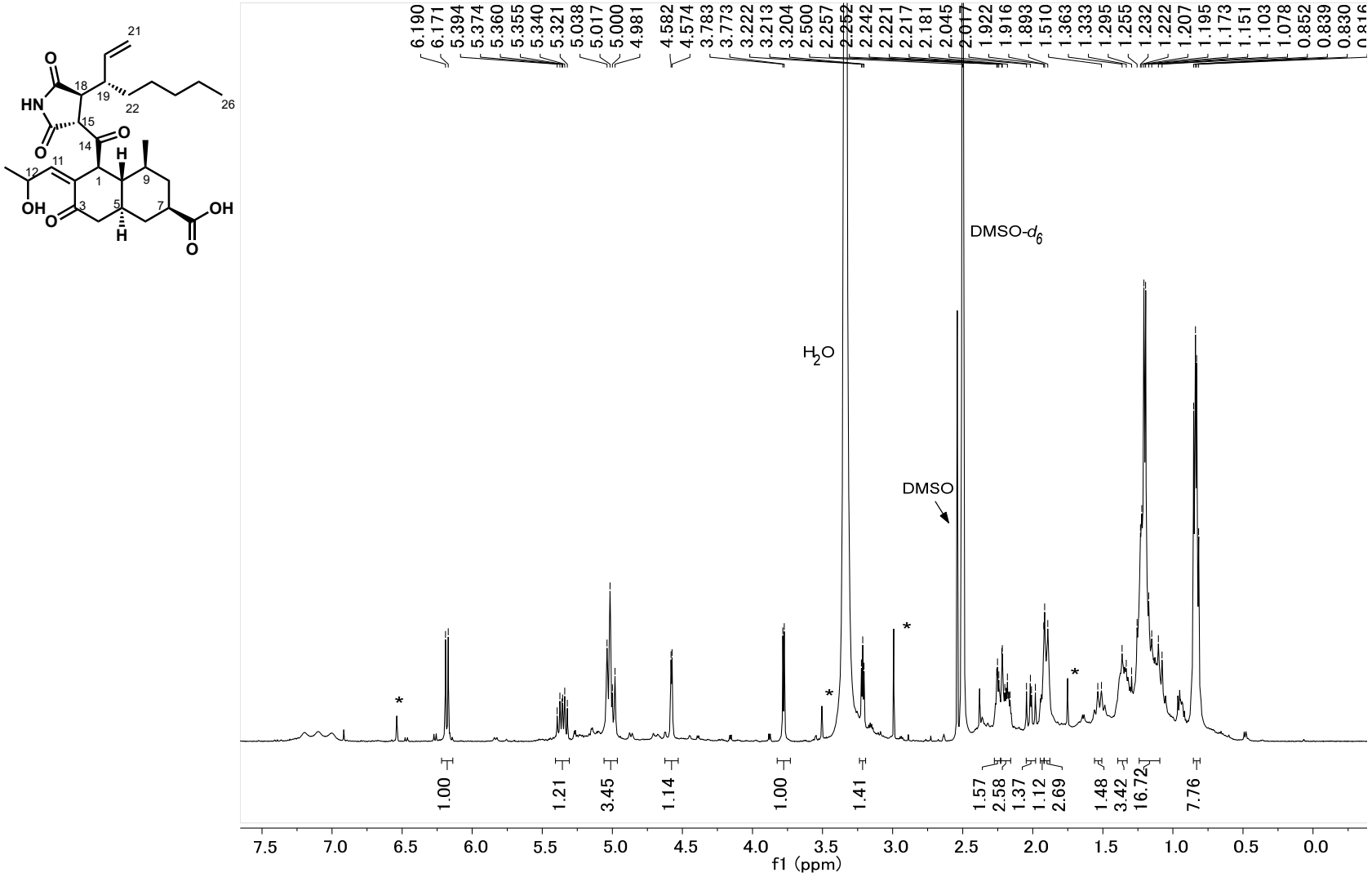

Figure S42. ^{13}CNMR spectrum of **6** in DMSO-d_6 (125 MHz)

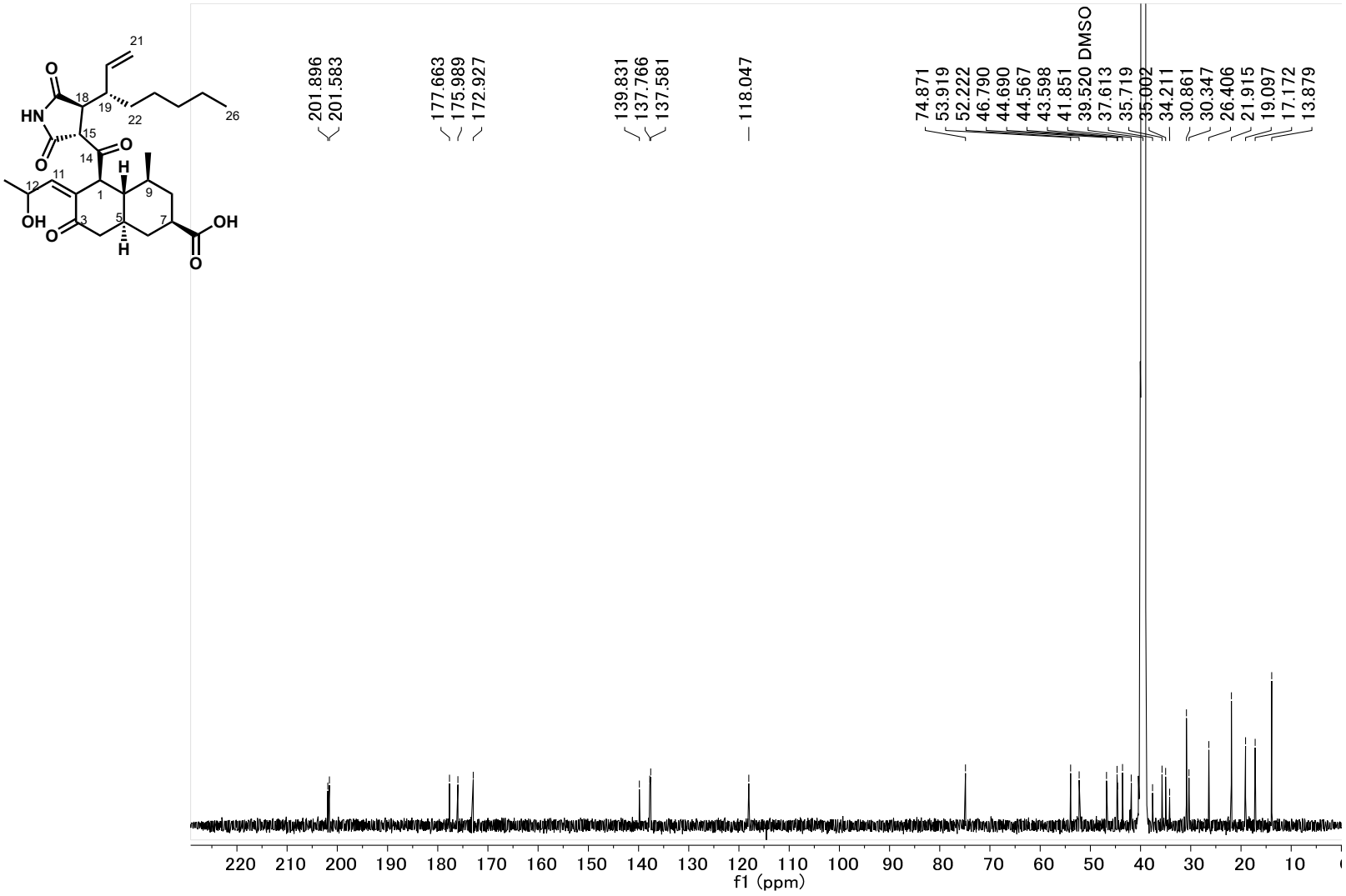

Figure S43. ^{1}H-^{1}H COSY spectrum of **6** in DMSO-*d*$_6$ (500 MHz).

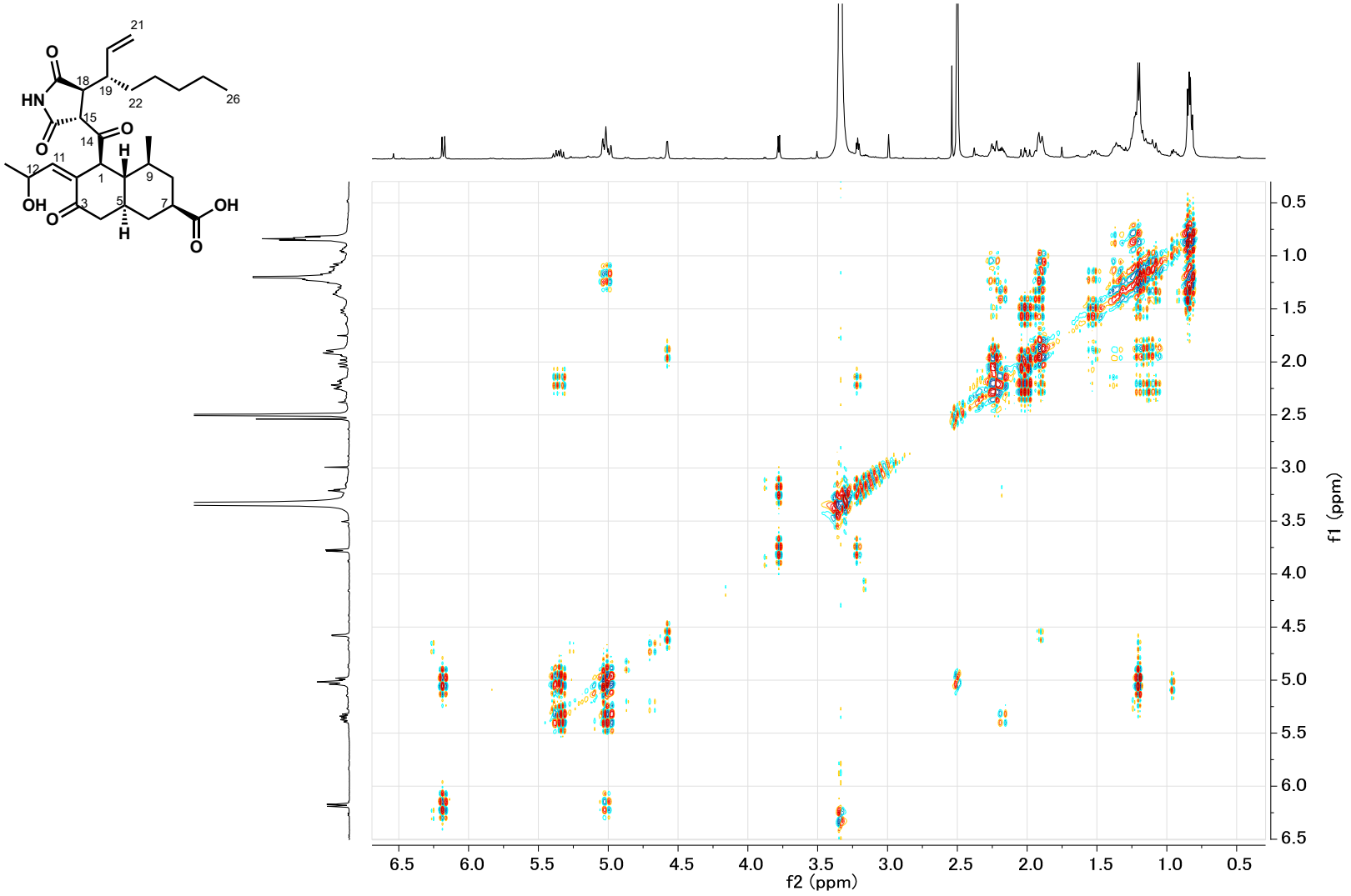

Figure S44. HSQC spectrum of **6** in DMSO-d_6 (500 MHz)

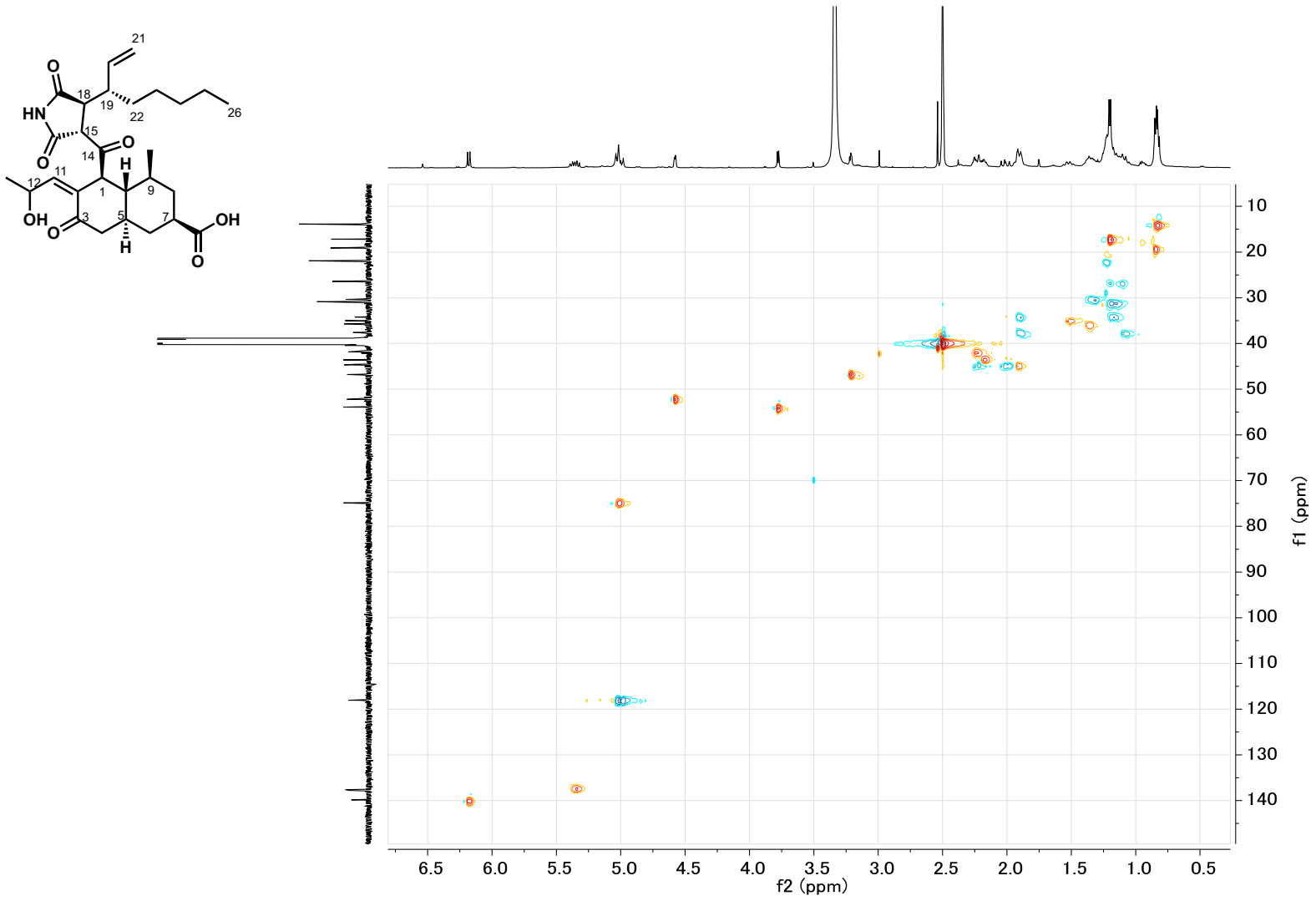

Figure S45. HMBC spectrum of **6** in DMSO-*d*$_6$ (500 MHz).

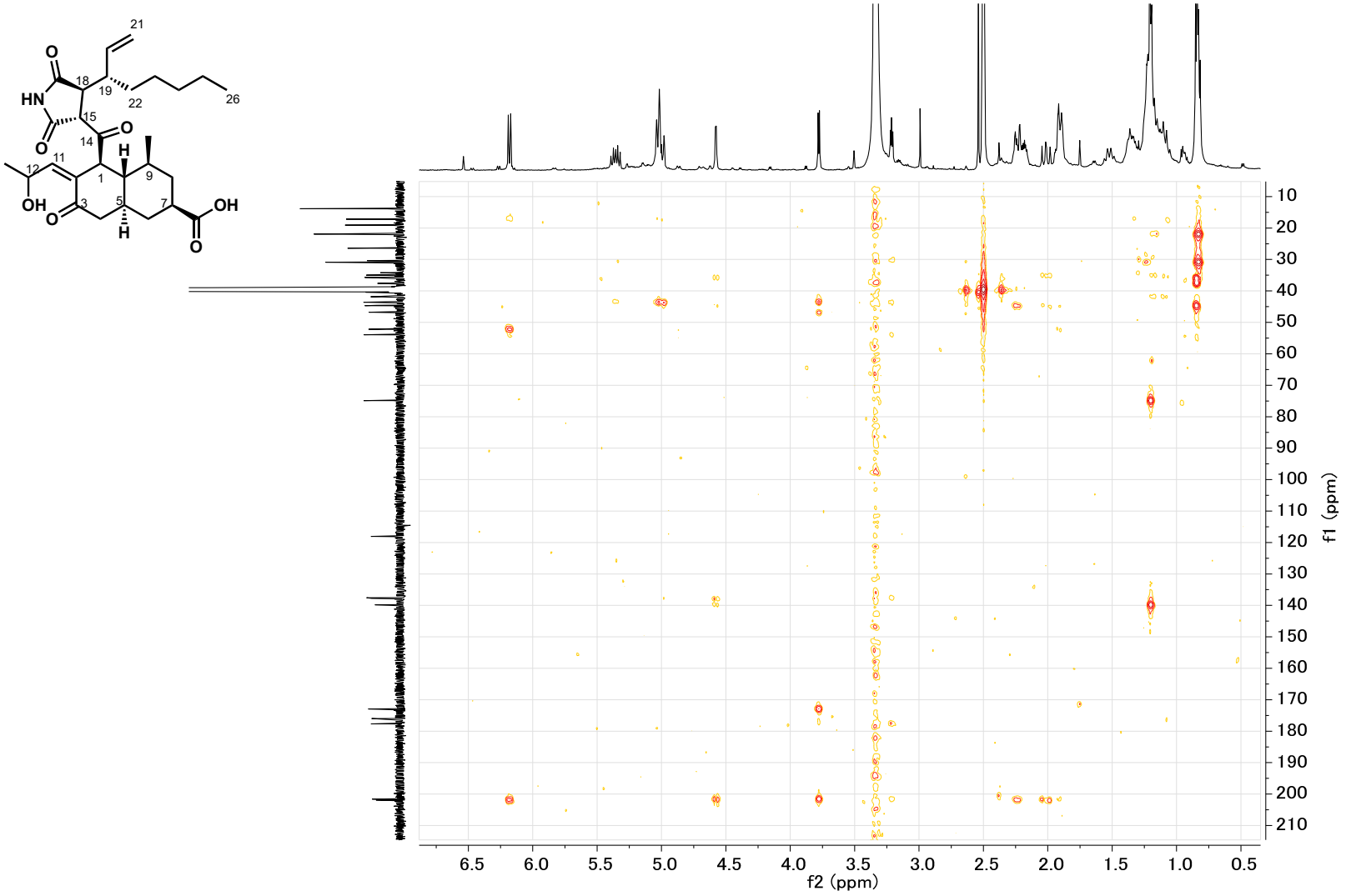

Figure S46. NOESY spectrum of **6** in DMSO-d_6 (500 MHz)

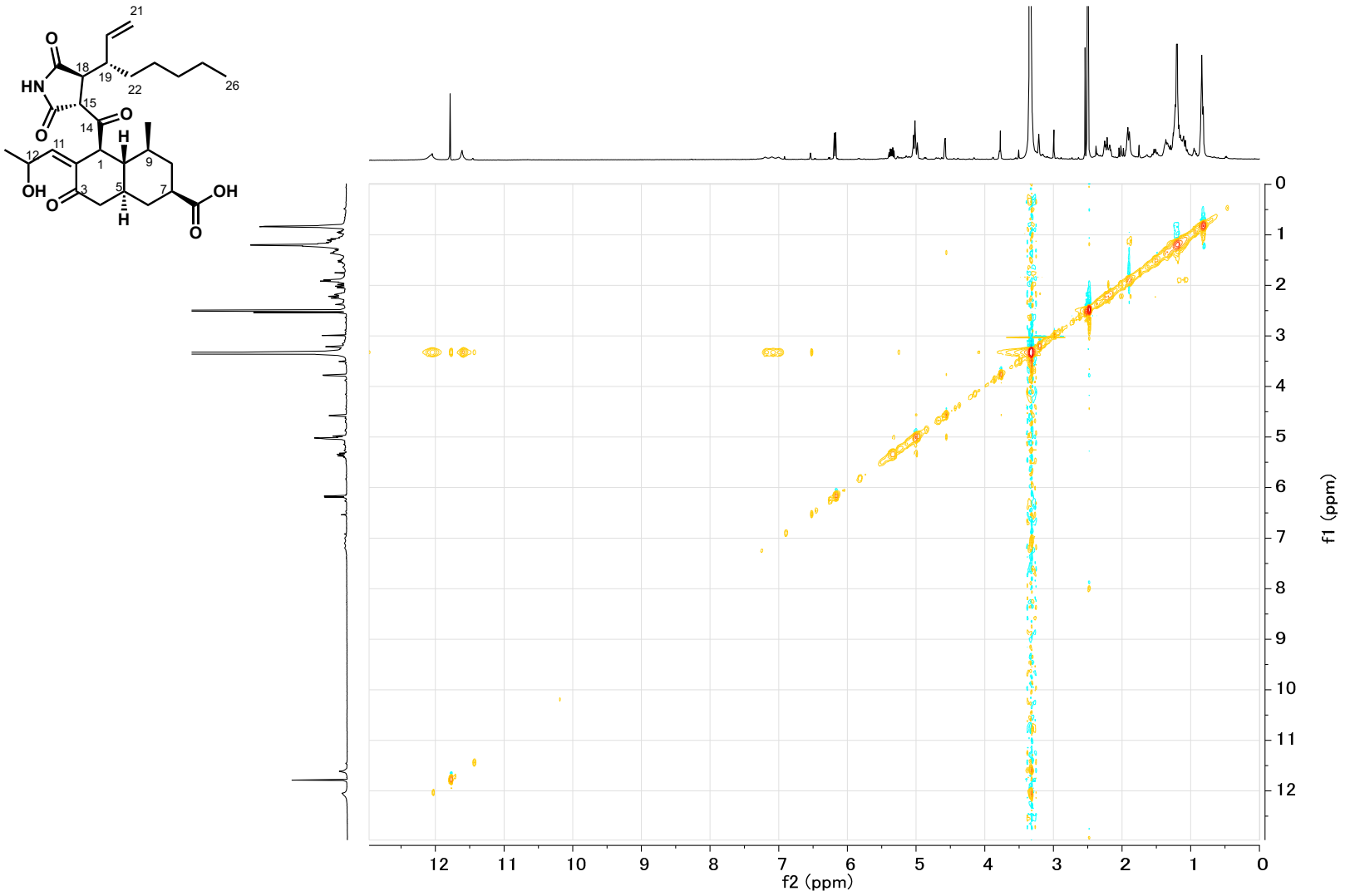

2.13. Chemical characterization of **7**

Table S10. NMR data of oxaleimide G (**7**) in DMSO-*d*$_6$. The molecular formula of **7** was established by mass data [ESI–MS: *m/z* 484 $(M–H)^–$; HRESIMS: *m/z* 484.2701 $(M–H)^–$, calcd. for $C_{28}H_{36}NO_6^–$, 484.2705, Δ = 0.4 mmu]; $[\alpha]_D^{31}$: 166.5 (*c* 0.52, MeOH).

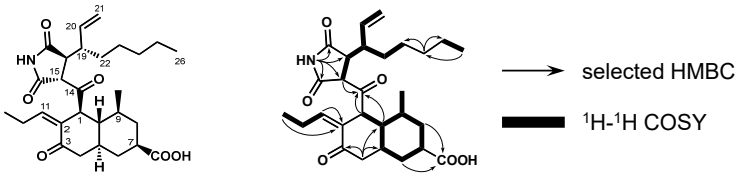

Position	δ_H [ppm]		mult. (*J* in Hz)	HMBC	δ_C [ppm]
1	4.02	1H	d (4.9)	2,9,10,11,14	59.8
2		1H			132.5
3		1H			202.6
4	1.86	1H	m	3,5,10	45.8
	2.28	1H	m	3,10	
5	1.52	1H	m		35.0
6	1.12	1H	m	5,7,8,10,7-CO	34.1
	1.91	1H	m		
7	2.32	1H	m		41.5
8	1.05	1H	m	7,9,10,7-CO	37.6
	1.88	1H	m		
9	1.36	1H	m		36.2
10	1.75	1H	ddd (11.4, 4.7, 4.7)	1,4,9,14,9-Me	44.2
11	6.34	1H	t (7.5)	1,2,3,12,13	146.1
12	2.26	2H	m	2,10,13	22.4
13	1.00	3H	t (7.5)	11,12	13.7
14					202.9
15	4.23	1H	d (4.9)	14,16,18,19	54.2
16					173.4
17					177.9
18	3.01	1H		14,15,17,19,20,22	47.7
19	2.22	1H			43.7
20	5.34	1H	ddd (17.1, 9.6, 9.6)	19,22	137.5
21	5.03	1H	d (16.8)	19,20	117.9
	5.04	1H	dd (8.1, 1.7)	19,20	
22	1.28	1H	m	23	30.2
	1.39	1H	m		
23	1.10	1H	m		26.2
	1.21	1H	m		
24	1.17	2H	m	23,25	30.9
25	1.22	2H	m	24	21.9
26	0.83	3H	t (7.0)	24,25	13.9
7-COOH					176.1
9-Me	0.78	3H	d (6.4)	8,9,10	19.2
NH	11.5	1H		15,16,17,18	

Figure S47. ^{1}H NMR spectrum of **7** in DMSO-*d*$_6$ (500 MHz)

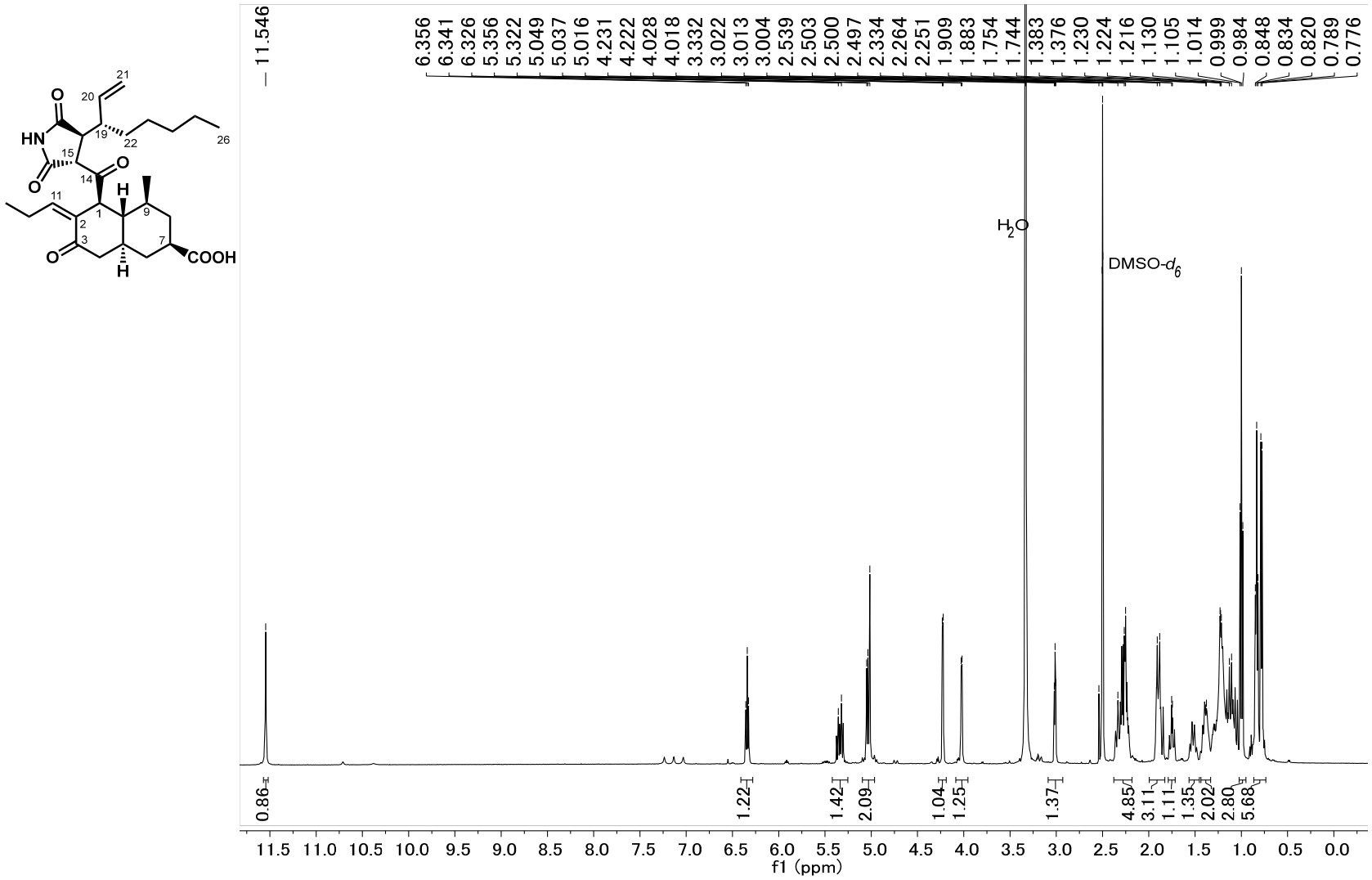

Figure S48. ^{13}CNMR spectrum of **7** in DMSO-*d*$_6$ (125 MHz)

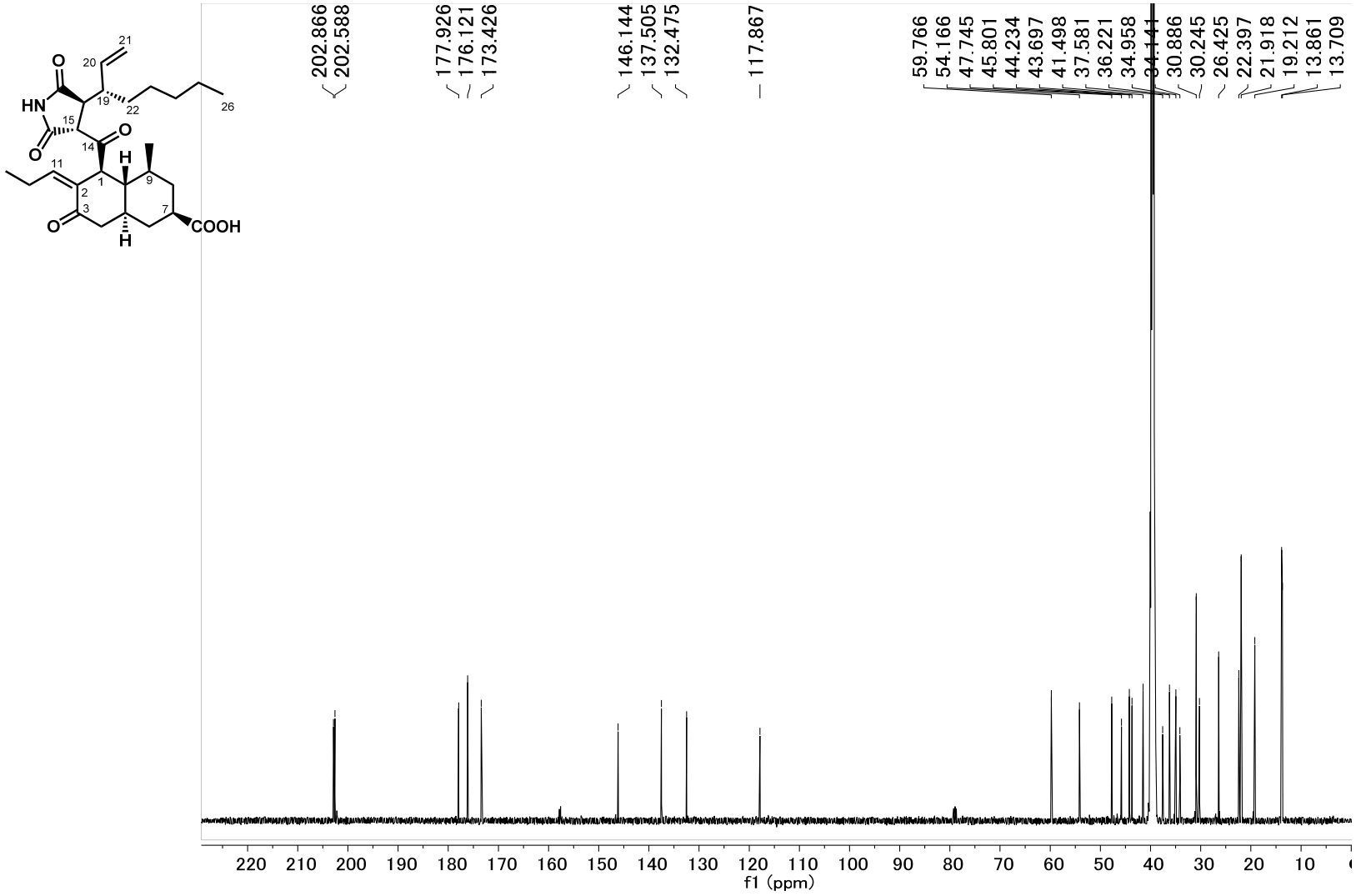

Figure S49. ^{1}H-^{1}H COSY spectrum of **7** in DMSO-*d*$_6$ (500 MHz)

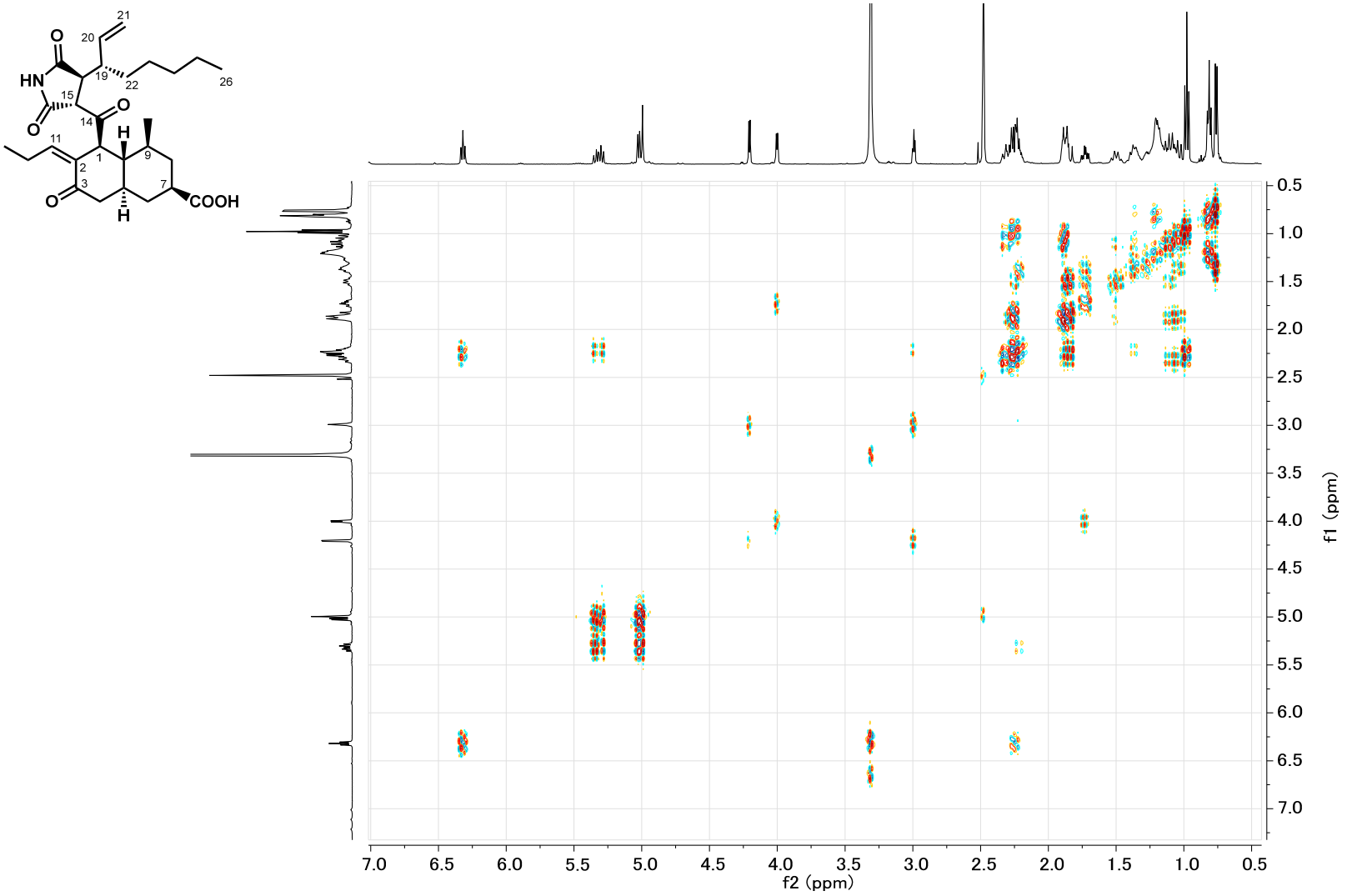

Figure S50. HSQC spectrum of **7** in DMSO-d_6 (500 MHz)

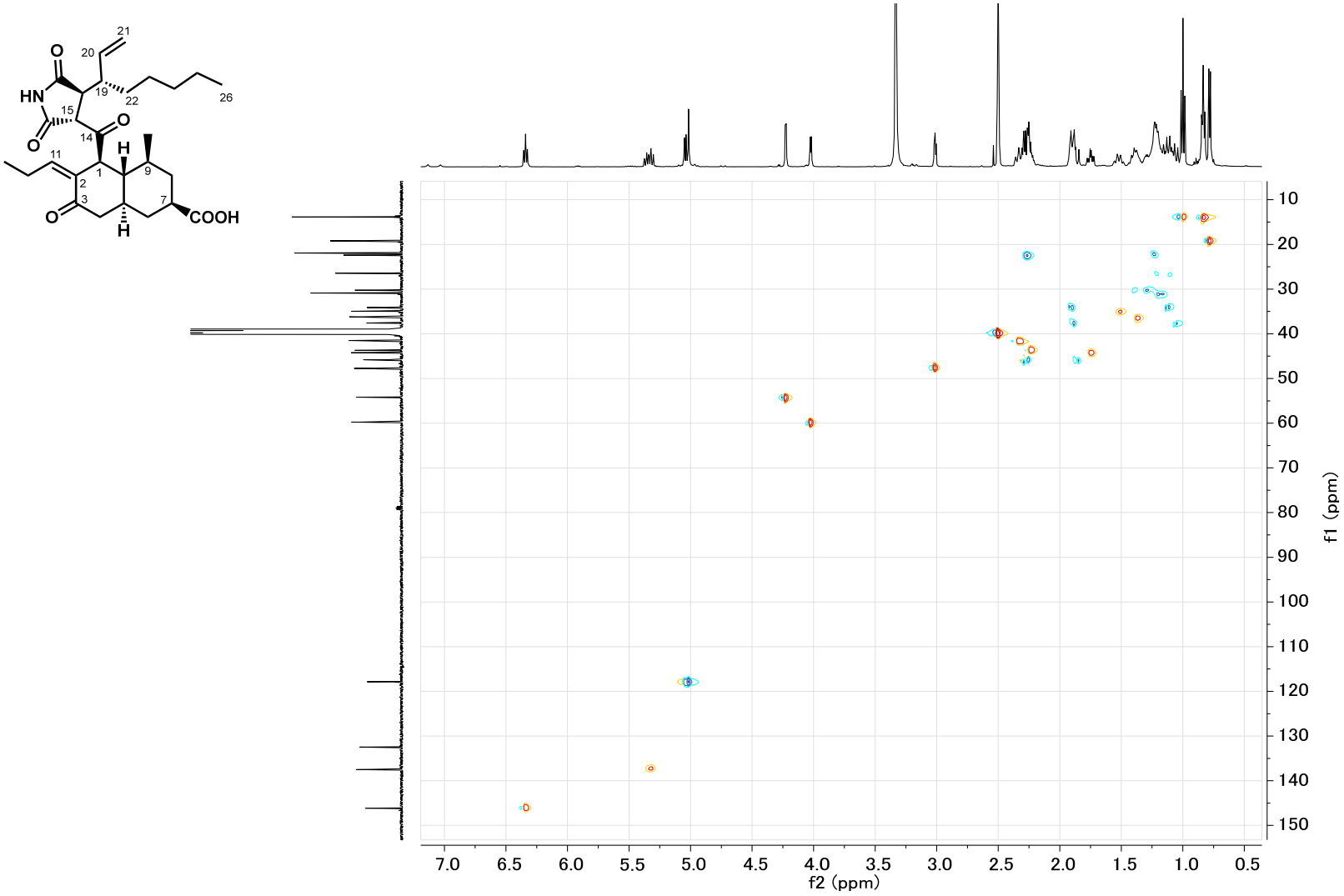

Figure. S51. HMBC spectrum of **7** in DMSO-*d*$_6$ (500 MHz).

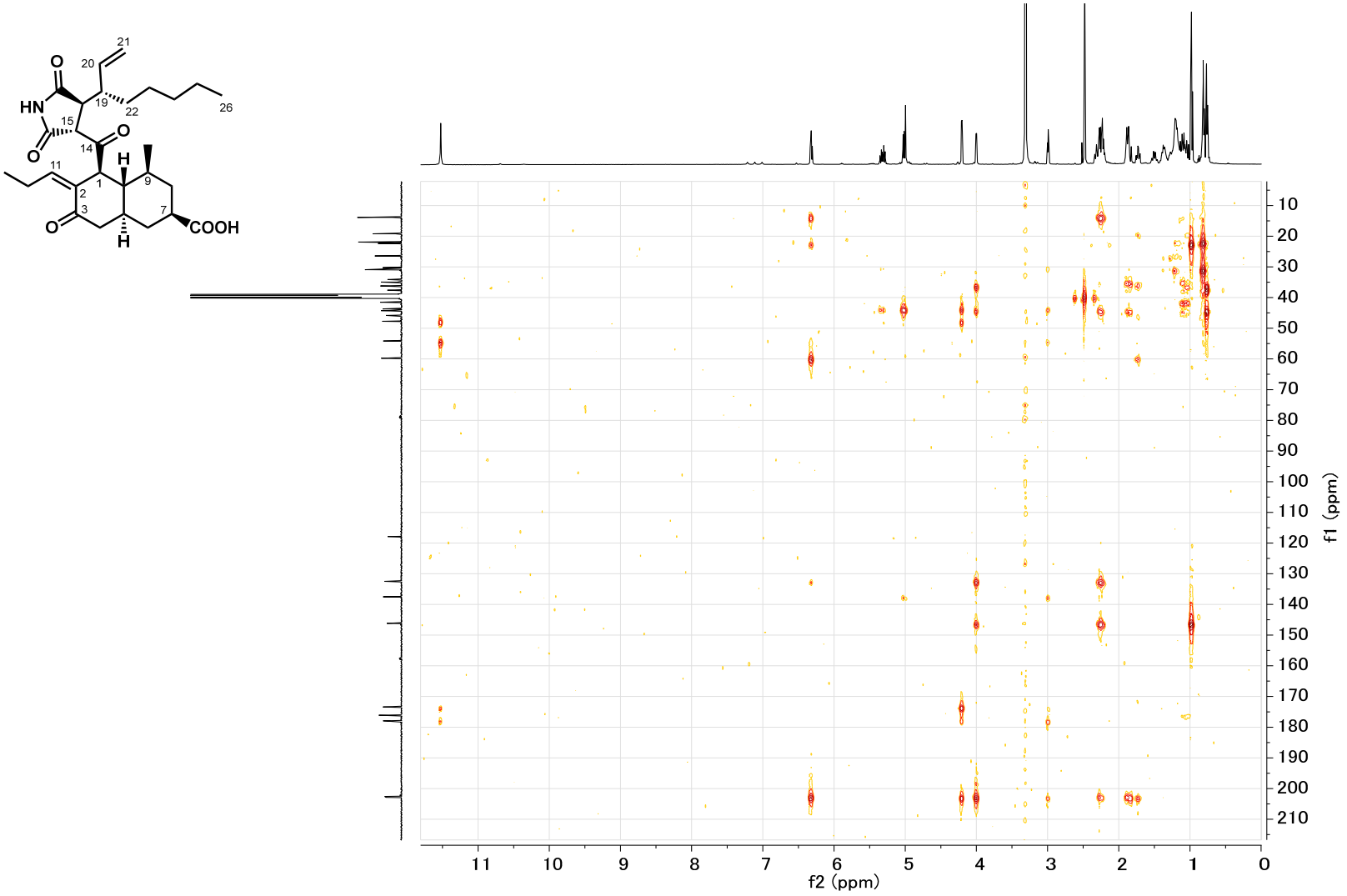

Figure S52. NOESY spectrum of **7** in DMSO-*d*$_6$ (500 MHz)

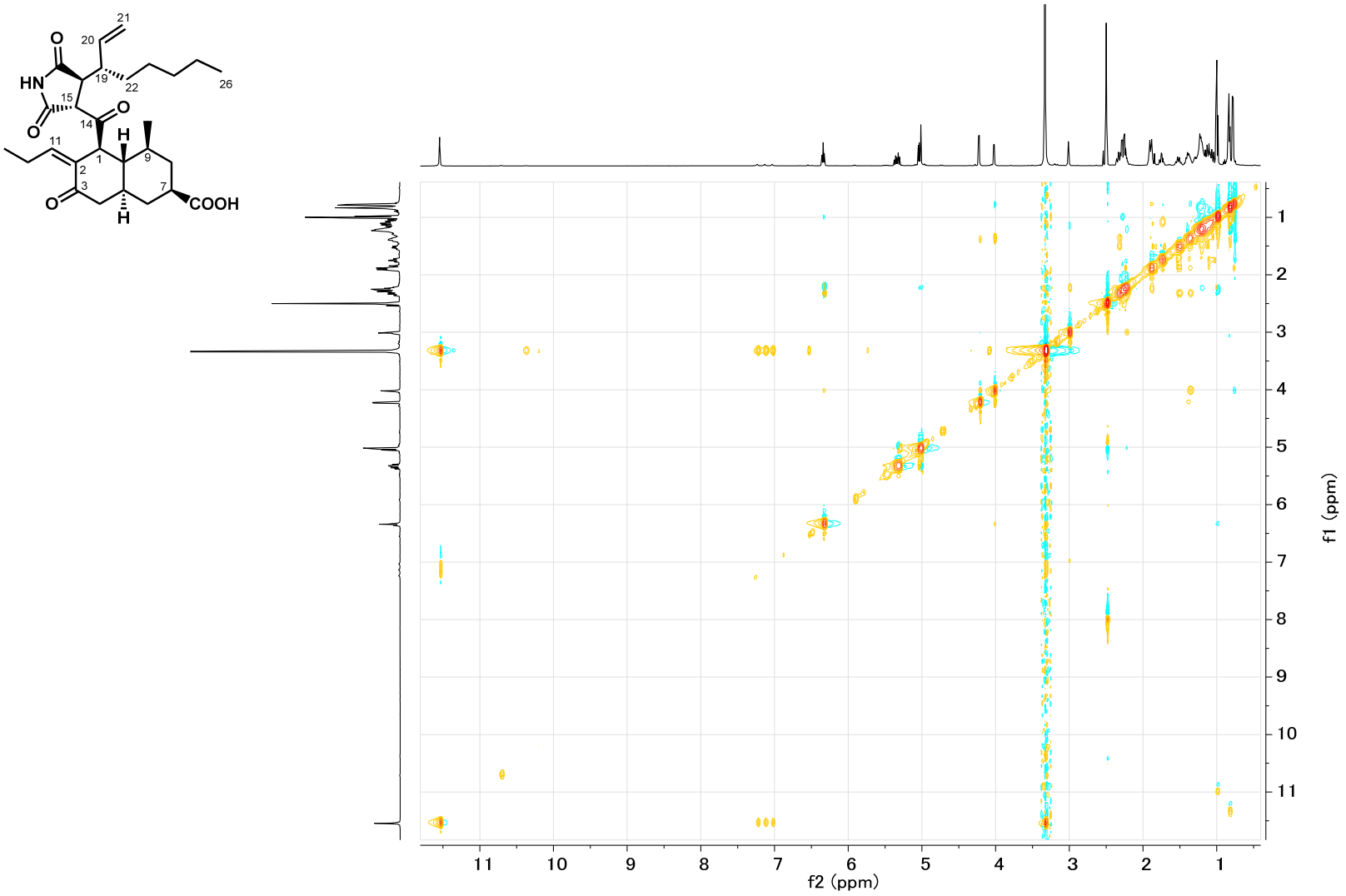

2.14. Chemical characterization of **8**

Table S11. NMR data of oxaleimide H (**8**) in $CDCl_3$. The molecular formula of **8** was established by mass data [ESI–MS: *m/z* 484 $(M–H)^–$; HRESIMS: *m/z* 484.2705 $(M–H)^–$, calcd. for $C_{28}H_{38}NO_6^–$, 484.2705, Δ = 0.01 mmu]; $[\alpha]_D^{31}$: 187 (*c* 0.76, MeOH).

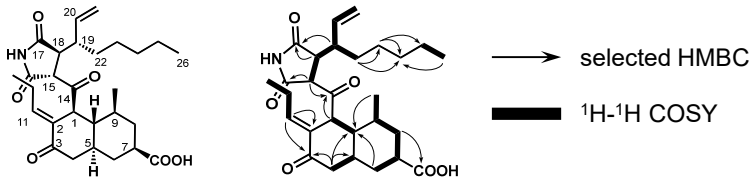

Position	δ_H [ppm]		mult. (*J* in Hz)	HMBC	δ_C [ppm]
1	4.50	1H	d (3.9)	2,3,9,10,11,14	52.4
2					133.6
3					201.8
4	2.10	1H	m	3,5,10	45.4
	2.29	1H	m	3,5,10	
5	1.41	1H			36.2
6	1.39	1H	m	8,10	34.4
	2.03	1H			
7	2.46	1H	m		42.2
8	1.29	1H	m	7,9,9-Me,7-CO	37.7
	2.07	1H	m		
9	1.42	1H			36.8
10	2.13	1H	m	1,3,9,14,9-Me	44.5
11	6.65	1H	dd (9.0, 6.3)	1,3,12,13	145.4
12	2.57	1H	m	2,11,13	22.1
	2.35	1H	m	2,11,13	
13	1.15	3H	t (7.5)	11,12	13.6
14					199.8
15	3.92	1H	d (5.4)	14,16,18,19	54.0
16					171.8
17					176.8
18	3.52	1H	dd (5.4, 3.6)	14-17,19,21,22	46.5
19	2.13	1H	m	15,17,18,20,22,23	44.8
20	5.37	1H	ddd (16.9, 9.6, 9.6)	19,22	137.0
21	5.00	1H	d (17.0)	19,20	119.0
	5.08	1H	dd (10.2, 1.6)		
22	1.44	1H	m	23,24	31.3
	1.51	1H	m	23,24	
23	1.18	1H	m	24,25	27.2
	1.27	1H	m		
24	1.23	2H	m	26	31.7
25	1.26	2H	m	24	22.6
26	0.86	3H	t (6.8)	24,25	14.2
7-COOH					179.6
9-Me	0.92	3H	d (6.3)	8,9,10	19.2
NH	8.05	1H	s		

Figure S53. ^{1}H NMR spectrum of **8** in $CDCl_3$ (500 MHz) (* are unidentified impurities)

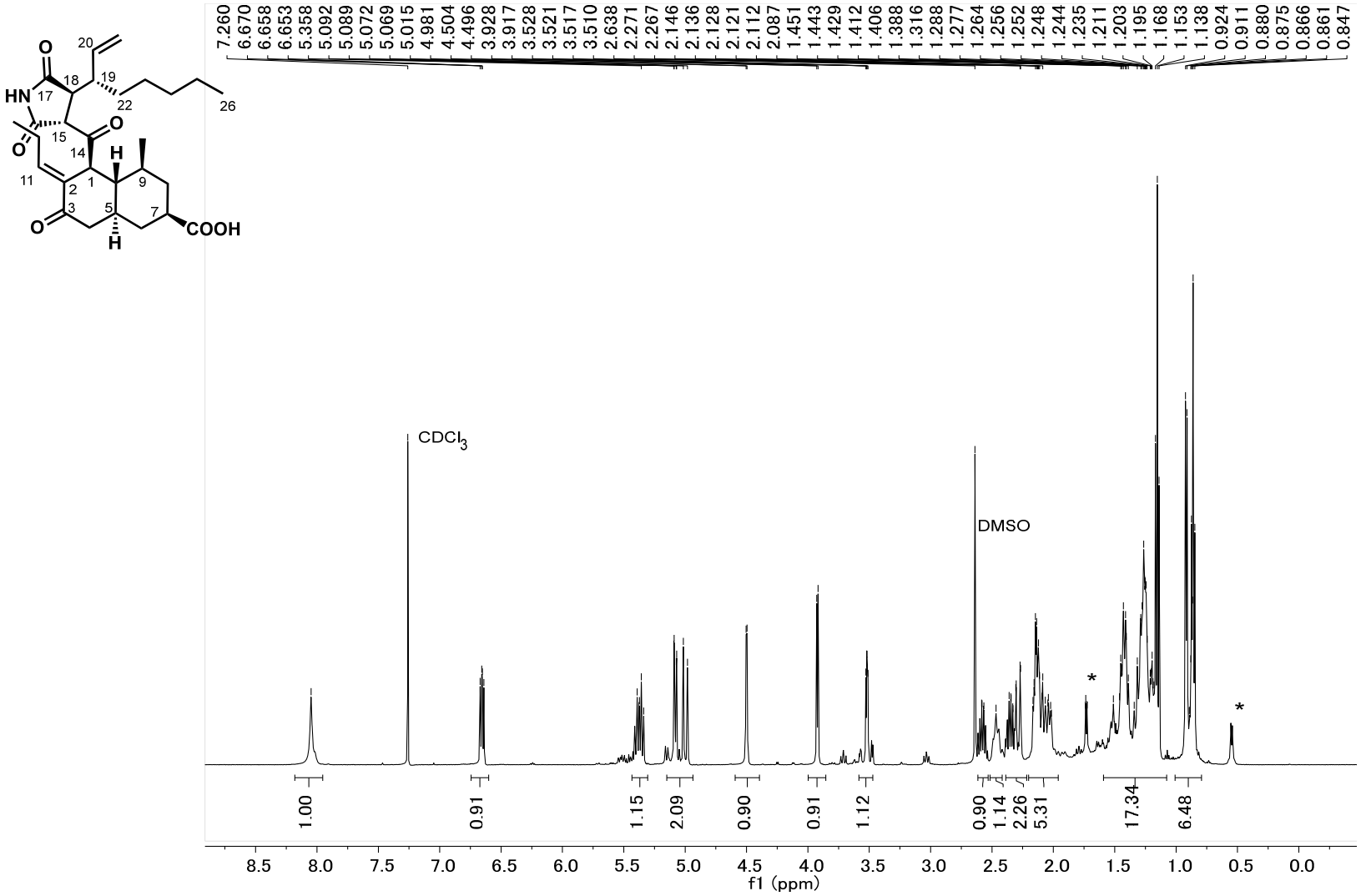

Figure S54. ^{13}CNMR spectrum of **8** in $CDCl_3$ (125 MHz)

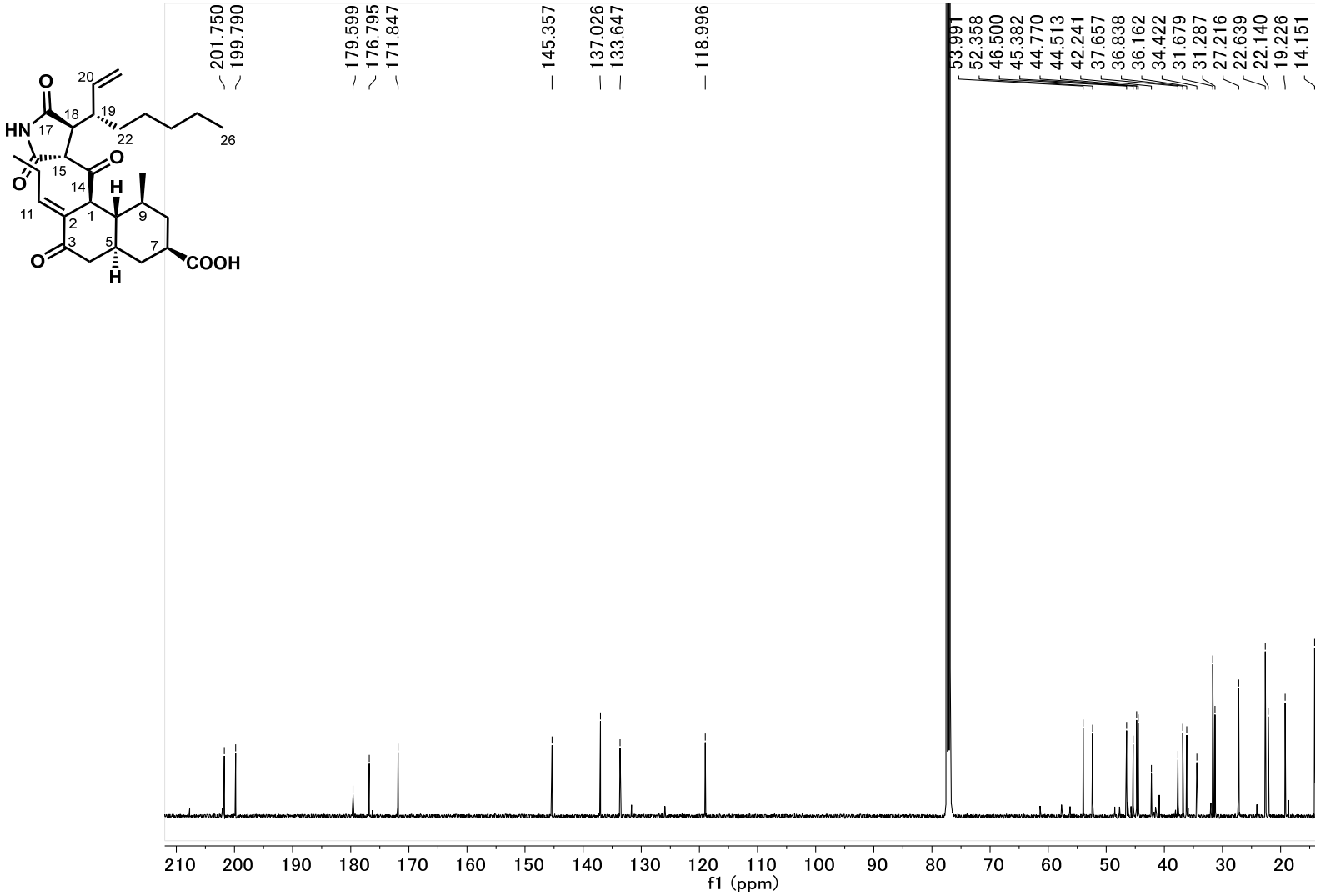

Figure S55. ^{1}H-^{1}H COSY spectrum of **8** in $CDCl_3$ (500 MHz)

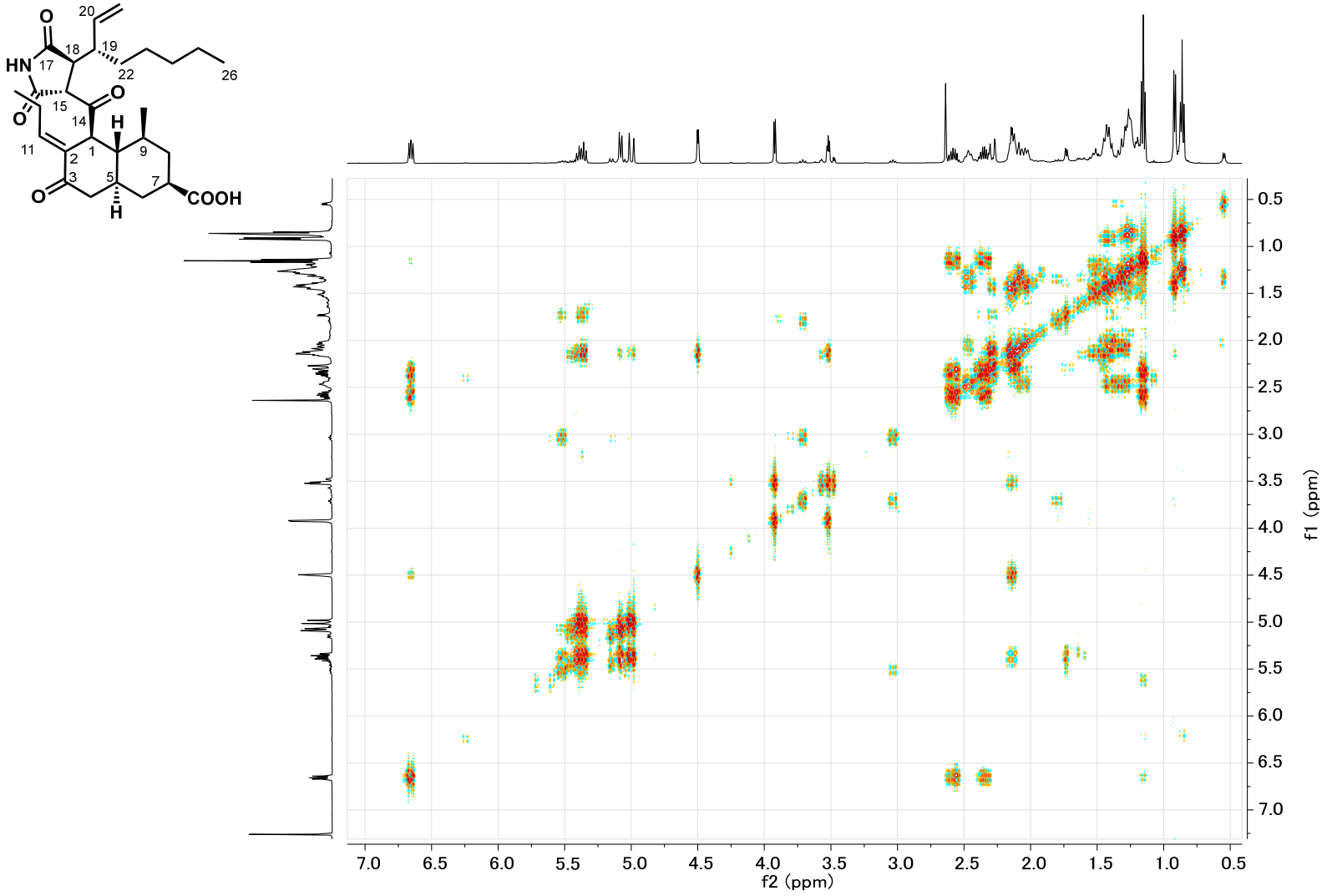

Figure S56. HSQC spectrum of **8** in $CDCl_3$ (500 MHz)

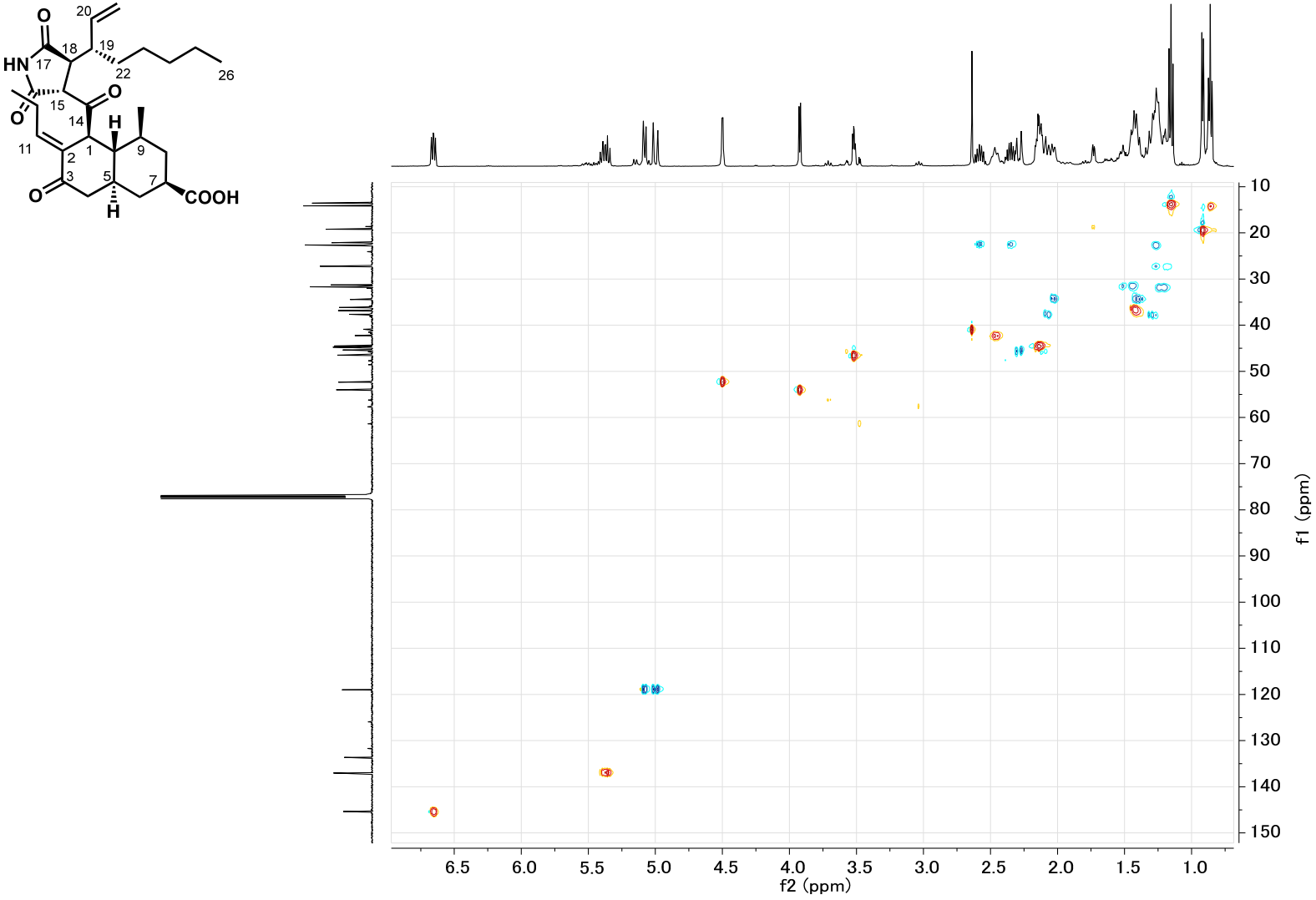

Figure S57. HMBC spectrum of **8** in $CDCl_3$ (500 MHz).

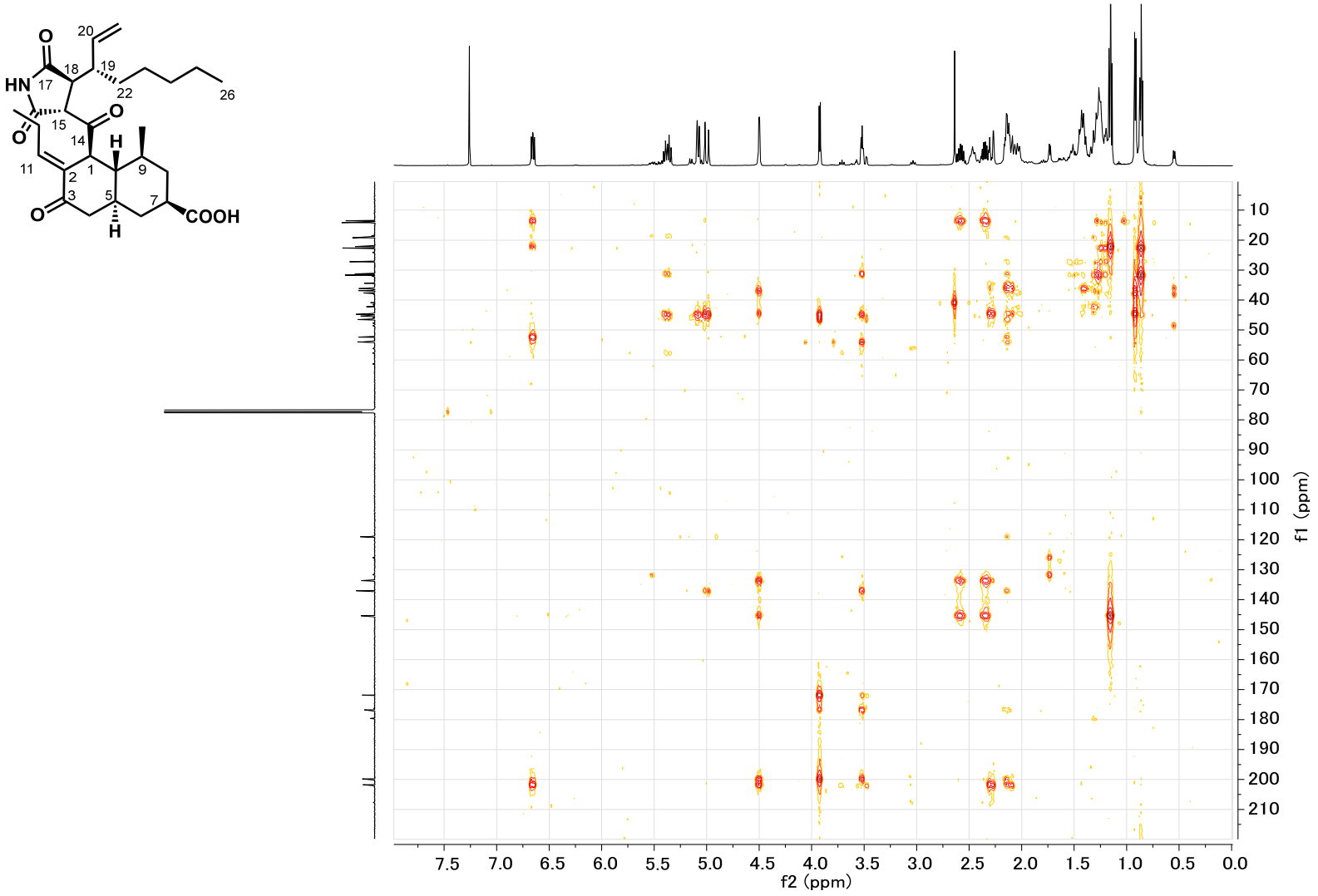

Figure S58. NOESY spectrum of **8** in $CDCl_3$ (500 MHz)

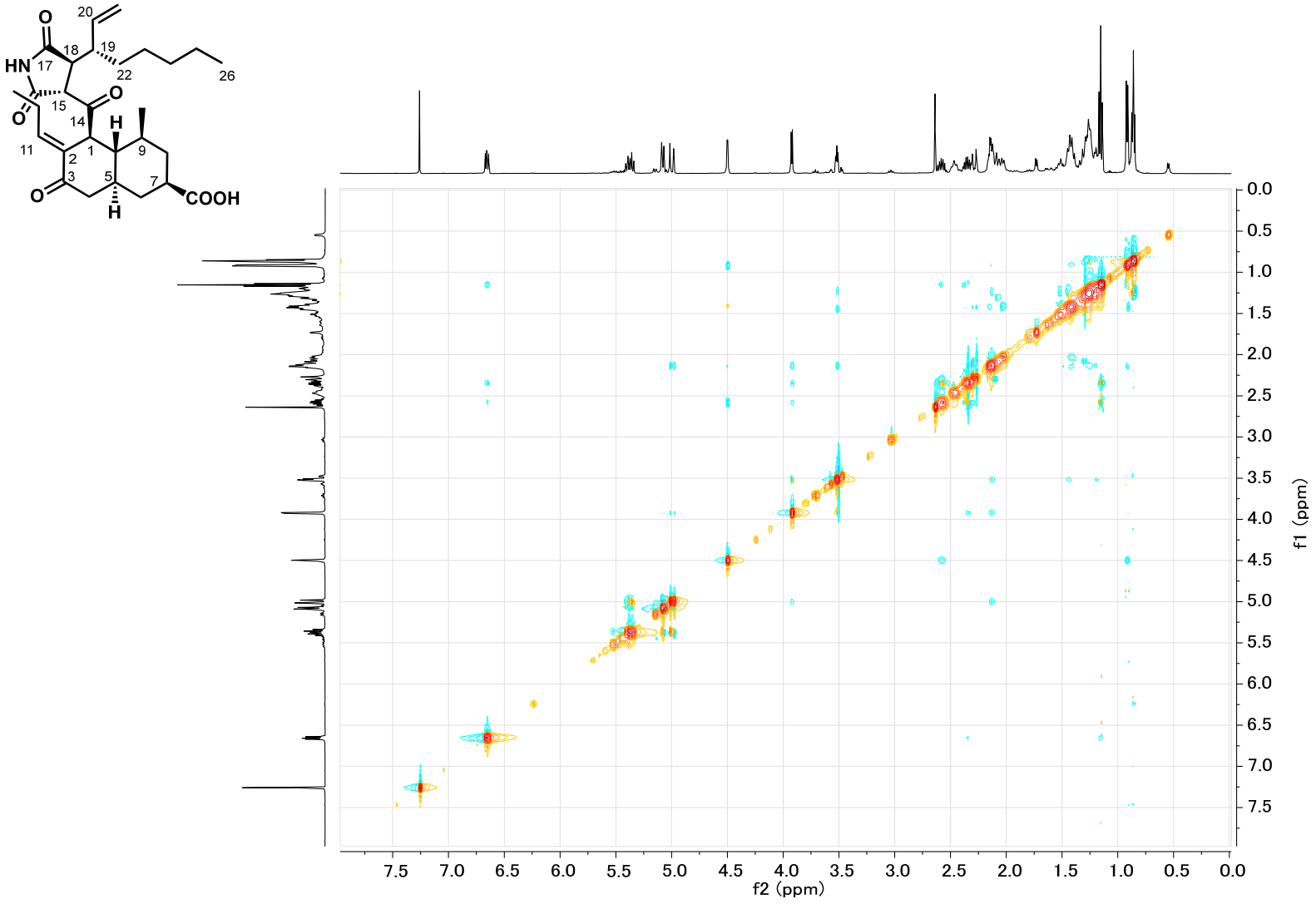

2.15. Chemical characterization of **9**

Table S12. NMR data of oxaleimide I (**9**) in $CDCl_3$. The molecular formula of **9** was established by mass data [ESI–MS: *m/z* 466 $(M–H)^–$; HRESIMS: *m/z* 466.2599 $(M–H)^–$, calcd. for $C_{28}H_{36}NO_5^–$, 466.2599, Δ = 0.01 mmu]; $[\alpha]_D^{31}$: -24.5 (*c* 0.4, MeOH).

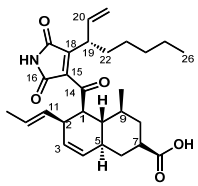

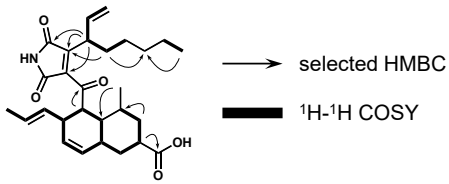

Position	δ_H [ppm]		mult. (*J* in Hz)	HMBC	δ_C [ppm]
1	3.97	1H	dd (8.2, 8.2)	2,3,9-11,14	53.8
2	3.03	1H	m		41.1
3	5.56	1H	m	1,2,5,6	129.1
4	5.67	1H	m	2,5,6	133.1
5	1.87	1H	brt (9.6)		39.9
6	2.22	1H	brd (12.1)		34.8
	1.48	1H	m	4,5,7,10,7-CO	
7	2.56	1H	m	6,8,7-CO	42.8
8	1.98	1H	brd (12.5)		38.2
	1.35	1H	m	6,7,9,10,7-CO	
9	1.51	1H	m		38.0
10	1.63	1H	m	1,5,6,9,14,9-Me	45.5
11	5.23	1H	m	2,12,13	131.1
12	5.38	1H	m	2,11,13	127.5
13	1.56	3H	d (6.0)	1,2,11,12	18.0
14					198.8
15					133.3
16					168.7
17					169.0
18					155.1
19	4.10	1H	dt (8.1, 7.3)	15,17,18,20-23	42.3
20	6.09	1H	ddd (16.8, 9.4, 9.4)	18,19,22	137.3
21	5.10	1H	d (18.2)	18,19,20,22	118.3
	5.11	1H	d (9.3)	18,19,20,22	
22	1.75	1H	m	18,19,20,23,24	33.3
	1.72	1H	m	18,19,20,23,24	
23	1.39	1H	m		27.4
	1.20	1H	m		
24	1.27	2H	m	25	31.6
25	1.27	2H	m	24	22.6
26	0.86	3H	m	24,25	14.1
7-COOH					180.1
9-Me	0.77	3H	d (6.4)	9,10	22.7
NH	7.45	1H			

Figure S59. ^{1}H NMR spectrum of **9** in $CDCl_3$ (500 MHz). (* are unidentified impurities)

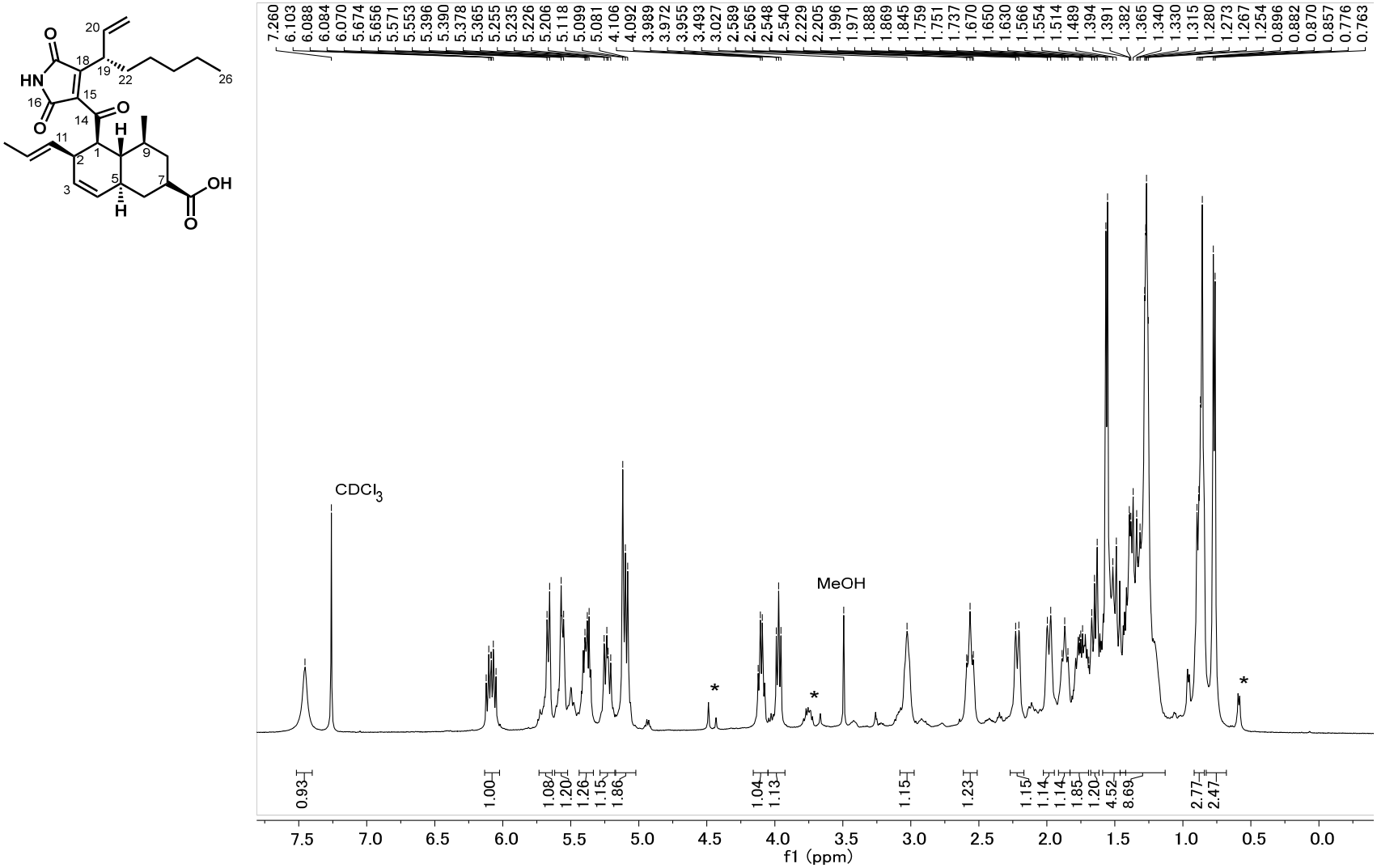

Figur S60. ^{13}CNMR spectrum of **9** in $CDCl_3$ (125 MHz)

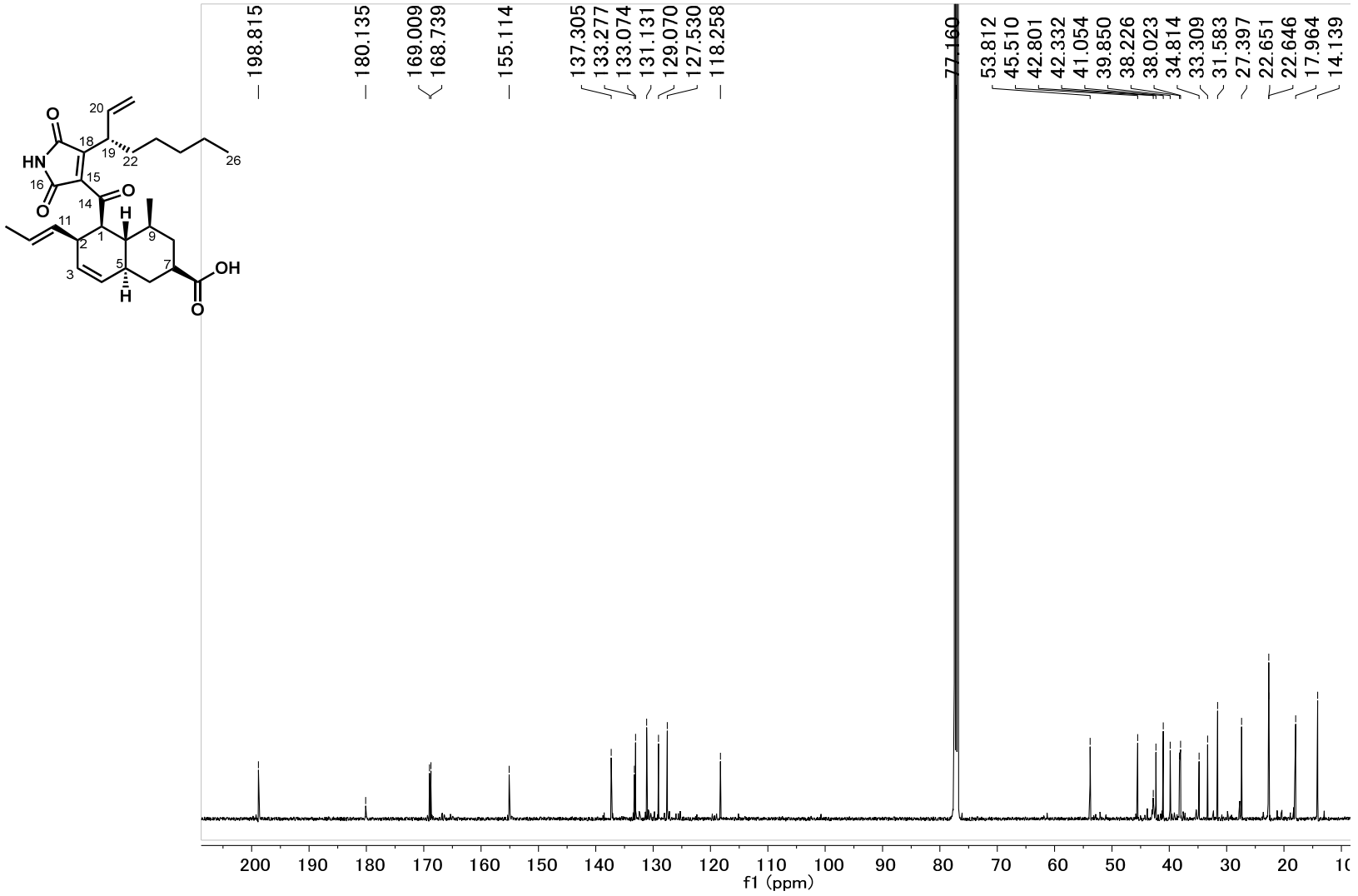

Figure S61. ^{1}H-^{1}H COSY spectrum of **9** in $CDCl_3$ (500 MHz).

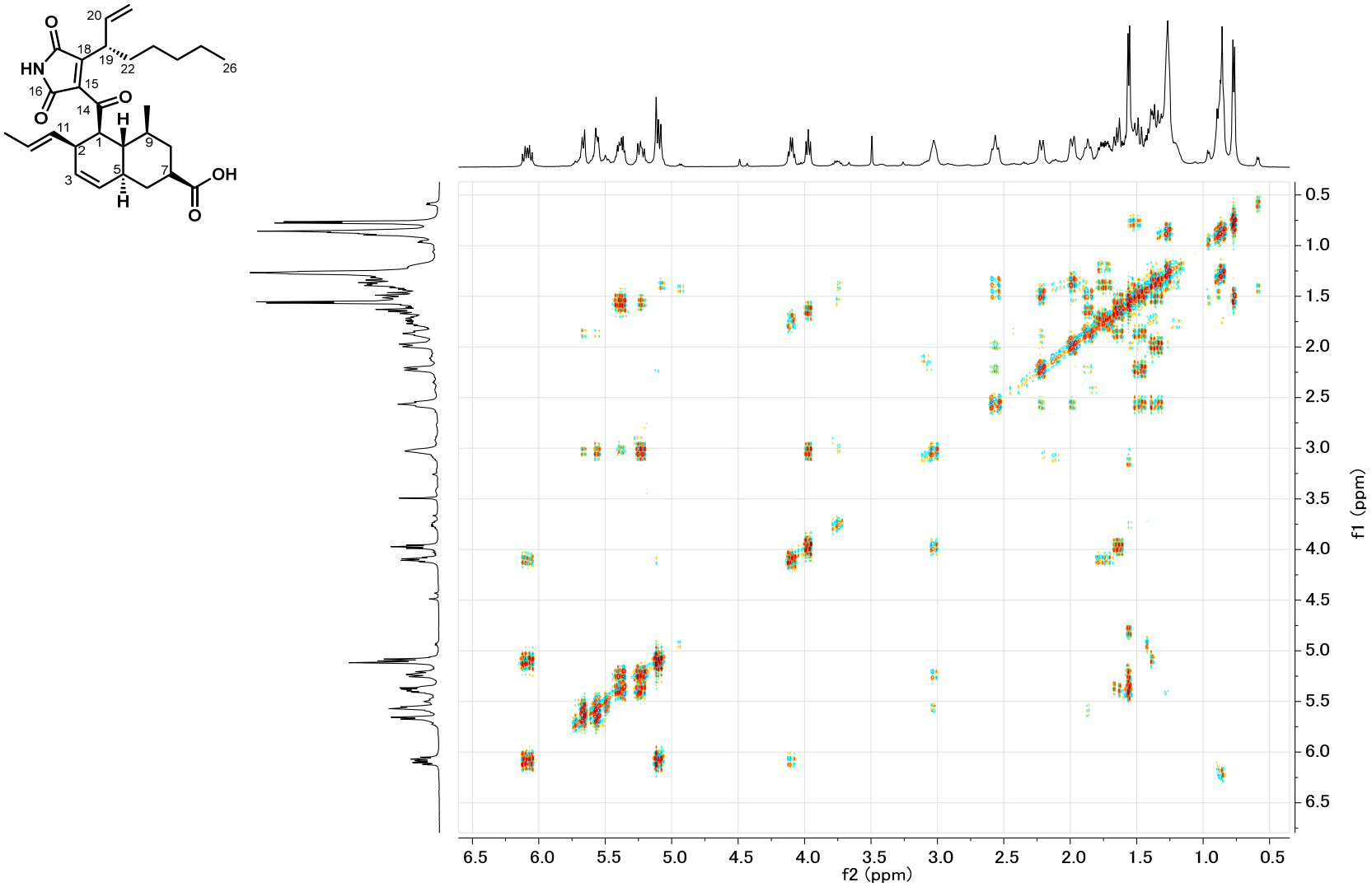

Figure S62. HSQC spectrum of **9** in $CDCl_3$ (500 MHz).

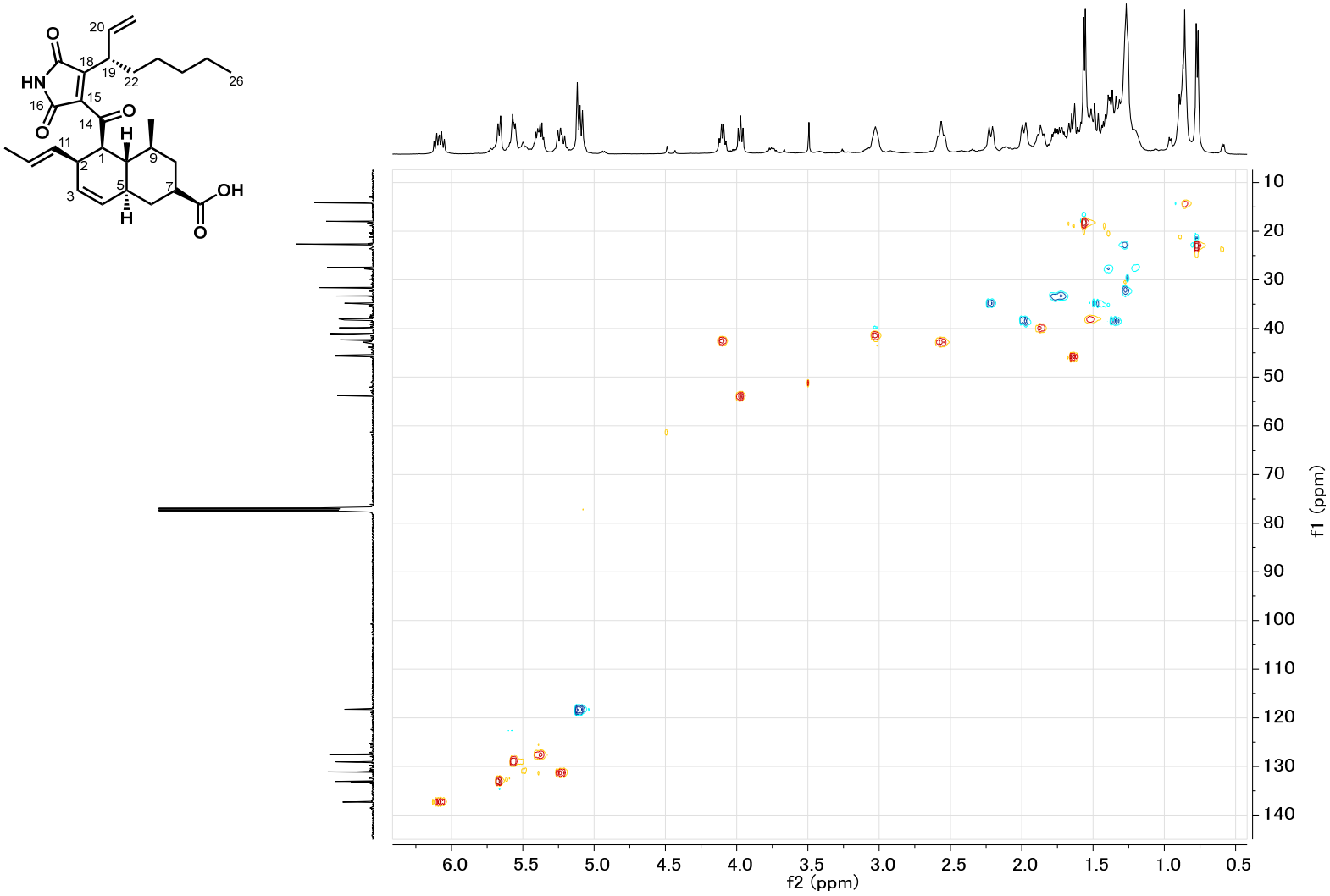

Figure S63. HMBC spectrum of **9** in $CDCl_3$ (500 MHz)

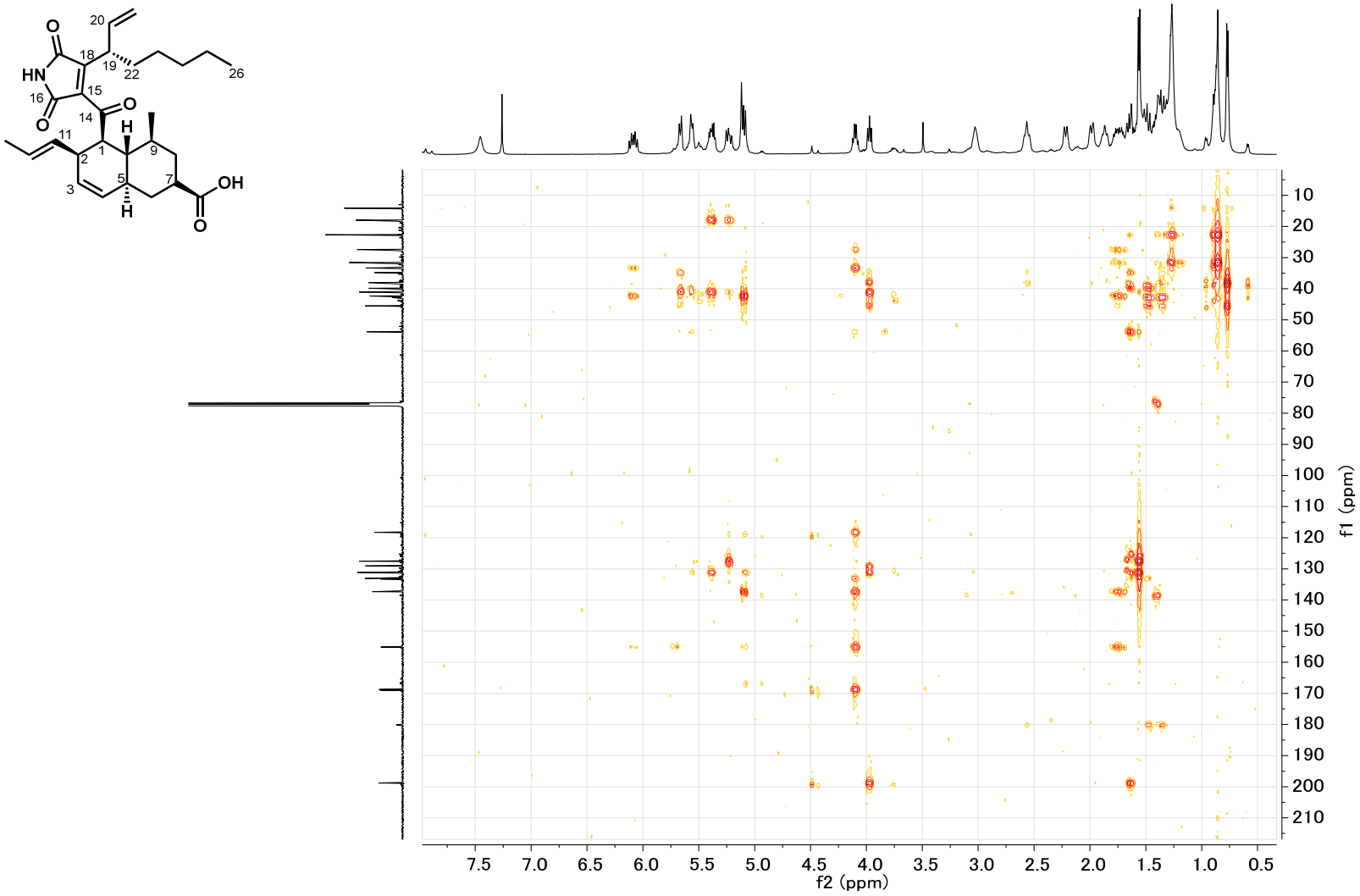

Figure S64. NOESY spectrum of **9** in $CDCl_3$ (500 MHz)

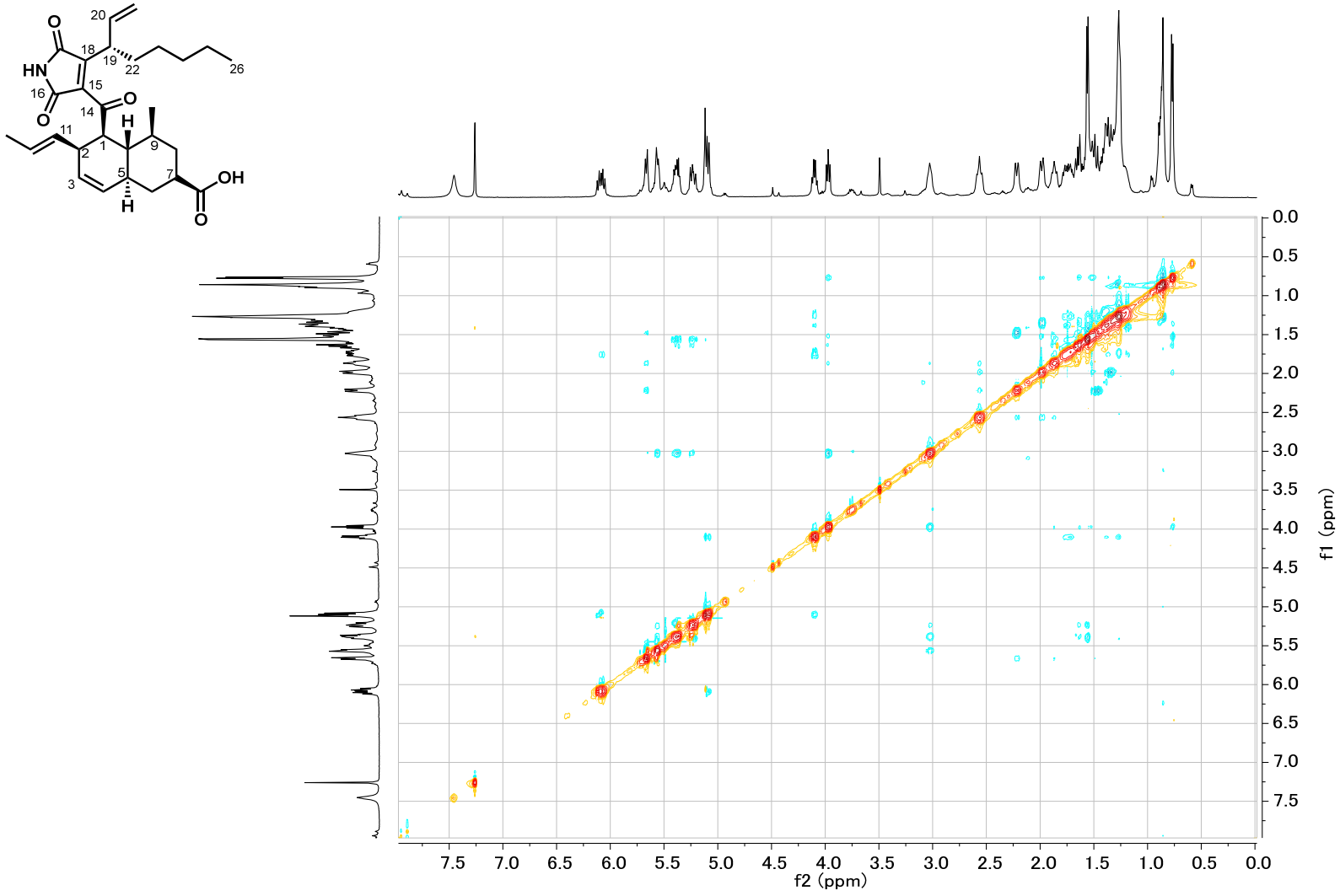

2.16. Chemical characterization of **10**

Table S13. NMR data of oxaleimide J (**10**) in $CDCl_3$. The molecular formula of **10** was established by mass data [ESI–MS: *m/z* 466 $(M–H)^–$; HRESIMS: *m/z* 466.2599 $(M–H)^–$, calcd. for $C_{28}H_{36}NO_5^–$, 466.2599, Δ = 0.02 mmu]; $[\alpha]_D^{31}$: –68.7 (*c* 1.1, MeOH).

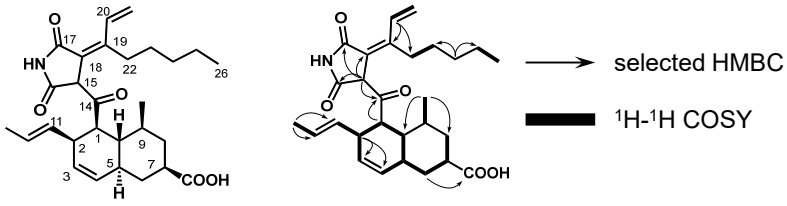

Position	δ_H [ppm]	mult. (Hz)	δ_C [ppm]	δ_H [ppm]	mult. (Hz)	δ_C [ppm]	HMBC
1	3.75	dd (10.8, 4.7)	52.1	3.21	dd (8.3, 5.7)	53.2	2,3,9,11,14
2	3.01	brs	41.5	2.76	brs	42.5	3,4,10,11,12
3	5.55	m	128.0	5.18	m	129.3	2
4	5.49	m	130.7	5.46	m	130.3	5,6
5	1.96	m	41.9	1.81	m	41.5	
6	2.07	m	35.3	2.07	m	35.2	
	1.37	m		1.37	m		4,7,7-CO
7	2.54	m	42.9	2.54	m	42.9	6,8,7-CO
8	1.88	m	39.1	1.97	m	39.0	10
	1.39	m		1.36	m		
9	1.41	m	37.2	1.43	m	37.8	
10	1.53	m	43.0	1.41	m	45.0	1,5,8,9
11	5.36	m	130.4	5.49	m	130.1	2,13
12	5.36	m	127.1	5.17	m	127.2	2,11
13	1.66	d (3.5)	18.1	1.57	d (5.0)	18.1	11,12
14			199.3			199.8	
15	4.48	s	61.3	4.43	s	61.9	14,16,17,18,19,20
16			168.7			169.0	
17			169.4			170.5	
18			119.7			119.4	
19			154.9			154.7	
20	8.00	dd (17.5,11.0)	132.4	7.95	dd (17.9, 11.1)	132.4	19,21,22
21	5.70	d (17.5)	122.4	5.72	d (17.7)	122.6	19,20
	5.58	m		5.58	m		19
22	2.43	m	30.8	2.34	m	30.5	18,19,20,23,24
	1.84	m		2.28	m		18,19,20,23,24
23	1.51	m	29.1	1.35	m	29.0	
24	1.26	m	32.3	1.29	m	32.4	23,25,26
25	1.31	m	22.8	1.31	m	22.6	24
26	0.89	t (6.4)	14.1	0.89	t (6.4)	14.1	24,25
7–COOH			180.0			179.9	
9–Me	0.58	d (5.8)	23.6	0.96	d (5.0)	23.5	8,9,10

Figure S65. ^{1}H NMR spectrum of **10** in $CDCl_3$ (500 MHz).

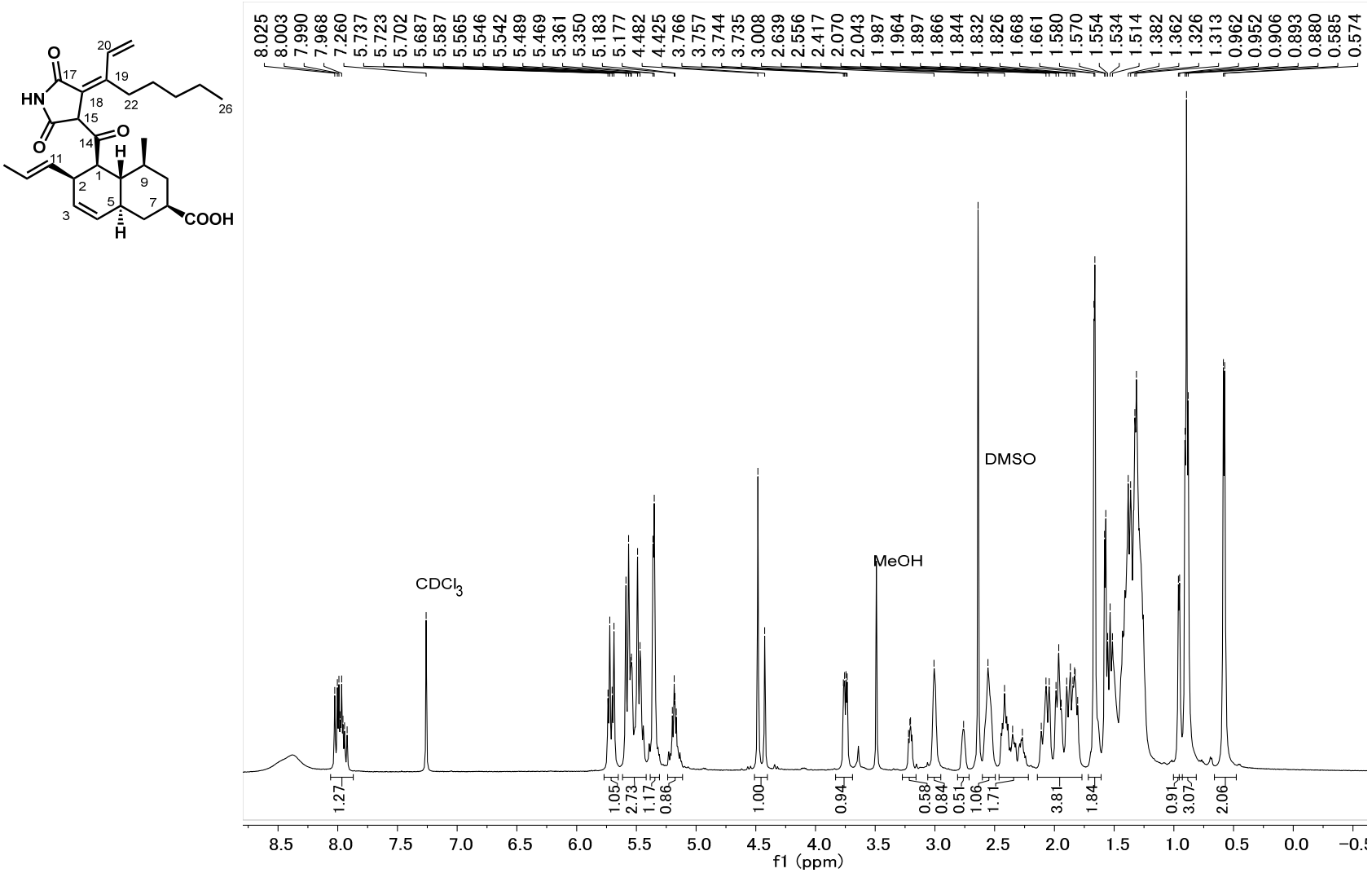

Figure S66. ^{13}CNMR spectrum of **10** in $CDCl_3$ (125 MHz)

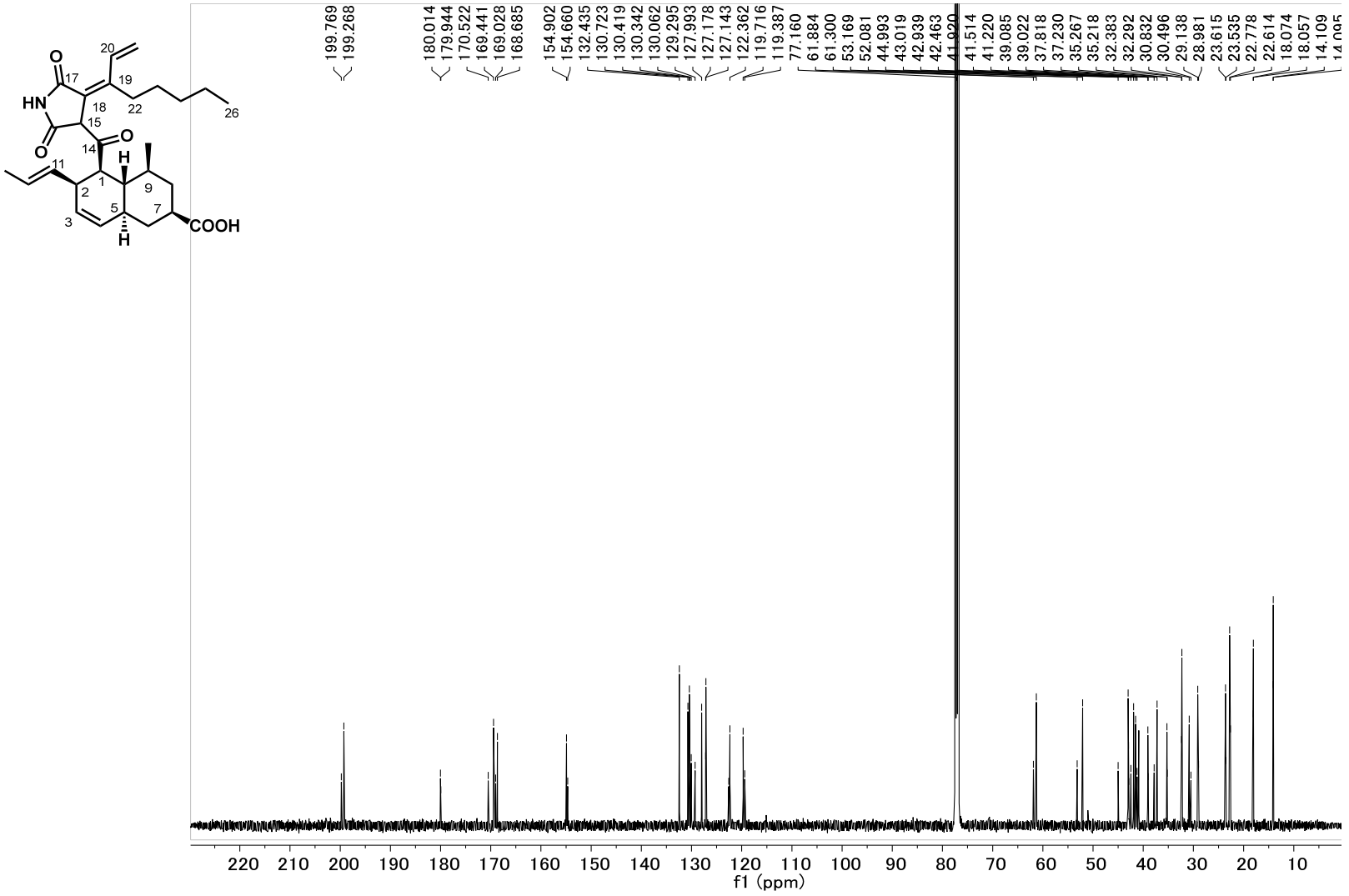

Figure S67. ^{1}H-^{1}H COSY spectrum of **10** in $CDCl_3$ (500 MHz)

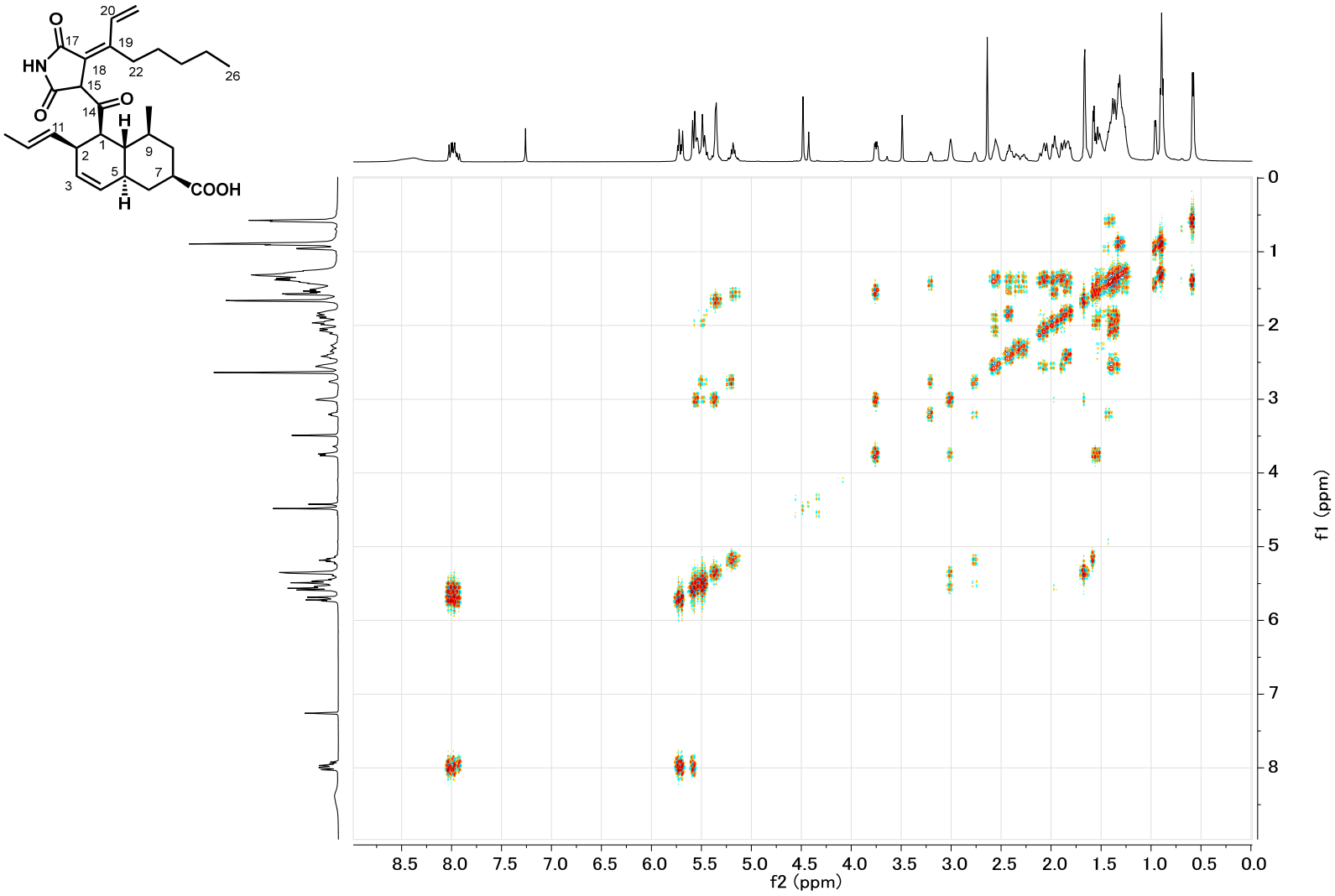

Figure S68. HSQC spectrum of **10** in $CDCl_3$ (500 MHz).

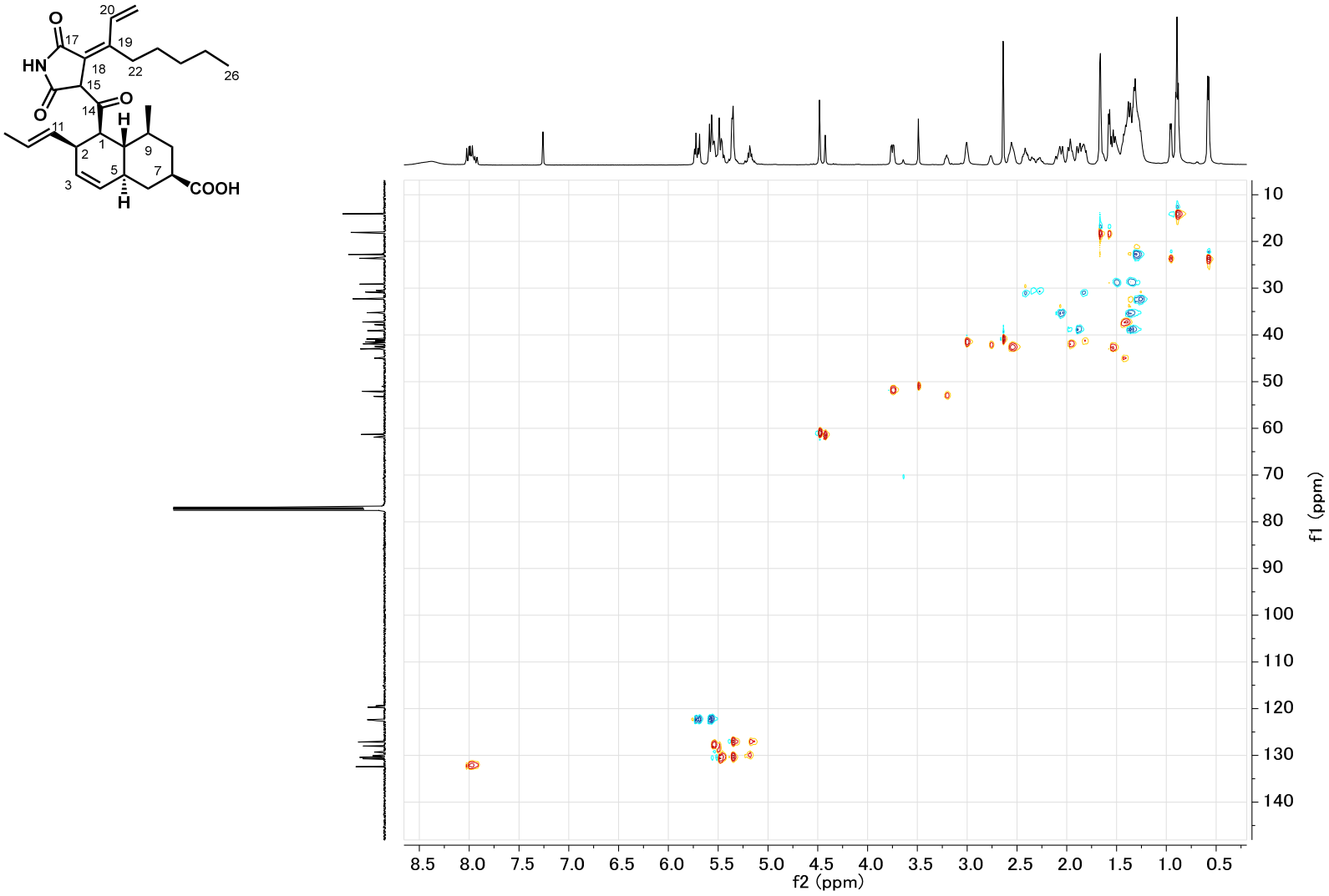

Figure S69. HMBC spectrum of **10** in $CDCl_3$ (500 MHz)

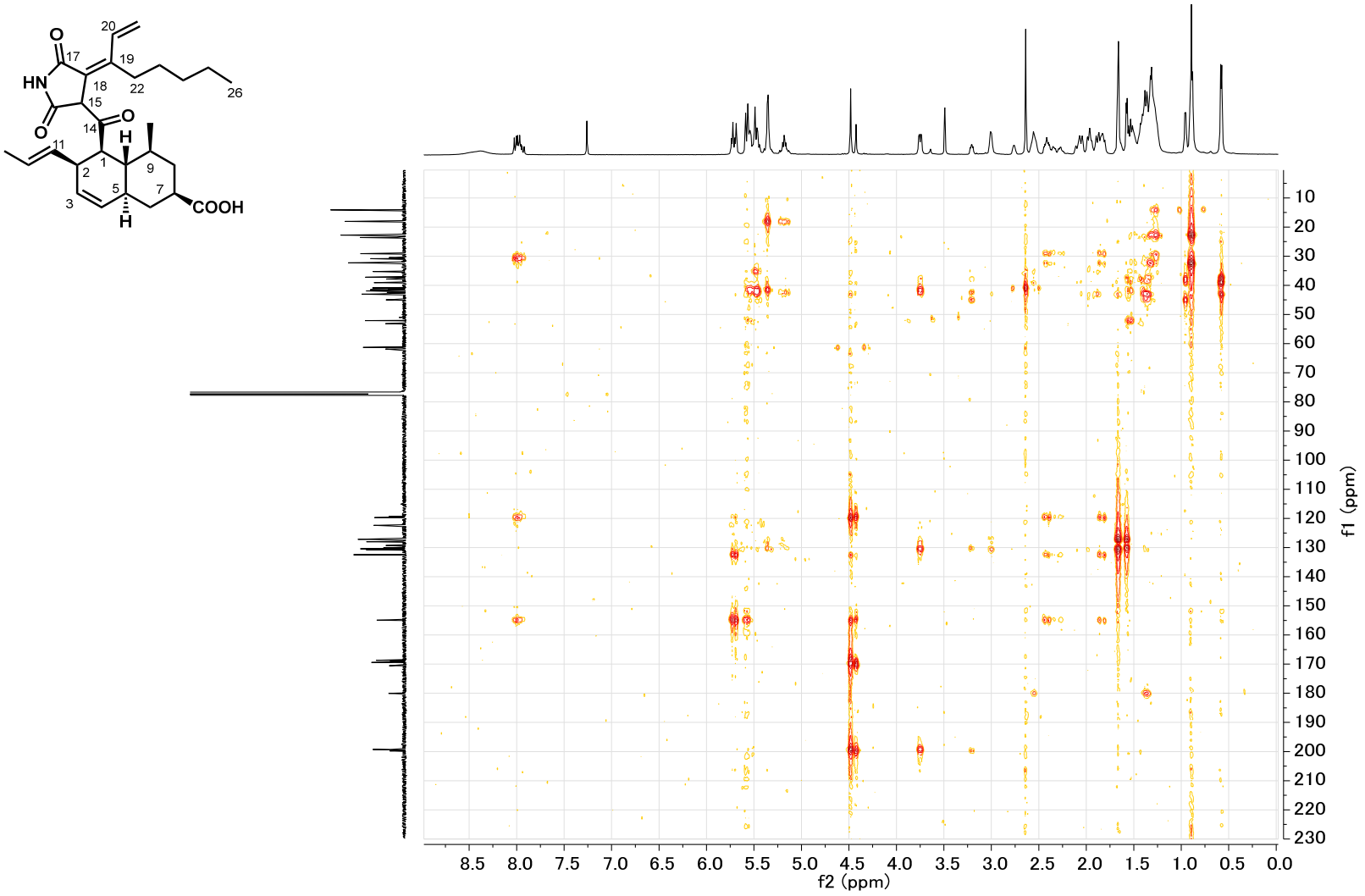

2.17. Chemical characterization of **12**

Table S14. NMR data of compound **12** in $CDCl_3$. The molecular formula of **12** was established by mass data [ESI–MS: *m/z* 442 $(M–H)^-$; HRESIMS: *m/z* 442.3324$(M–H)^-$, calcd. for $C_{28}H_{44}NO_3^-$, 442.3327, Δ = 0.25 mmu]; $[\alpha]_D^{31}$: 15.2 (*c* 0.1, MeOH).

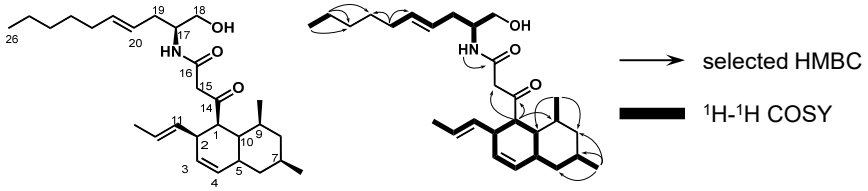

Position	δ_H [ppm]		mult. (*J* in Hz)	HMBC	δ_C [ppm]
1	2.84	1H	dd (8.3, 8.3)	2,9,10,11,12,14,15	58.0
2	2.95	1H	m	1,11,12,14	40.6
3	5.62	1H	m	1,11,12	128.3
4	5.65	1H	m	5	134.3
5	1.75	1H	m	6	40.4
6	1.87	1H	brd (11.1)	5,7,8,10	41.5
	0.93	1H	m	4	
7	1.56	1H	m	6,8,7-Me	32.7
8	1.64	1H	m		45.5
	0.81	1H	m		
9	1.34	1H	m	10	38.9
10	1.24	1H	m	1,5,8,9,14,9-Me	46.3
11	5.25	1H	dd (15.2, 8.8)	2,3,13	130.6
12	5.47	1H	m	2,13	127.2
13	1.65	3H	d (6.2)	11,12	18.1
14					210.4
15	3.40	1H	d (25.4)	14,16	49.4
	3.36	1H	d (25.4)	14,16	
16					167.0
17	3.91	1H	m	16,18,19,20	52.7
18	3.67	1H	dd (11.1, 3.0)	19	65.9
	3.57	1H	dd (11.1, 6.3)	17,19	
19	2.25	1H	m	17,18,20,21	34.5
	2.20	1H	m	17,18,20,21	
20	5.34	1H	dt (15.1,6.9)	17,19,21,22	124.8
21	5.56	1H	m	19,20,22,23	135.1
22	1.99	1H	dt (7.1,7.0)	20,21,23,24	32.6
23	1.35	2H	m	21,24,25	29.2
24	1.25	2H	m		31.6
25	1.29	2H	m	23,24,26	22.7
26	0.86	3H	t (7.0)	24,25	14.2
7-Me	1.56	3H	t (6.4)	6,7,8	32.7
9-Me	0.74	3H	d (6.6)	8,9,10	22.0
NH	7.43	1H	brd (6.6)	16,17,19	

Figure S70. ^{1}H NMR spectrum of compound **12** in $CDCl_3$ (500 MHz).

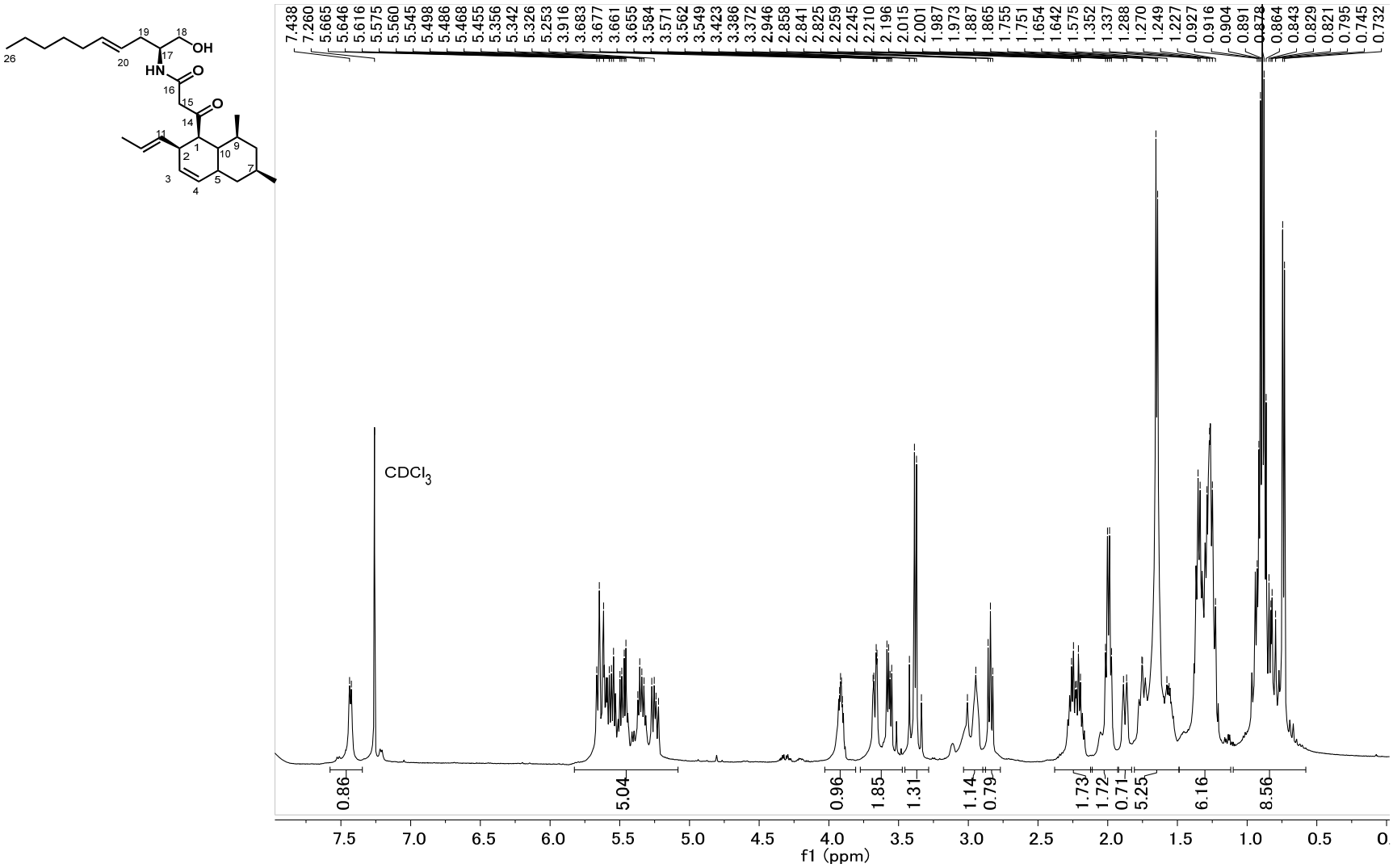

Figure S71. ^{13}CNMR spectrum of compound **12** in $CDCl_3$ (125 MHz)

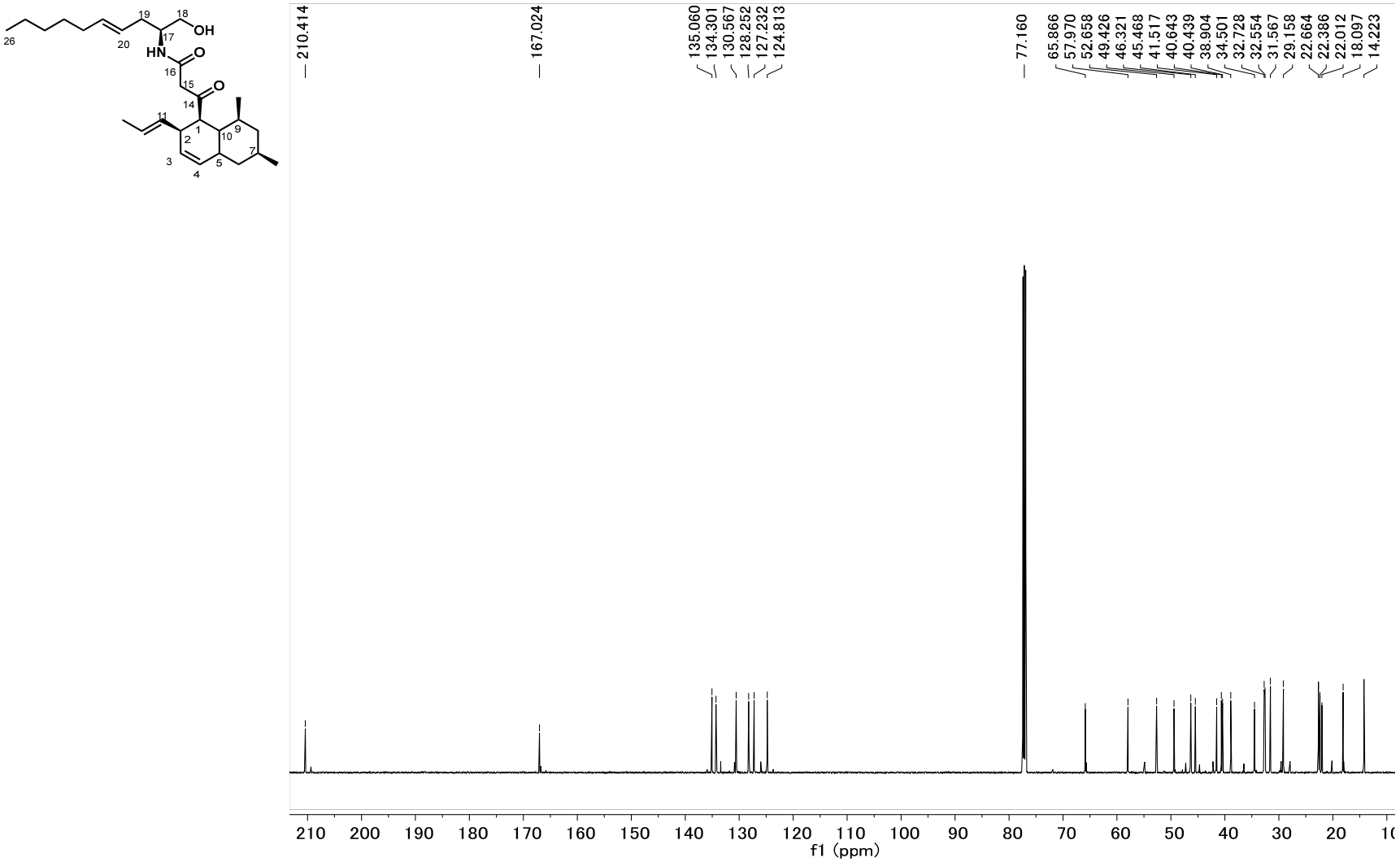

Figure S72. ^{1}H-^{1}H COSY spectrum of compound **12** in $CDCl_3$ (500 MHz).

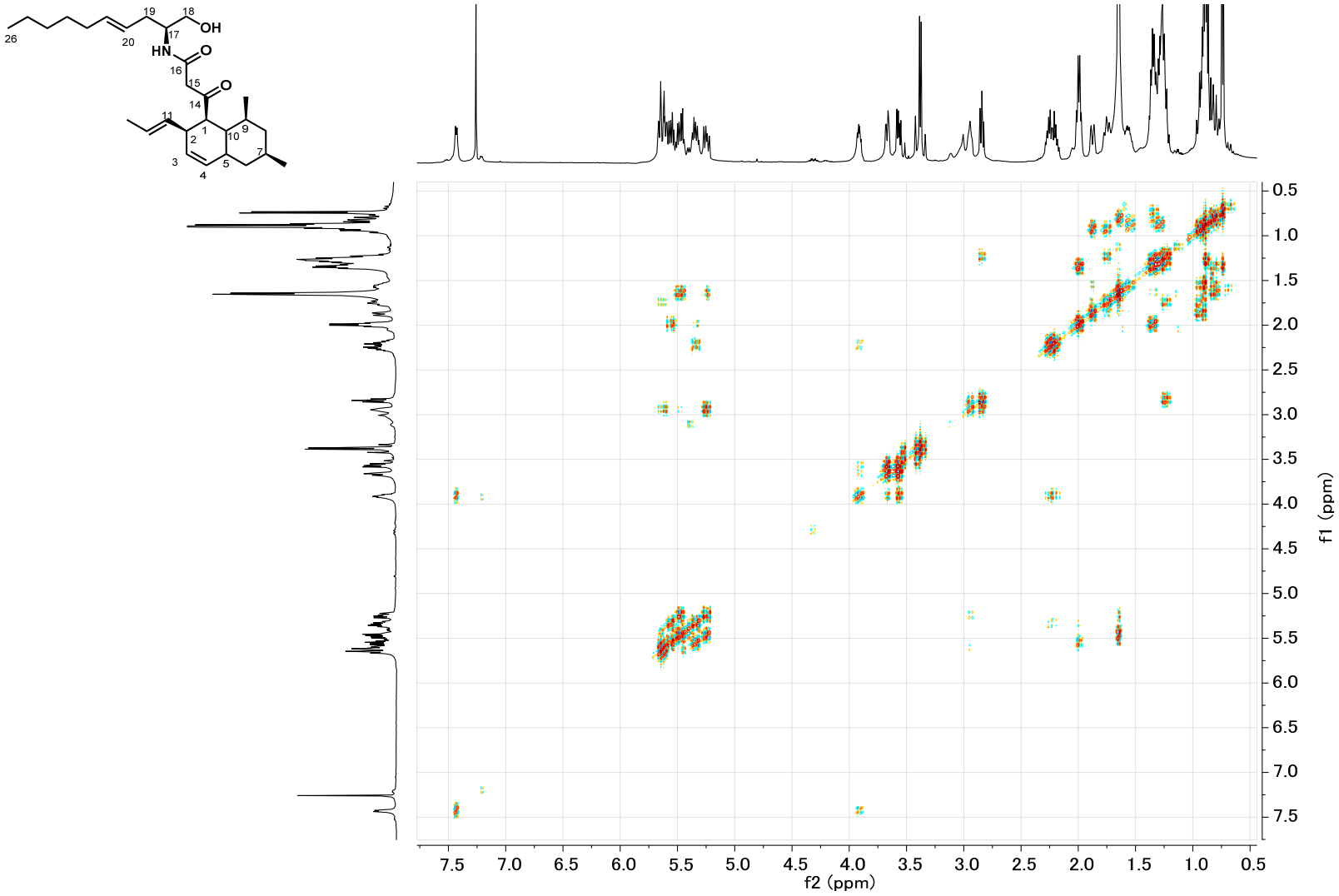

Figure S73. HSQC spectrum of compound **12** in $CDCl_3$ (500 MHz).

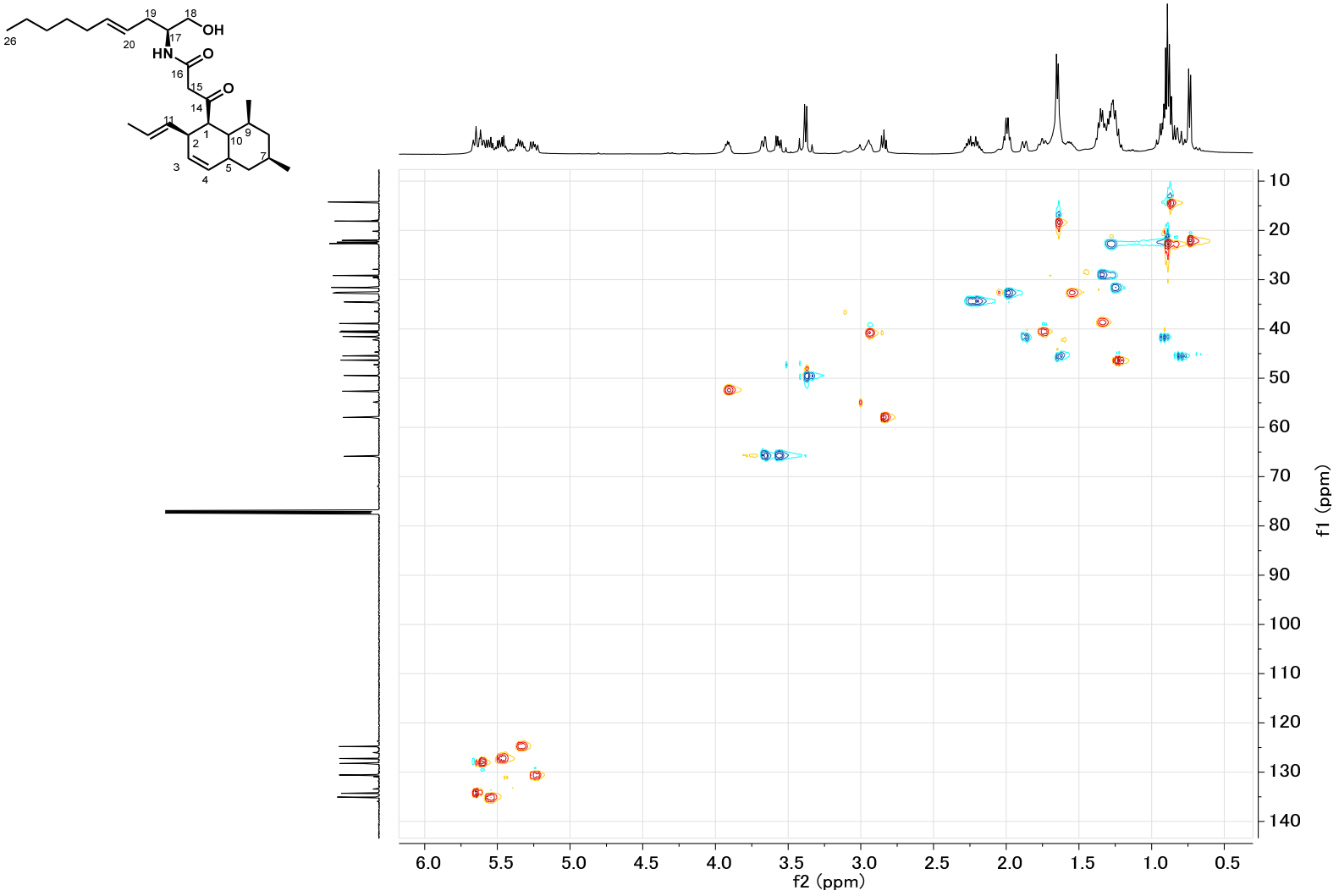

Figure S74. HMBC spectrum of compound **12** in $CDCl_3$ (500 MHz)

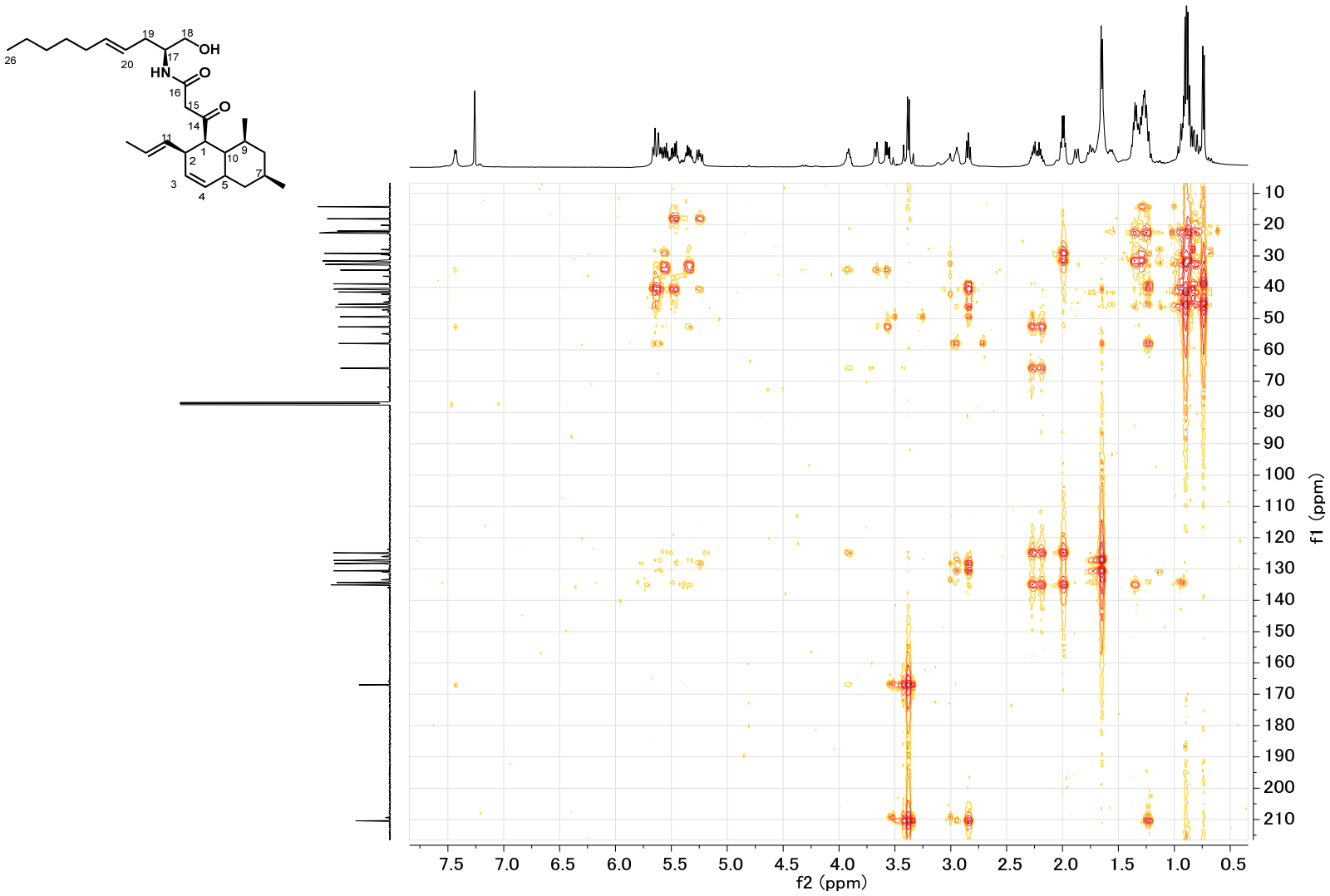

Figure S75. NOESY spectrum of compound **12** in $CDCl_3$ (500 MHz)

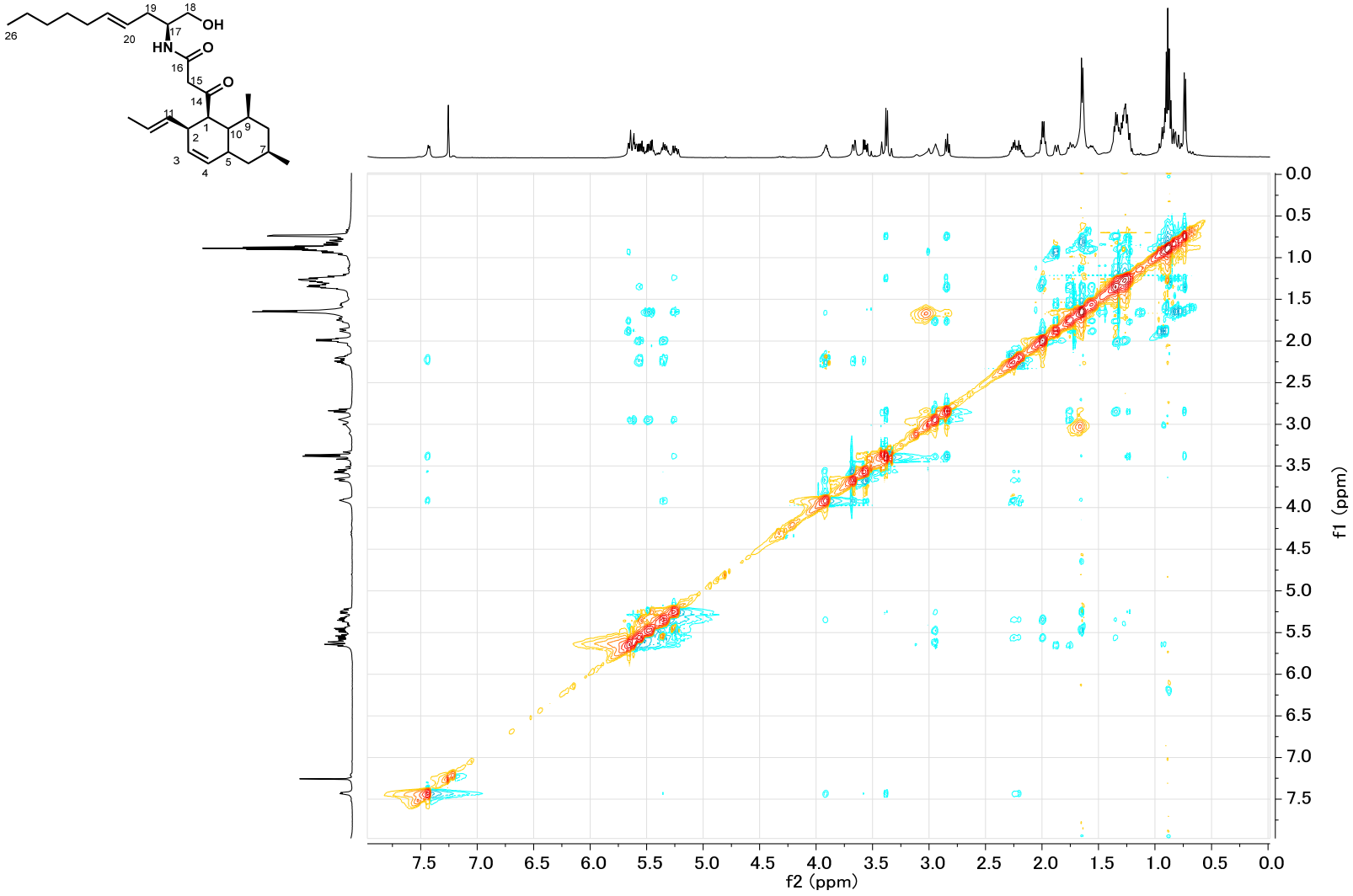

2.18. Chemical characterization of **14**

Table S15. NMR data of compound **14** in CD_3OD. The molecular formula of **14** was established by mass data [ESI–MS: *m/z* 186 $(M+H)^+$; HRESIMS: *m/z* 186.1485 $(M+H)^+$, calcd. for $C_{10}H_{20}NO_2^+$, 186.1489, Δ = 0.3 mmu] ; $[\alpha]_D^{30}$: –22.1 (*c* 0.19, MeOH).

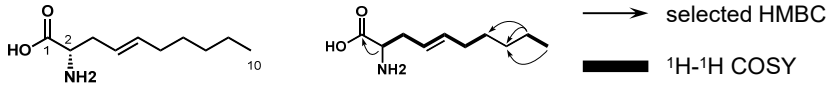

Position	δ_H [ppm]		mult. (*J* in Hz)	HMBC	δ_C [ppm]
1					174.3
2	3.51	1H	dd (7.5, 4.5)	1,3,4	55.9
3	2.69	1H	m	2,4,5	35.8
	2.49	1H	m	2,4,5	
4	5.41	1H	dt (15.2, 7.1)	3,6	124.5
5	5.66	1H	dt (15.2, 6.6)	3,6,7	137.2
6	2.05	2H	dt (7.3, 7.2)	4,5,7,8	33.7
7	1.40	2H	m	5,8,9	30.0
8	1.30	2H	m	9	32.6
9	1.32	2H	m	7,8,10	23.6
10	0.91	3H	t (7.1)	8,9	14.4

Figure S76. ^{1}H NMR spectrum of compound **14** in CD_3OD (500 MHz)

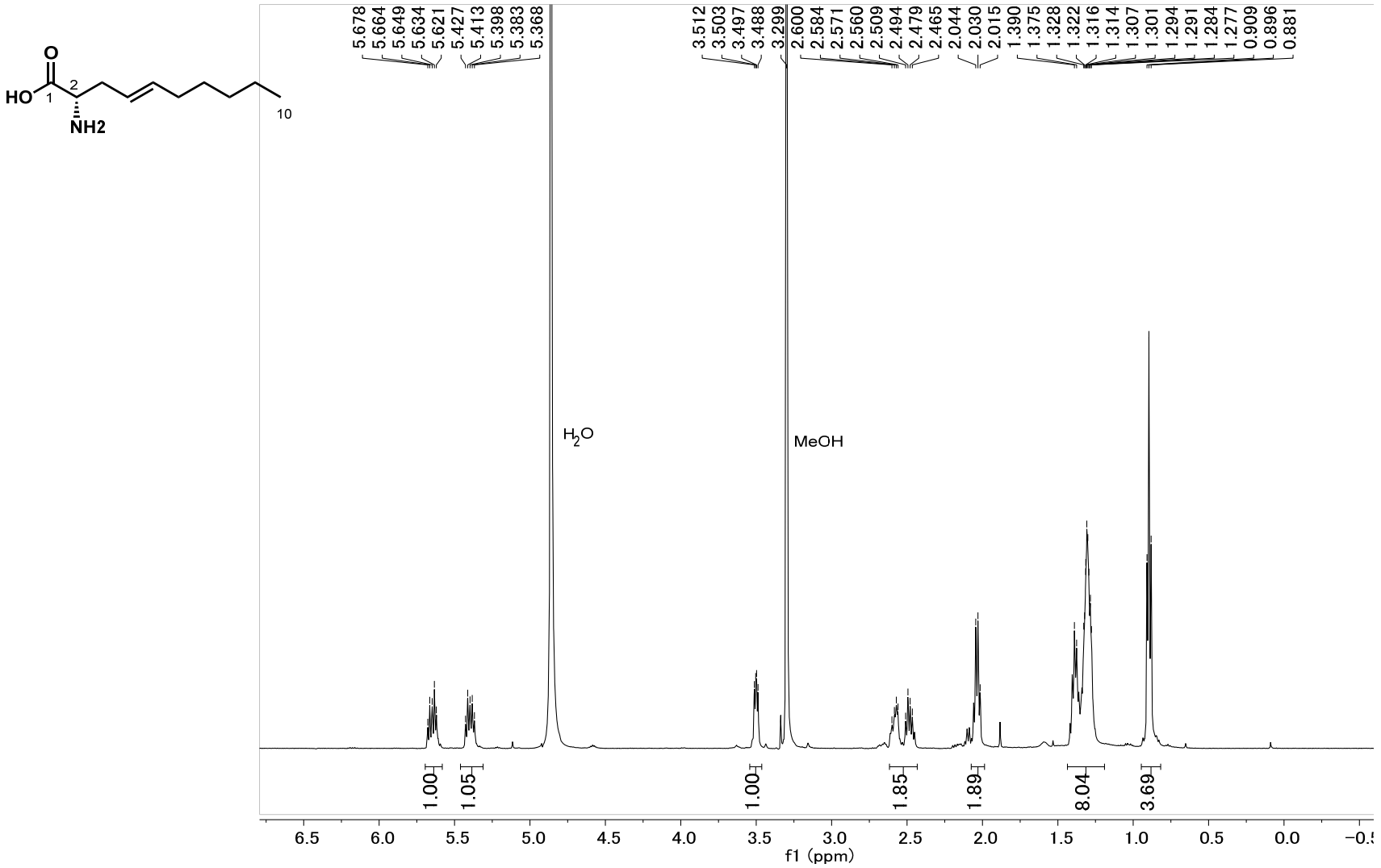

Figure S77. ^{13}CNMR spectrum of compound **14** in CD_3OD (125 MHz)

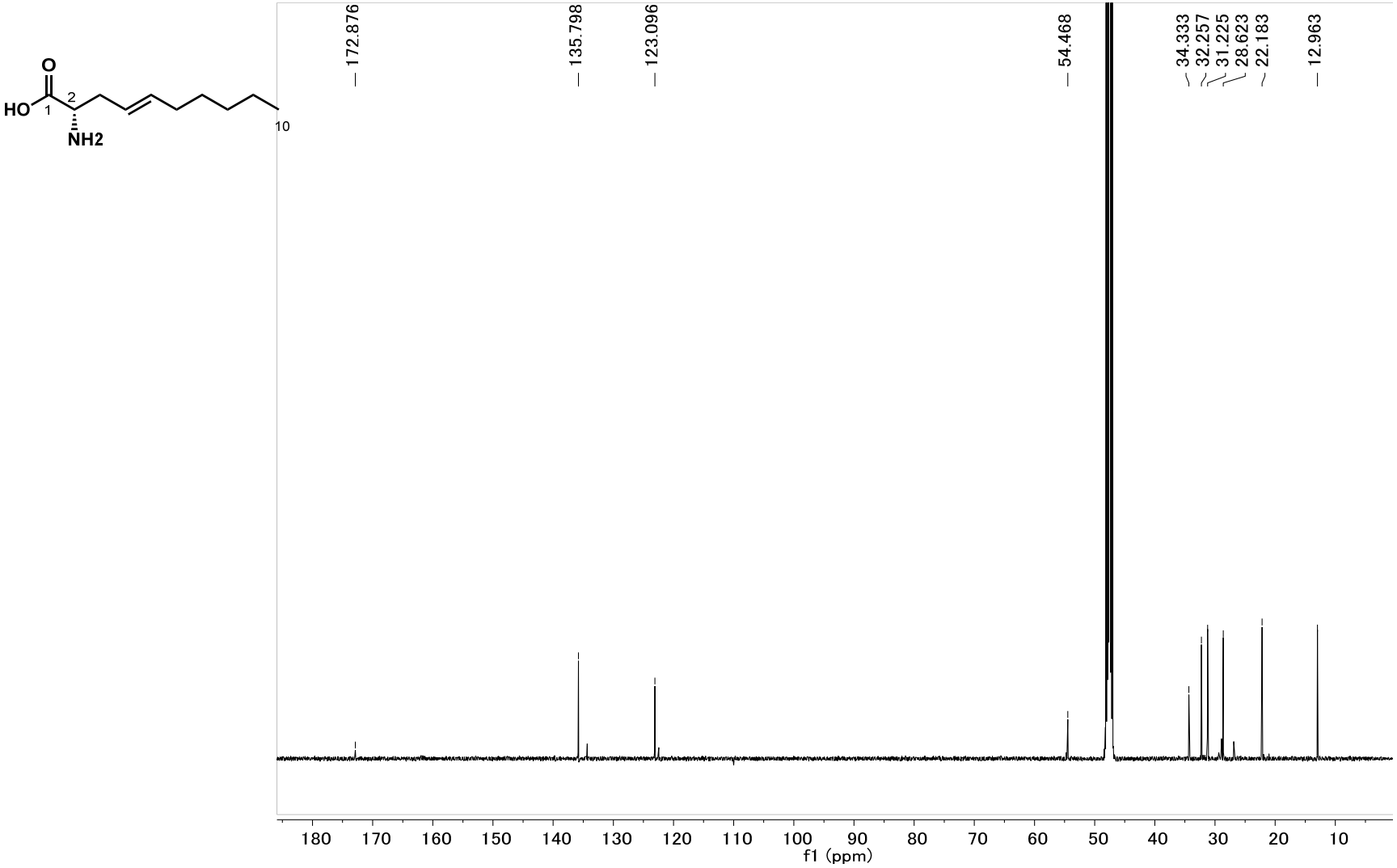

Figure S78. ^{1}H-^{1}H COSY spectrum of compound **14** in CD_3OD (500 MHz)

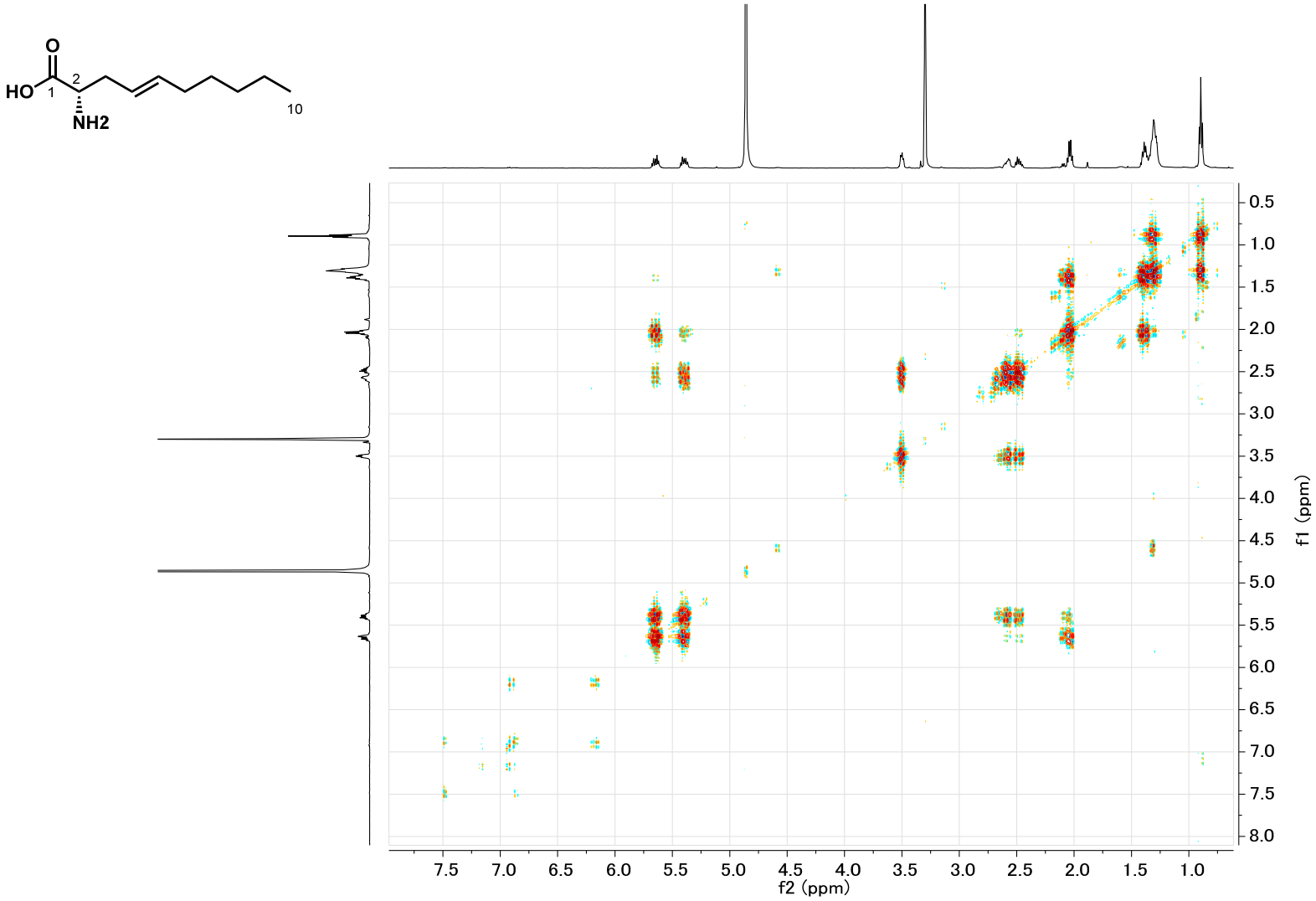

Figure S79. HSQC spectrum of compound **14** in CD_3OD (500 MHz).

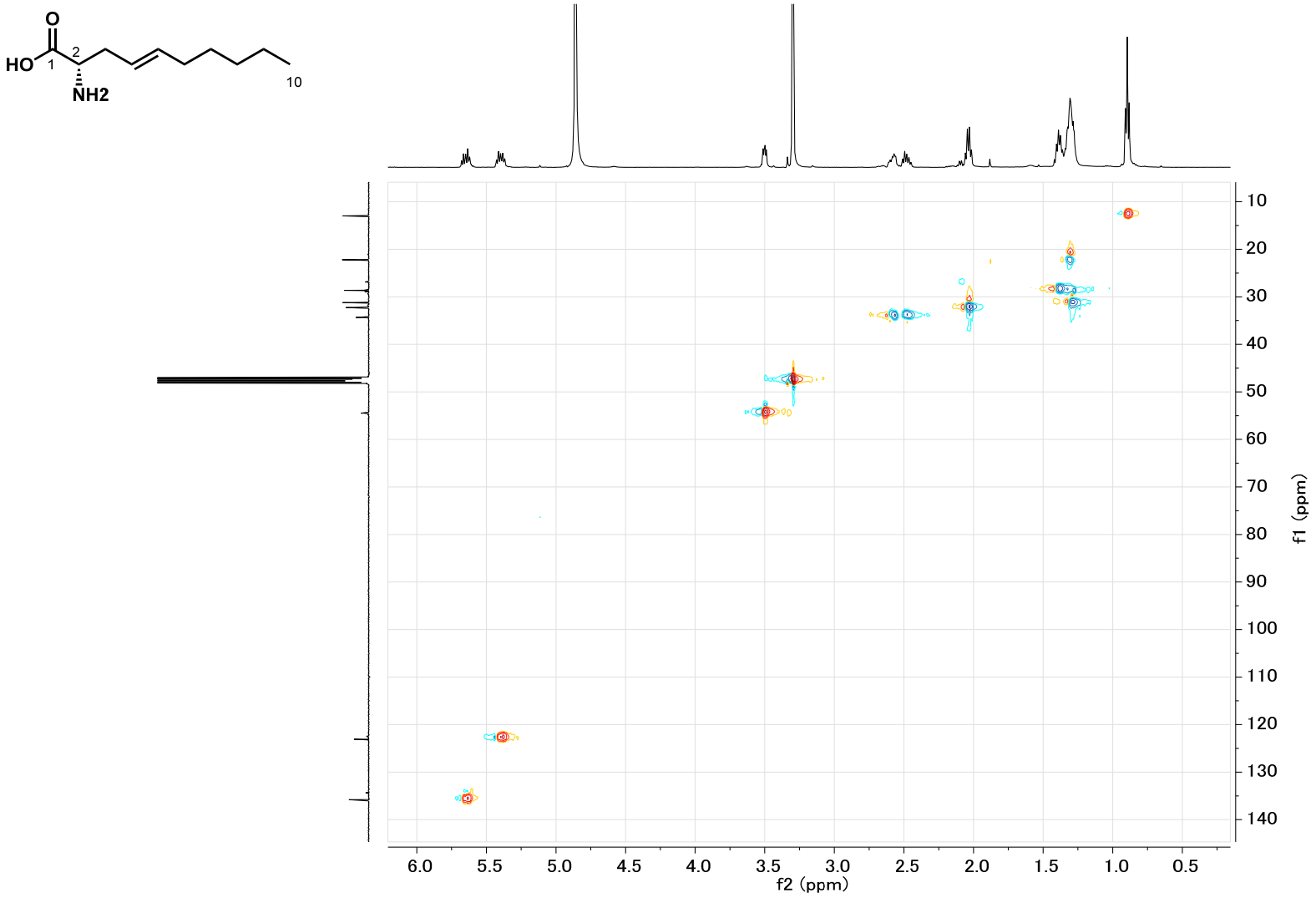

Figure S80. HMBC spectrum of compound **14** in CD_3OD (500 MHz)

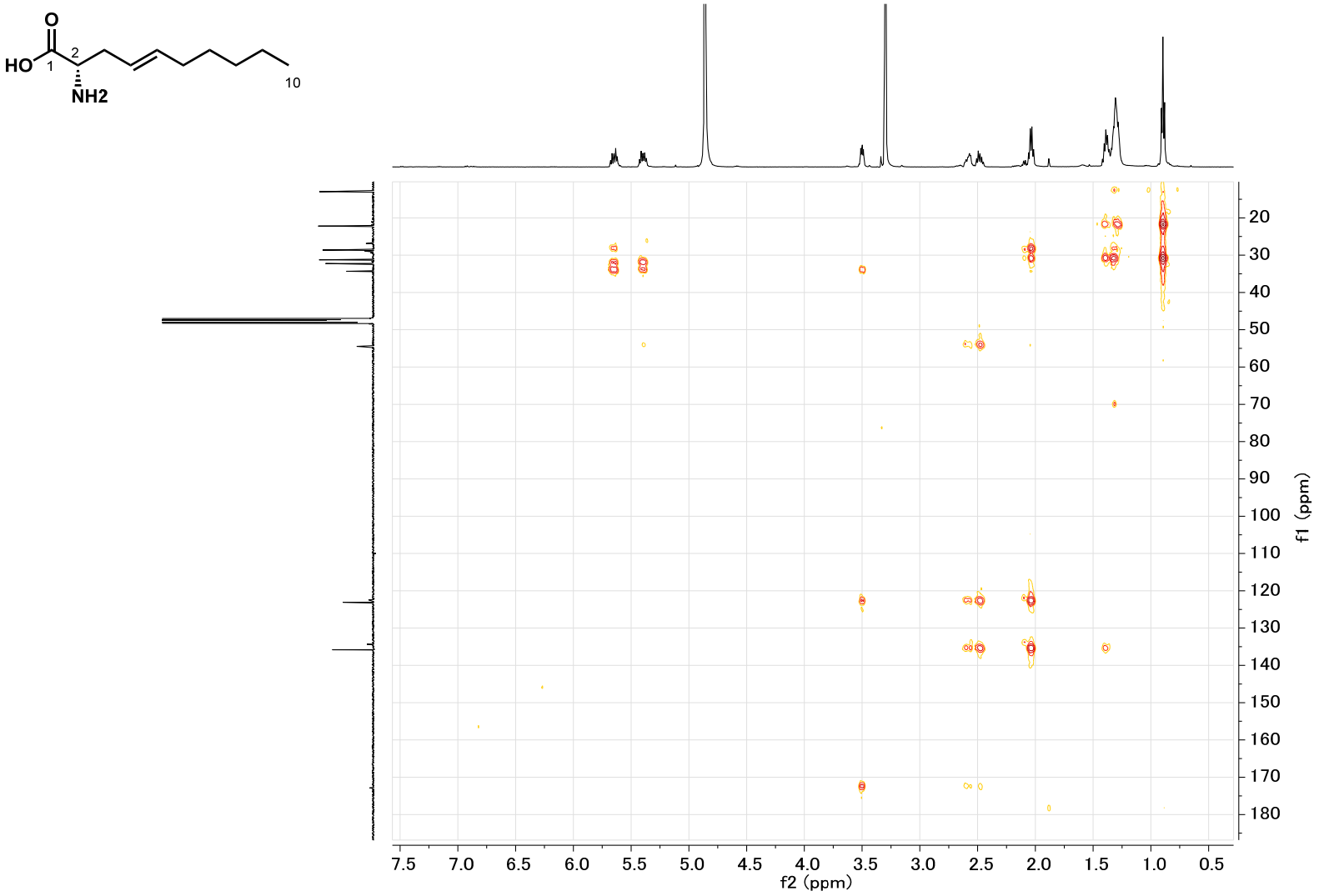

2.19. Chemical characterization of **15**

Table S16. NMR data of compound **15** in $CDCl_3$. The molecular formula of **15** was established by mass data [ESI–MS: *m/z* 185 $(M–H)^–$; HRESIMS: *m/z* 185.1185 $(M–H)^–$, calcd. for $C_{10}H_{17}O_4^–$, 185.1183, Δ = 0.15 mmu]

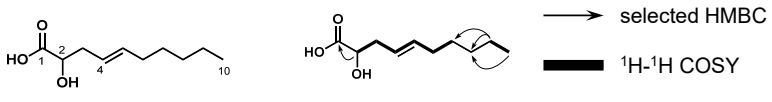

Position	δ_H [ppm]		mult. (*J* in Hz)	HMBC	δ_C [ppm]
1					176.9
2	4.30	1H	brt (5.7)	1,3,4	70.0
3	2.59	1H	m	2,4,5	37.5
	2.45	1H	m	2,4,5	
4	5.40	1H	dt (15.2, 7.2)	3,6	122.9
5	5.63	1H	dt (15.2, 6.7)	3,6,7	136.8
6	2.02	2H	dt (7.2, 7.1)	4,5,7,8	32.7
7	1.36	2H	m	5,8,9	29.1
8	1.26	2H	m	9	31.5
9	1.29	2H	m	7,8,10	22.6
10	0.88	3H	t (6.6)	8,9	14.2

Figure S81. ^{1}H NMR spectrum of compound **15** in $CDCl_3$ (500 MHz)

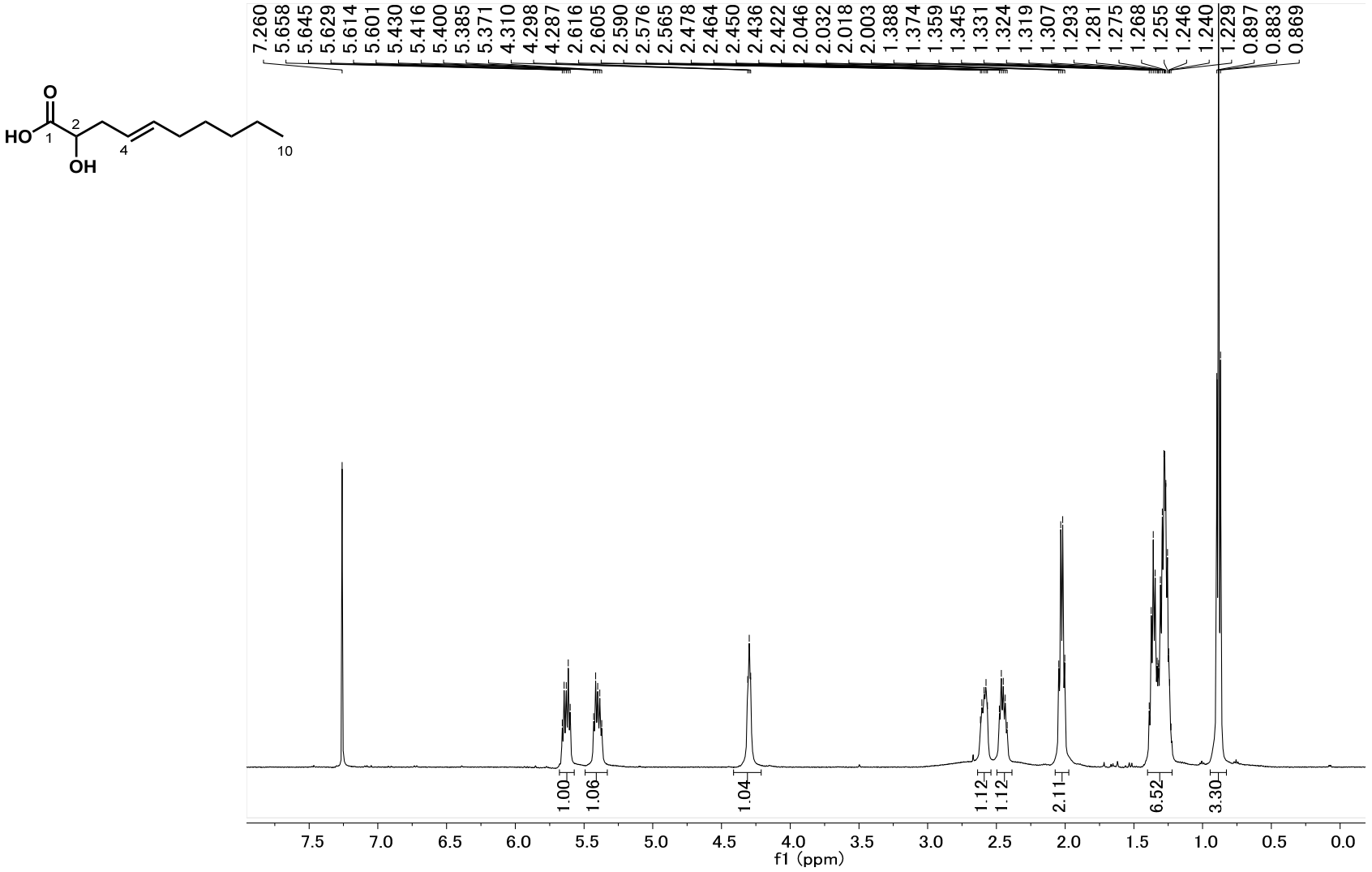

Figure S82. ^{13}CNMR spectrum of compound **15** in $CDCl_3$ (125 MHz)

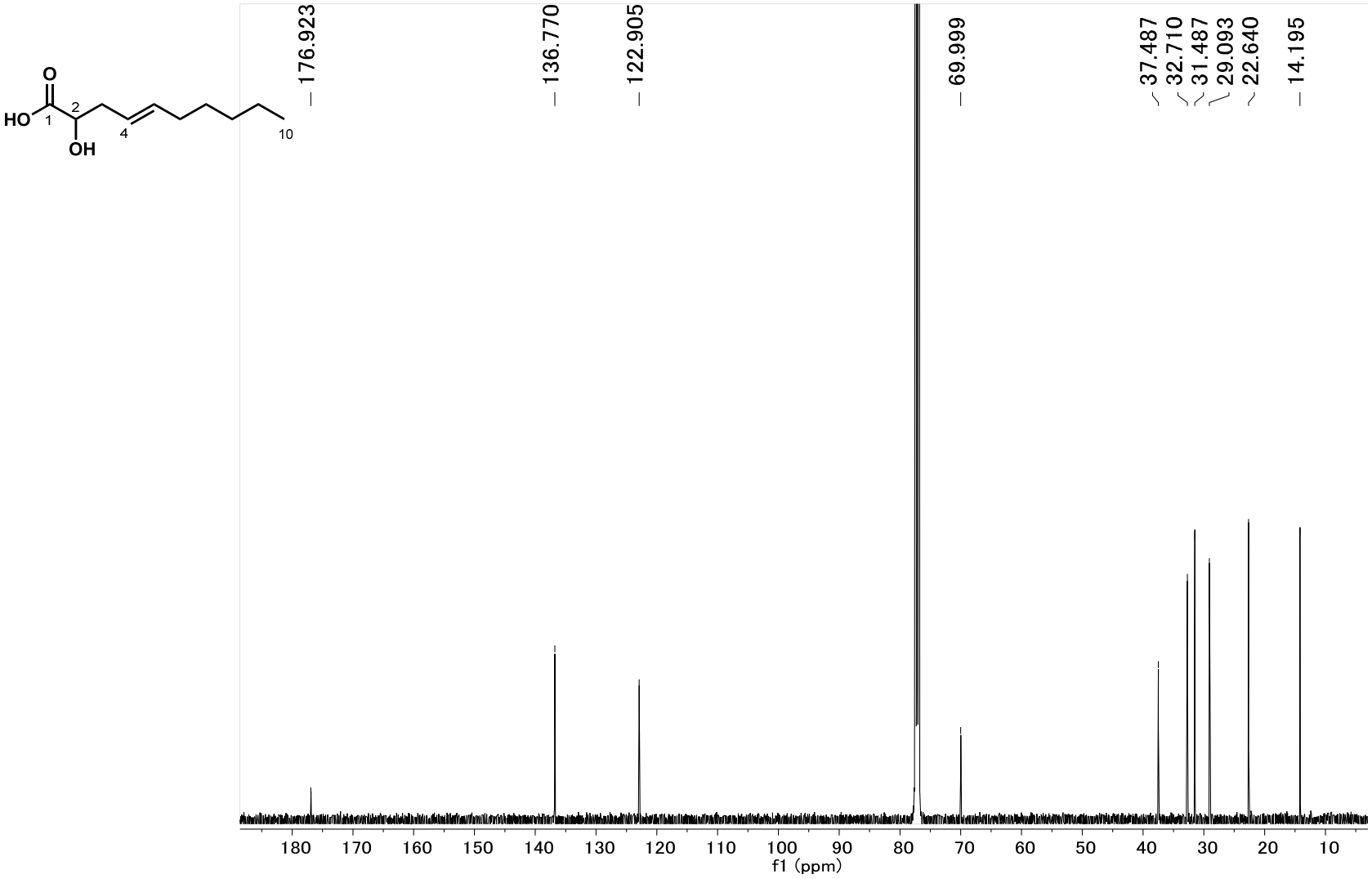

Figure S83. ^{1}H-^{1}H COSY spectrum of compound **15** in $CDCl_3$ (500 MHz)

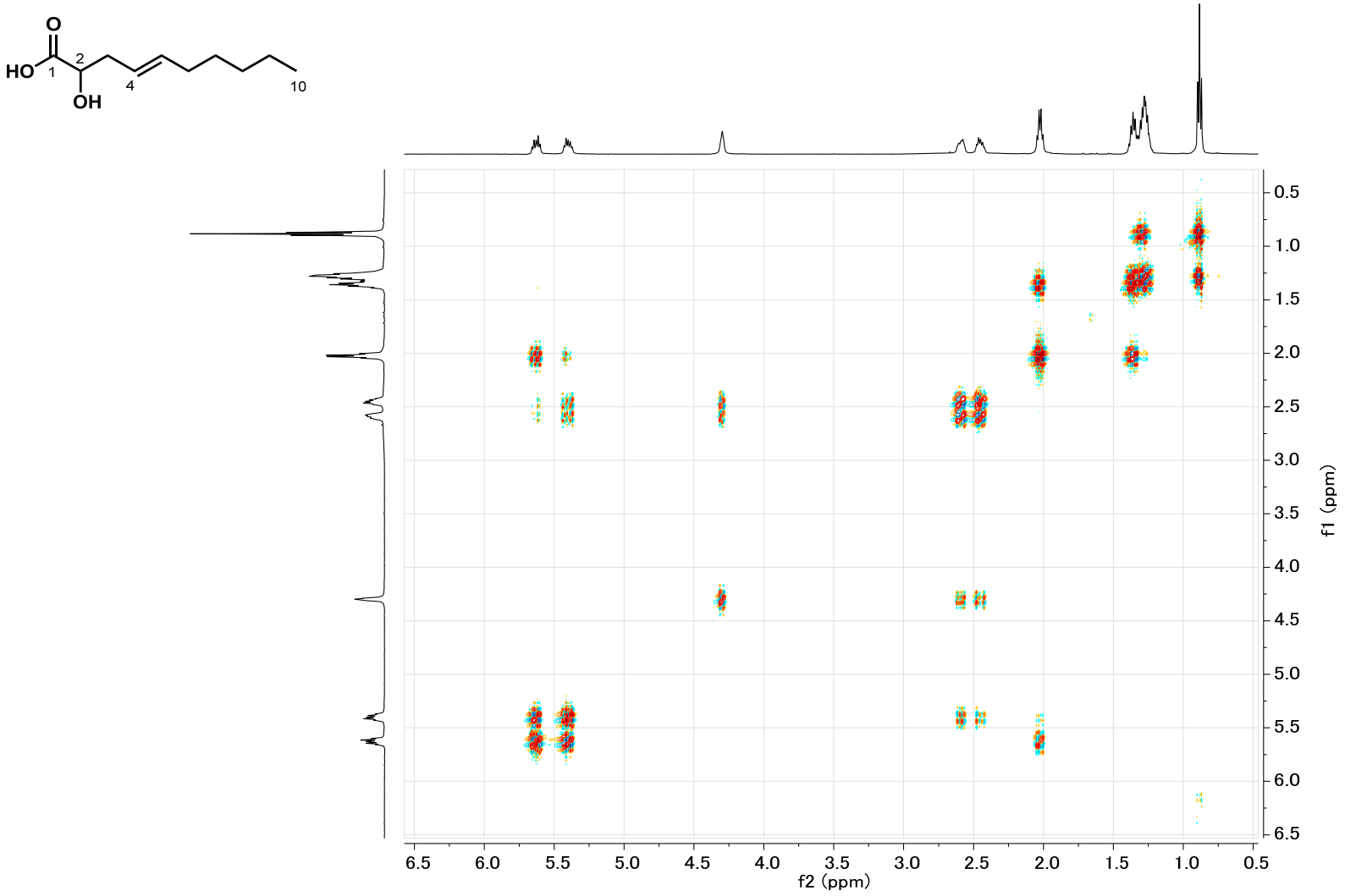

Figure S84. HSQC spectrum of compound **15** in $CDCl_3$ (500 MHz).

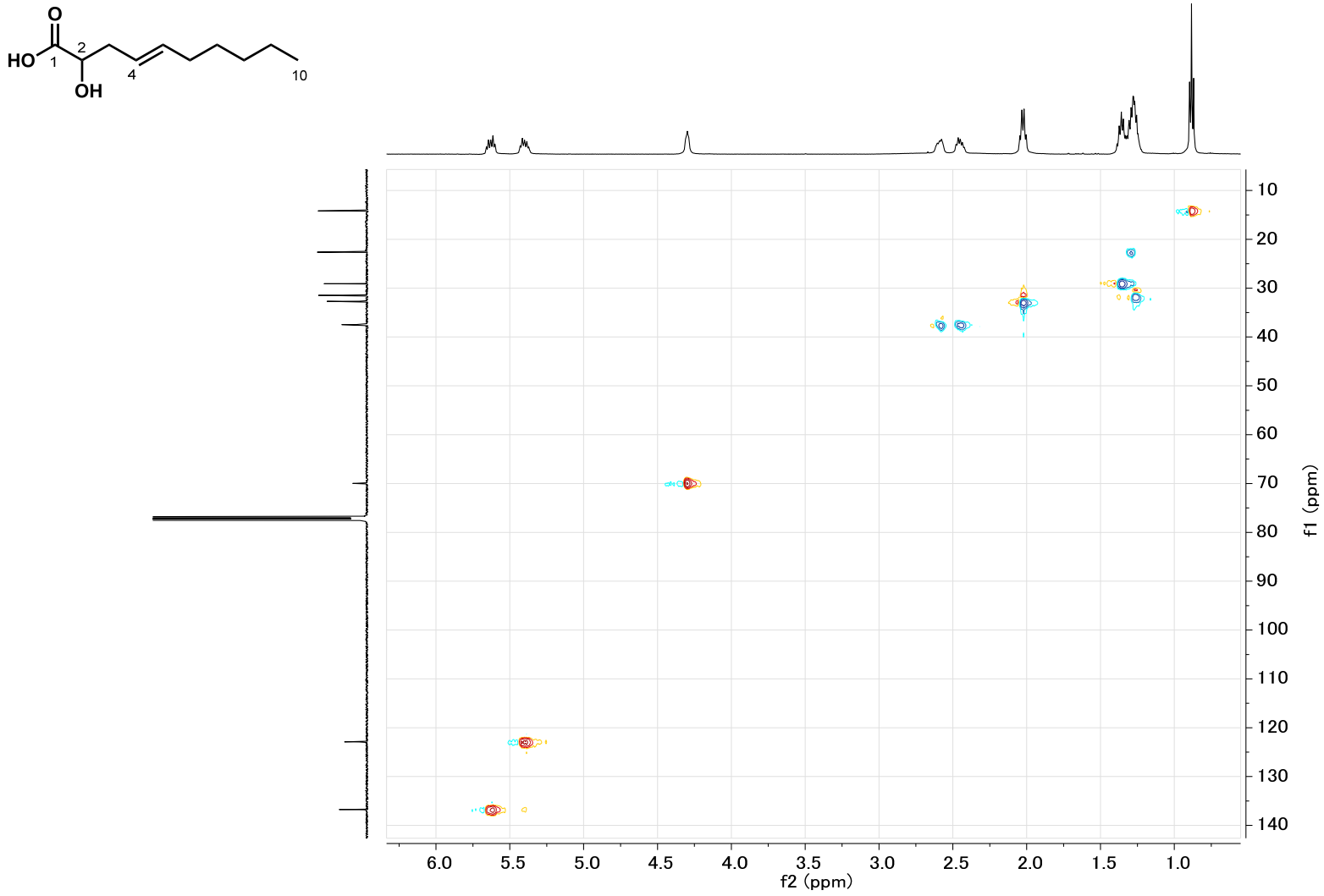

Figure S85. HMBC spectrum of compound **15** in $CDCl_3$ (500 MHz)

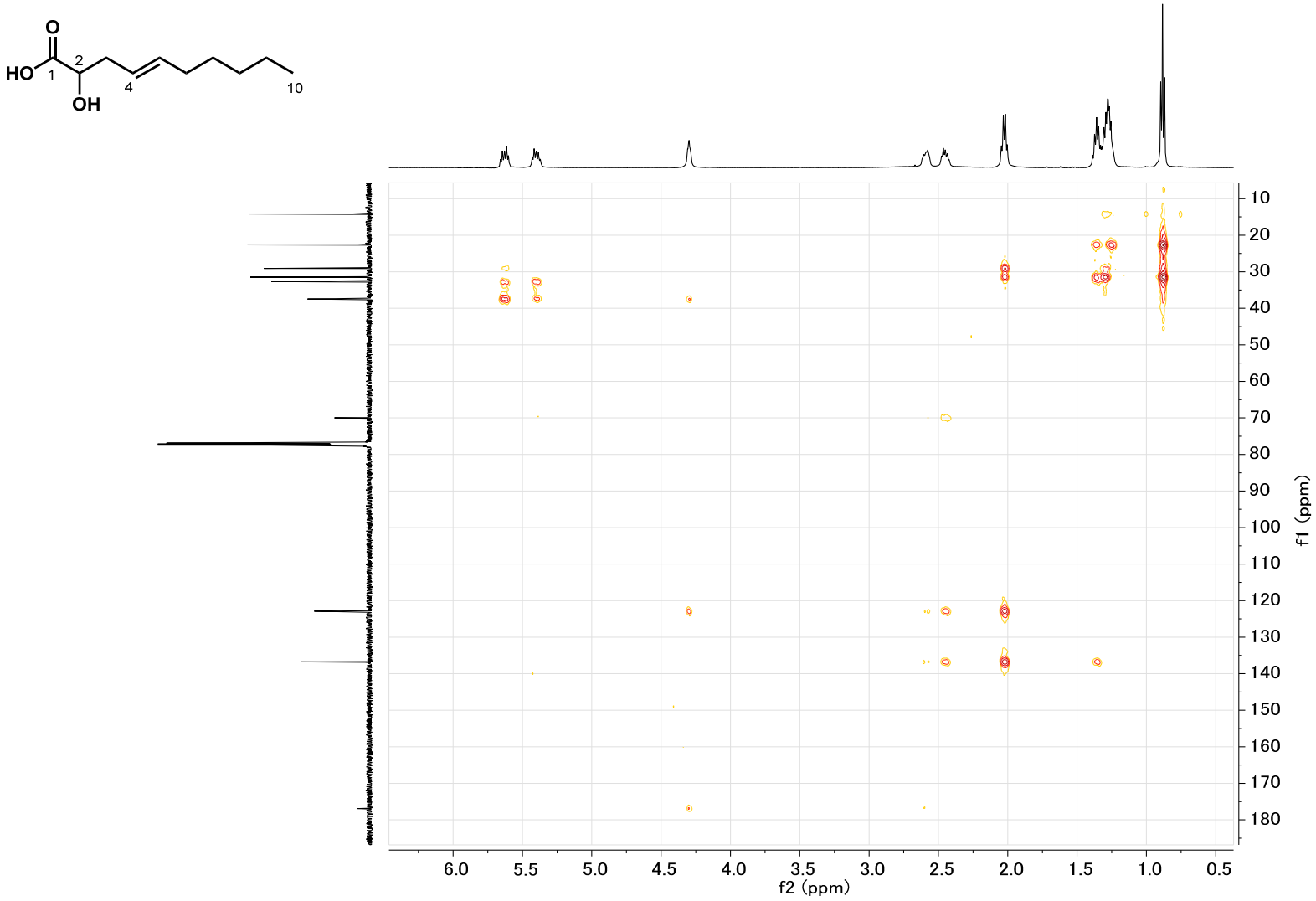

3. Supporting References

1. Gottlieb, H. E.; Kotlyar, V.; Nudelman, A. *J. Org. Chem.* **1997***, 62*, 7512–7515
2. Punt, P. J.; Oliver, R. P.; Dingemanse, M. A.; Pouwels, P. H.; van den Hondel, C. A. *Gene* **1987,** *56*, 117-124.
3. Kanwal, A.; Paraszkiewicz, K.; Dlugonski, J. *Microbios* **2001,** *104*, 27-38.
4. Lee, K. K.; Da Silva, N. A.; Kealey, J. T. *Anal. Biochem.* **2009,** *394*, 75-80.
5. Li, L.; Yu, P.; Tang, M. C.; Zou, Y.; Gao, S. S.; Hung, Y. S.; Zhao, M.; Watanabe, K.; Houk, K. N.; Tang, Y. *J. Am. Chem. Soc.* **2016,** *138*, 15837-15840.
6. Yamamoto, T.; Tsunematsu, Y.; Hara K.; Suzuki T.; Kishimoto, S.; Kawagishi, H.; Noguchi, H.; Hashimoto, H.; Tang, Y.; Hotta, K.; Watanabe, K. *Angew Chem Int Ed Engl*. **2016**, 55, 6207.
7. Johnson, M.; Zaretskaya, I.; Raytselis, Y.; Merezhuk, Y.; McGinnis, S.; Madden, T. L. *Nucleic Acids Res.* **2008,** *36*, W5-9.
8. Offenzeller, M.; Santer, G.; Totschnig, K.; Su, Z.; Moser, H.; Traber, R.; Schneider-Scherzer, E. *Biochemistry* **1996,** *35*, 8401-8412.